Molecular Dynamics simulation of methane

by

OOI SU KHI

1071112324

Session 2011/2012

The project report is prepared for
Faculty of Engineering
Multimedia University
in partial fulfilment for
Bachelor of Engineering

FACULTY OF ENGINEERING
MULTIMEDIA UNIVERSITY
April 2012

Declaration

I hereby declare that this work has been done by myself and no portion of the work contained in this report has been submitted in support of any application for any other degree or qualification of this or any other university or institute of learning.

I also declare that pursuant to the provisions of the Copyright Act 1987, I have not engaged in any unauthorised act of copying or reproducing or attempt to copy / reproduce or cause to copy / reproduce or permit the copying / reproducing or the sharing and / or downloading of any copyrighted material or an attempt to do so whether by use of the University's facilities or outside networks / facilities whether in hard copy or soft copy format, of any material protected under the provisions of sections 3 and 7 of the Act whether for payment or otherwise save as specifically provided for therein. This shall include but not be limited to any lecture notes, course packs, thesis, text books, exam questions, any works of authorship fixed in any tangible medium of expression whether provided by the University or otherwise.

I hereby further declare that in the event of any infringement of the provisions of the Act whether knowingly or unknowingly the University shall not be liable for the same in any manner whatsoever and undertakes to indemnify and keep indemnified the University against all such claims and actions.

Signature: ________________________

Name:

Student ID:

Date:

Acknowledgements

I would like to express my special thanks to my helpful and supportive supervisor, Mr Cheong Soon Nyean, as well as Dr Lim Thong Leng for their patience and willingness to teach and provide me with all the guidance to enable a smooth completion of this project. Their kind effort is greatly appreciated.

My sincere and grateful thanks also go to Dr Yoon Tiem Leong as well as Mr Min Jun Kit from School of Physics, University Science Malaysia (USM) for without their help in providing a computer cluster in USM, knowledge sharing, training and guidance, this project will not be able to proceed smoothly.

I would also like to express my utmost gratitude to the staff of Faculty Of Engineering for their hard work in arranging and preparing the necessary equipment and location for presentation and other things required to complete this course. Last but not least, I would also like to thank my parents and friends for the support they provided.

Abstract

As we all know, as time goes by, scarce natural resource such as petroleum will continue to decrease as daily demand for such resources are ever increasing. Therefore it is important that other alternative source of energy is discovered and research needed to be done on it to further understand it. Among the many alternative, methane (CH4) is one of the alternative which can be commonly found in our environment in area such as swamp, landfill and many others. Methane despite being rather common, its phase transitions are still not too well known. Many researches have been carried out for pure methane as well as other variation of it. In this project however, it will only focus on the different phases of methane detectable using molecular dynamics simulation by using an open source software called LAMMPS. There are two sets of simulation done in this project. The first set involves simulation of methane with constant pressure and varying temperature while the second set involves simulation with constant temperature and varying temperature. From the simulation, it is found that the data obtained is similar to that obtained in previous research and simulation. When pressure is made constant at 100MPa and the temperature is increase, transition from phase III to II happen at 17°K, phase II to I at 27°K and reaches its melting point at 118°K. As for the setting of 300MPa constant pressure, Phase IV to III transition took place at 29°K and phase III to I at 39°K. It reaches melting point at 157°K. Transition from phase IV to V took place at 29°K follow by phase V to IV at 79°K, Phase IV to B at 94°K, while transition from phase B to A happens at 113°K and lastly from phase A to I at 128°K are the transitions detectable when pressure is set at a constant of 2000MPa with increasing temperature. When constant pressure of 20GPa is used, the only detectable transition took place at 241°K from phase HP to B. When temperature is fix at 130°K and the pressure is increase from 1MPa to 30GPa, transition from liquid to phase I took place at 175MPa, Phase I to A transition took place at 1994MPa follow by phase A to B at 2904MPa and entering HP phase at 10167MPa. As for temperature being set at 165°K, liquid to phase I transition happen at 252MPa follow by phase I to A at 2550MPa and lastly entering HP phase at 12780MPa. By setting the temperature at 295°K and variying the pressure, it is found that liquid to phase I transition happens at 1392MPa, phase I to A happens at 5042MPa, changing to phase B at 8432MPa and lastly entering HP phase at 22737MPa. The values obtained only differ slightly due to the usage of a different value of forcefield parameters. Thus it is concluded that the forcefield parameters being used is quite accurate. Besides that, simulation also shows that lennard-jones pair potential can

describe the intermolecular interaction of methane molecules adequately. Under high pressure, it is also observable that methane still maintains it solid form.

Table of Contents

LIST OF FIGURES

LIST OF TABLES

CHAPTER 1: INTRODUCTION

As time goes by, the availability of natural resources such as petroleum will continue to decrease with the increase in daily usage. Therefore it is important that alternate source of energy needs to be discovered and utilize so that when petroleum runs out, our daily activity will not be affected drastically. Methane is one of the alternatives to fossil fuel and it can be found commonly.

1.1 Objective

Methane being a simple and commonly found molecule has a different phase under different influence of pressure and temperature. Its phase transition is not well known. Therefore in this project, it is aimed to study the phase transition of methane under pressure with the usage of molecular dynamics. Two types of simulation will be done. The first type involves making the pressure constant while varying the temperature and the second one involves varying the pressure while maintaining the temperature constant.

1.2 Motivation

Molecular dynamics simulation offers a variety of tools to study the material of interest. Properties of material such as phase transition, diffusivity as well as the heat capacity can be simulated with the help of molecular dynamics. No doubt that phase transition is hard to determine due to a strong hysteresis in the physical quantity. However at phase change, there will be a sudden increase of potential energy and the volume of the material. These changes will provide the information needed to determine the melting and boiling point of a material. With molecular dynamics simulation, cost of research or experiment of new material or under extreme environment can be reduce as properties of material can be studied without performing the full experiment in the lab. As molecular dynamics is suitable to study static and dynamic system and it provides acceptably accurate result, therefore for this project is has been chosen as the method being used.

The motivation behind this project is to study the different behavior of methane's phase when under the influence of high pressure as well as various temperature. It will provide further understanding about this commonly found material and it is possible with a better understanding of it to come out with possible modes for transportation and storage of methane since it is an alternative source of energy.

CHAPTER 2: BACKGROUND THEORY

2.1 Methane

Methane is a form of colorless and odorless gas widely obtainable in our planet's natural environment. Naturally, methane is form when organic compounds are decomposed under anaerobic condition by bacteria commonly occurring near swamps as well as wetlands and landfills [1]. Since it is a byproduct of decaying organic material, therefore methane is a form of renewable resources. It is also a main component in natural gas consisting of an estimate of 75% of it, 15% made up of ethane and the remaining 5% was form from other hydrocarbons such as butane and propane [1]. It is usually found together with petroleum and it undergoes processing to separate methane from other hydrocarbons. Besides that some non hydrocarbon gases found inside natural gas must also be filtered before it is being distributed. Methane consists of one single carbon atom and four hydrogen atoms. Its molecule is arrange in such a manner where the carbon atom is in the center surrounded by four hydrogen atoms thus forming a tetrahedral structure as shown in Figure 1.

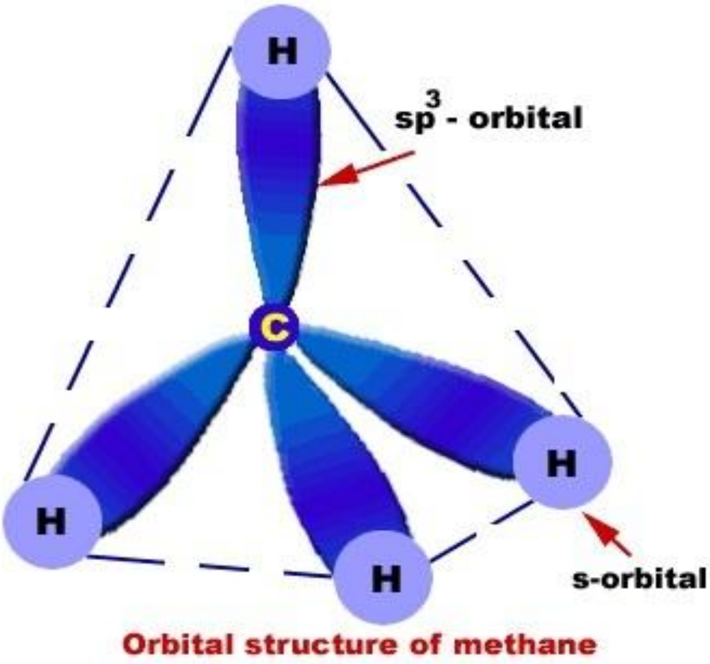

Figure 1: Orbital structure of methane

The bonding between the hydrogen atoms with the carbon atom forms an angle of 109.5^o between each other as shown in Figure 2 bellow.

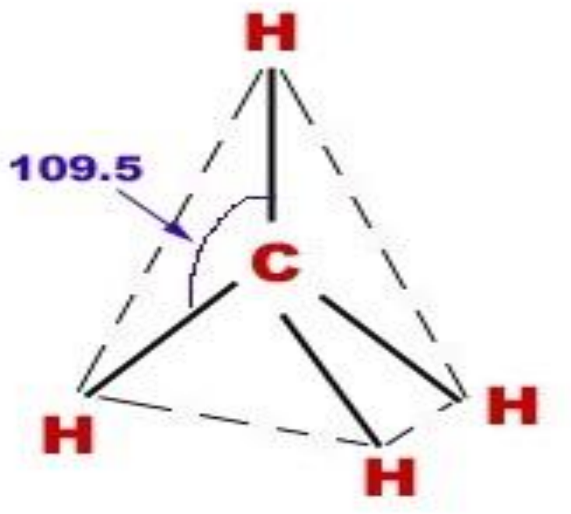

Figure 2: Bonding angle of methane

It has a molecular formula of CH_4 as well as a molecular mass of 16 [1]. Methane is a non-polar molecule which is insoluble in water due to the fact that there is no separation of charge during the formation of its covalent bond therefore no positive and negative poles are form. In order to dissolves methane, a non-polar solvent such as alcohol or carbon tetrachloride can be used. Methane is also a non-toxic gas. However it can cause suffocation when inhaled due to the reduction of concentration of oxygen taken in.

Generally under normal atmospheric pressure and room temperature, methane appears in a gas phase and it has a melting point of -182.5 ^{o}C and a boiling point of -169.5^{o}C. It is lighter than air when in gas form. Methane is easily combustible and it is an exothermic reaction which release a large amount of energy in terms of heat as well as water and carbon dioxide when sufficient oxygen is provided ($CH_4 + 2O_2 \rightarrow CO_2 + 2H_2O$) thus its wide application as an energy source in both domestic and industrial sector. It is also used to generate electric power. However a higher concentration of it in the air can cause explosion therefore commercial natural gases are added with organic sulphur compound such as dimethyl sulphide ($CH_3{-}S - CH_3$) to provide an easily detectable odour in case of any leakage.

For commercial purposes, methane is synthesized by heating carbon and hydrogen mixture [1], via the reduction process or by distillation of bituminous coals which are coals containing more than 15% volatile material. In other words, it is the amount of mass which is vaporized when the coal is heated to a temperature of 900 ^{o}C without the presence of air. It can also be created by the heating of sodium hydroxide and sodium acetate $CH_3COONa + NaOH \rightarrow CH_4 + Na_2CO_3$. Methane is also a raw material in the chemical industry for manufacturing methanol (CH_3OH), chloroform (CH_3Cl) as well as few other chemicals. Methane also reacts with chlorine and fluorine under the exposure of ultraviolet light and substitution process takes place. This reaction is also known as halogenations in which the hydrogen atom in methane is replaced with another halogen atom for example: $CH_4 + Cl_2 \rightarrow CH_3Cl + HCl$ which produced chloro methane. Besides the chemical industry, methane is also used in shoe polish, tyre manufacturing and many more.

2.2 Computer Simulation

Computer simulation is carried out in order to further understand the properties of a cluster of molecules in various aspects such as their structure as well as the microscopic interactions which happens between those molecules [2]. This allows us to learn something new in which we might not be able to find out in terms of normal experiment. It helps by acting as a link between the real laboratory experiment environment and the microscopic environment of the test molecules. Molecules' interaction can be predicted to certain accuracy with the computer resources as the main limitation. Simulation using computer also allows a theory to be tested using the same model as the real experiment. Result obtain via simulation is then compared with the results obtain using real experiment to confirm the accurateness of the theory. Computer simulations also allows experiments to be done on molecule systems under extreme conditions which most likely is difficult to be carried out in real experiments such as under conditions of extreme temperature of pressure [3]. There are two main families of simulation techniques available namely molecular dynamics (MD) as well as Monte Carlo (MC) [4].

2.3 Monte Carlo (MC)

Monte Carlo simulation method imposes on the system under test with relatively large motions to determine the feasibility of the altered structure's energy at the simulated temperature rather than determining incremental atomic motions via evaluating forces [5]. Instead of evolving smoothly through time, the Monte Carlo system jumps from conformation to conformation in an abrupt manner. This method of simulation only placed importance of the relative energy of the conformations before and after the jump therefore it can traverse barriers of system while ignoring it. Besides that, this method cannot provide time dependent quantities due to the fact that the sampling of conformation space is obtain without a realistic dynamics trajectory. When sampling of many system configurations is important, in terms of estimating the average thermodynamics properties, Monte Carlo method may be much better compare to Molecular Dynamics method. An example of the method in which Monte Carlo simulation runs is as shown in Figure 3.

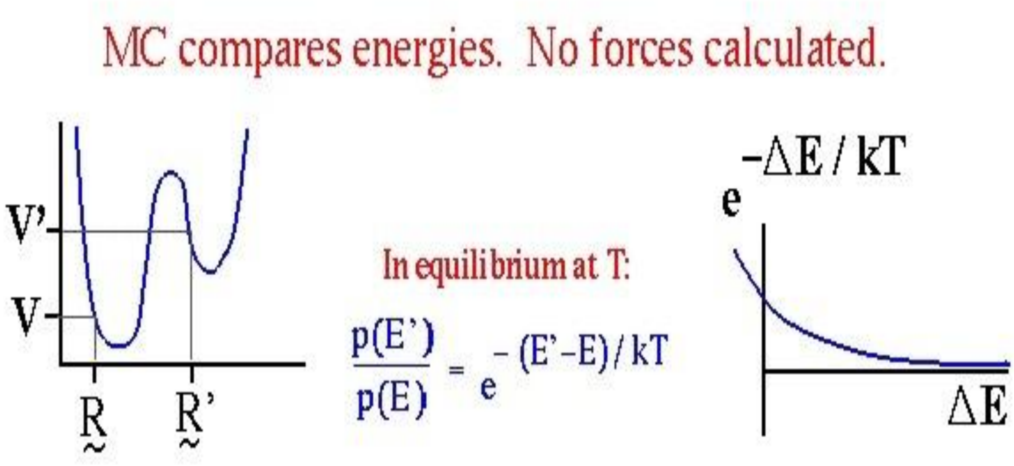

Figure 3: Explanation of how MC method samples data

2.4 Molecular Dynamics (MD)

Generally, prediction of structure from sequence as well as protein folding pathway modeling are not done using Molecular Dynamics simulation as this method usually begins where experimental structure determination leaves off. In molecular dynamics simulation each atom is assigned an initial velocity follow by applying Newton's laws to propagate the system's motion through time at the atomic level, motion of particles which forms the investigated system are then numerically integrated using Newton's classical equations of motion where r_i represents the position vectors while the forces acting upon the N particles in the system is represented by F_i [4].

$$m\frac{d^2 r_i}{dt^2} = F_i(r_1, r_2, \dots, r_N), \qquad i = 1, 2, \dots., N \quad (1)$$

For a system with specific geometric arrangement of particles, the forces derive from potential functions can be represented as in below.

$$F_i(r_1, r_2, \dots, r_N) = -\nabla_{r_i} U(r_1, r_2, \dots, r_N) \quad (2)$$

From the conservation of energy, this implies that the total amount of energy in the system $E = E_{kin} + U$, in which the instantaneous kinetic energy is E_{kin}. Without any influence from external forces, the potential function can be further simplified and represented as a summation of pairwise interactions between the atoms given by:

$$U = \sum_{i=1}^{N} \sum_{j>i}^{N} u(r_{ij}) \qquad (3)$$

Where $r_{ij} = r_i - r_j$. In order to avoid redundant particle pairs, it is made that j > i. In order to reduce computational effort, beyond certain cut off limit, the inter pair potential is assume to be negligible.

2.4.1 Lennard-Jones potential

For the interaction potential between a pair of atoms having Van Der Waals intermolecular force, the most popular model used is the Lennard-Jones potential which was initially proposed for liquid argon. Lennard-Jones potential is given by:

$$u_{LJ}(r_{ij}) = 4\varepsilon\left[\left(\frac{\sigma}{r_{ij}}\right)^{12} - \left(\frac{\sigma}{r_{ij}}\right)^{6}\right] \qquad (4)$$

The ε parameter represents the strength of the interaction and the length scale is given by σ. At short distances, the LJ potential is strongly repulsive with the term $\left(\frac{\sigma}{r_{ij}}\right)^{12}$ dominating in which it models the repulsion between atoms being brought very close together. This phenomenon can be supported by relating it to Pauli principle which stated that when there is a start of overlap in the electronic clouds surrounding the atoms, the energy of the system will increase rapidly. When $r_{ij} = \sigma$, the potential passes through 0. The potential reaches minimum when $r_{ij} \cong 1.1225\sigma$ [4]. The second term $\left(\frac{\sigma}{r_{ij}}\right)^{6}$ starts to dominate at large distance which contributes to the potential exhibiting an attractive tail effect [2] as shown in Figure 4. Due to fluctuating dipoles, the dipole-dipole interaction took place which further gives rise to the Van Der Waals dispersion forces. These forces are those that show the bonding characteristic of rare gases such as argon which represents the closed shell system. However due to the fact that strong localized bonds are formed for open shell systems, the Lennard-Jones potential is inappropriate to be used to represent such systems.

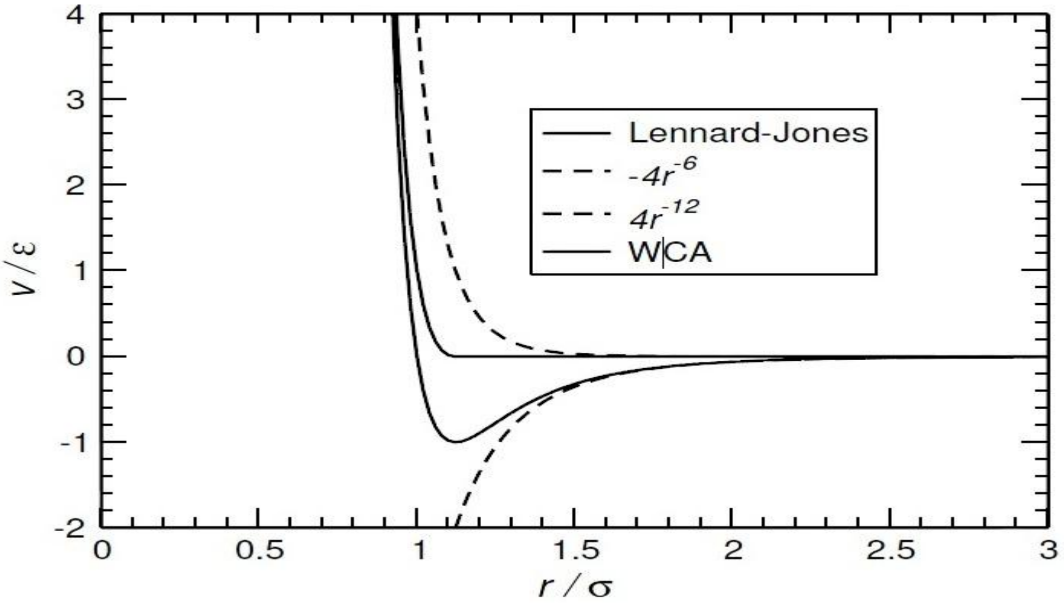

Figure 4: LJ Pair potential showing the value of both the term in the equation

MD units which are a dimensionless reduced unit are useful in modeling fluids with major advantages as below [4]:

- Instead of using small values link with the atomic scale, it enables researcher to deal with mathematical values of the order of one or unity.
- Due to the assimilation of the specification defining the model into units, the equation of motions can be simplified.
- Scaling of the results for an entire class of systems defined with the same model is also made possible

2.4.2 Thermodynamics Properties

The energy and the pressure of a system can be effortlessly asserted by taking into account that both the temperature and the density are independent variables. These values give the connection between both the microscopic and the macroscopic level thus making calculation in molecular dynamics (MD) simulation simplified. In MD simulation, it is noted that the energy is fixed instead of the temperature of the systems. Therefore it is stated that the average temperature should be used instead of temperature itself [4].

Temperature can be express in terms of kinetic energy of the system giving:

$$T = \frac{2k_B E_{kin}}{3N} \; where \; N = numbers \; of \; atoms, k_B = 1 \quad (5)$$

Pressure can thus be obtained for the case of pair potential to be:

$$PV = Nk_B T + \frac{1}{3}\left\langle \sum_{i<j}^{N} r_{ij} . f_{ij} \right\rangle \qquad (6)$$

By taking into account the relationship between kinetic energy and temperature of the system of atoms given by equation (5), the pressure can further be simplified into equation 7.

$$P = \frac{\rho}{3N}\left\langle 2E_{kin} + \sum_{i<j}^{N} r_{ij} . f_{ij} \right\rangle \qquad (7)$$

2.4.3 Time Dependence

In molecular dynamics simulation, assessment of forces in the system is the most tedious work of all. Multiple forces evaluation or time step needed for a process in considered as incompetent. Among the various similar algorithm in which one of the commonly used method is the Verlet Algorithm. The Velocity Verlet algorithm has several advantages namely [4]:

- Energy of the system is maintained
- Better dependability then the predictor corrector method
- Occupy less memory location for the process in comparison with the predictor corrector methods

In this method, the movement of a particle can be express in the terms of interval, t [4]

$$v(t+\Delta t) = v(t) + a(t)\Delta t + O((\Delta t)^2) \qquad (8)$$

$$r(t+\Delta t) = r(t) + v(t)\Delta t + \frac{1}{2}a(t)(\Delta t)^2 + O((\Delta t)^3) \qquad (9)$$

The predictor corrector methods is seldom used as it is a multiple value method involving many previous time step's output values in which the step size cannot be modified easily or it involves higher derivatives which requires additional computations and memory allocation.

2.4.4 Periodic Boundary Conditions

The way finite systems behaved is vastly different when compare with that of an infinite or relatively massive systems. The number of particles involve in simulation of bulk properties for a macroscopic system is important to determine the outcome if a group of atom with well defined number of segments is not being used in the simulation [2]. In comparison with the amount of particles available in a macroscopic system, the number of particles in a large simulated system is still comparatively negligible [2]. For a macroscopic system, the number of atoms located nearby the boundaries of the vessel in which contains the system accounted to only a small fraction therefore the effect of these particles in the vicinity of the wall is assumingly negligible. However the typical size a MD simulation can handle is still relatively small which means that the fraction of atoms near the boundary is very significant to the extent where the behavior of the system would be dominated by the surface effect. In this case, if the surface effects are not of particular interest, the best way to solve the problem is to use the periodic boundary conditions in which it could both resolve the problem of a finite system size as well as reducing the surface effect to its minimum. By using such conditions, we enclosed the particles in a box and surround that box with replicas of it which is translated in all three directions on the Cartesian graph. The particles in the replicas move accordingly with the particles in the original box which is simulated. With the aid of this condition, when a particle exits or enters the region under simulation, the replicated particle enters or exits that simulated region as well thus maintaining the total number of particles in the simulation region as shown in Figure 5. With this, it can be deem that the surface effects are being eliminated and render the position of the boundaries effect less in the simulation [2].

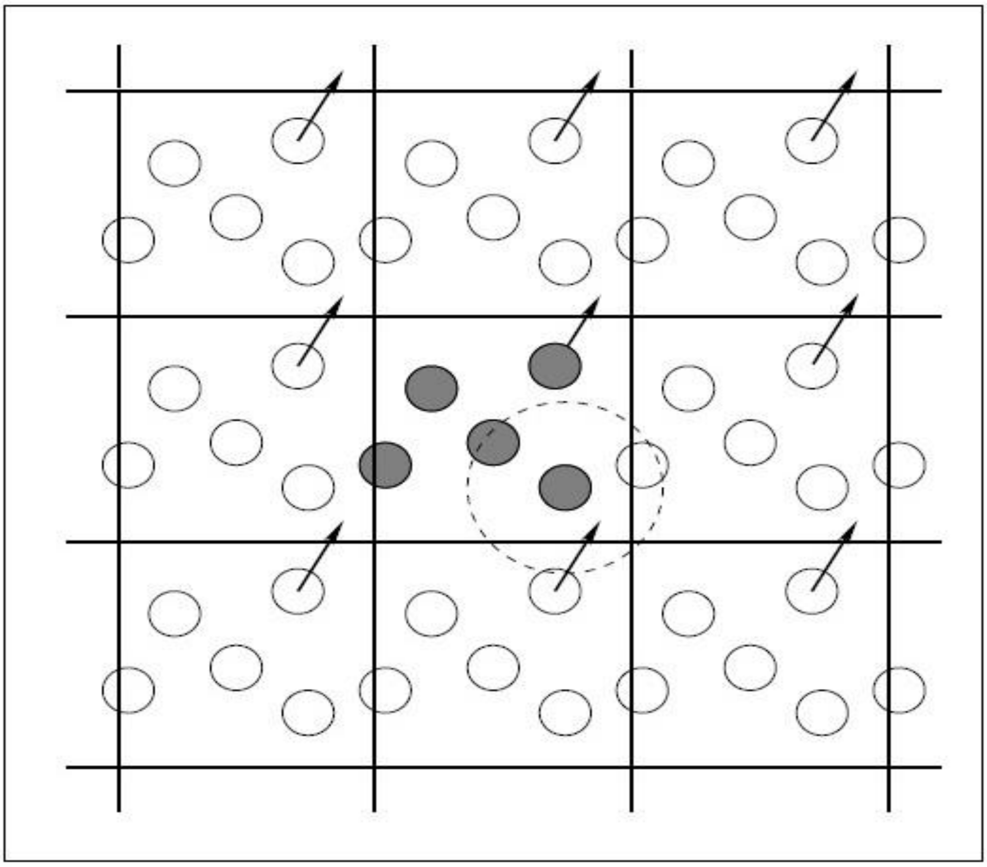

Figure 5: Periodic Boundary Condition showing how a particle in the simulation region leaves the box and the replica's particle entering it.

Due to the usage of the periodic boundary conditions, each of the particles in the region of interest seems to interact with other particles as well as with their own replicas thus making the total number of pairs interacting with each other to increase largely. This unwanted situation can be avoided by using a potential with a limited range in which two particles which is separated by a length exceeding that of the cutoff distance can be neglected. By making the assumption that the size of the box is two times larger than the cutoff distance in all direction, it can be observe that at most one of the pairs formed by the particle in the box with the other periodic replicas of another particle will fall inside the cutoff region thus causing an interaction. This criterion of evaluation is called minimum image criterion which states that only the closest image particle is considered while the rest are neglected as shown in Figure 6.

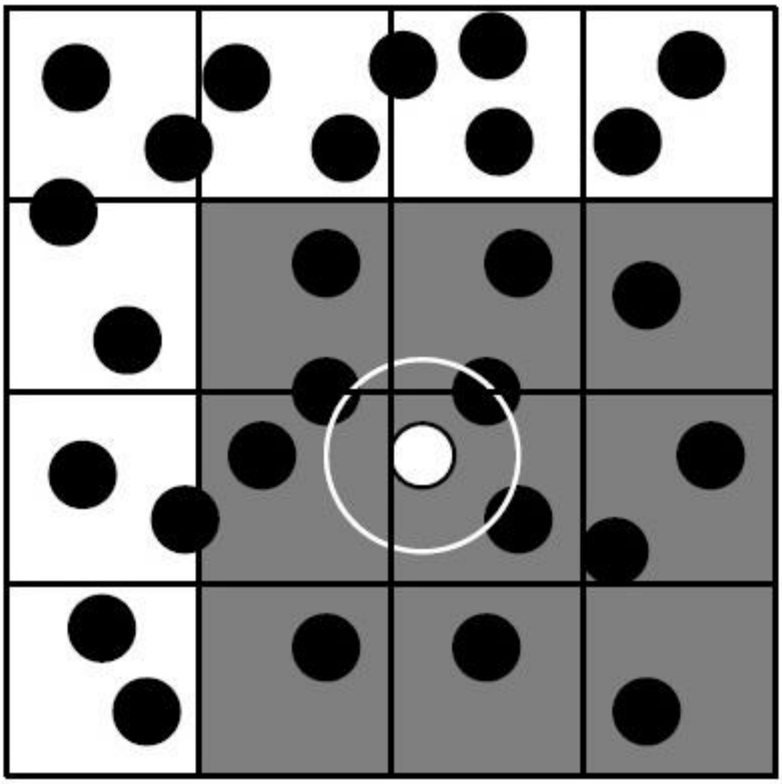

Figure 6: The structure of the box with the atom's cutoff distance shown in white.

After every integration step, the particle's coordinate needs to be examined. In the process, if it is found that a particle have left the simulation area, coordinate readjustment needs to be done to retrieve it back into the interior of the box which is also same as bringing a replicated particle into the region from the opposite boundary. This step is also known as Correcting Particle Coordinates.

CHAPTER 3: PREVIOUS RESEARCH

Various testing of methane were done to discover its phase diagram which is quite complex due to the variation of its orientation disorder and lattice constant of methane molecules at different phases. For low temperature (phase I and II), Neutron scattering experiment [6] as well as optical spectroscopic techniques [7] was done and it was discovered that at phase I methane molecule have a face center cubic structure and being completely orientationally disordered while being partially orientationally ordered in phase II.

The phase transitions from phase I to II, II to III and III to IV propose that there exist for methane different types of structure available for methane. Those phase transition was discovered when various experiments such as NMR [8], Raman spectrum [9], as well as neutron scattering [10] was perform on methane. Under high pressure as well as with a temperature up to room temperature level, Optical studies and IR investigations was done as well to further enhance understanding of the various complex phase of methane. From those experiments done, it was proposed that for methane, when it is in phase III, IV and A, it is tetragonal in nature while it is in hexagonal close packing (hcp) crystal structure during phase V, VI, B and high pressure (HP) phase [11]. In order to understand the phase diagram of methane, many other types of theoretical investigation was done. From those experiments, the phase diagram of methane is plotted as depicted by Figure 7.

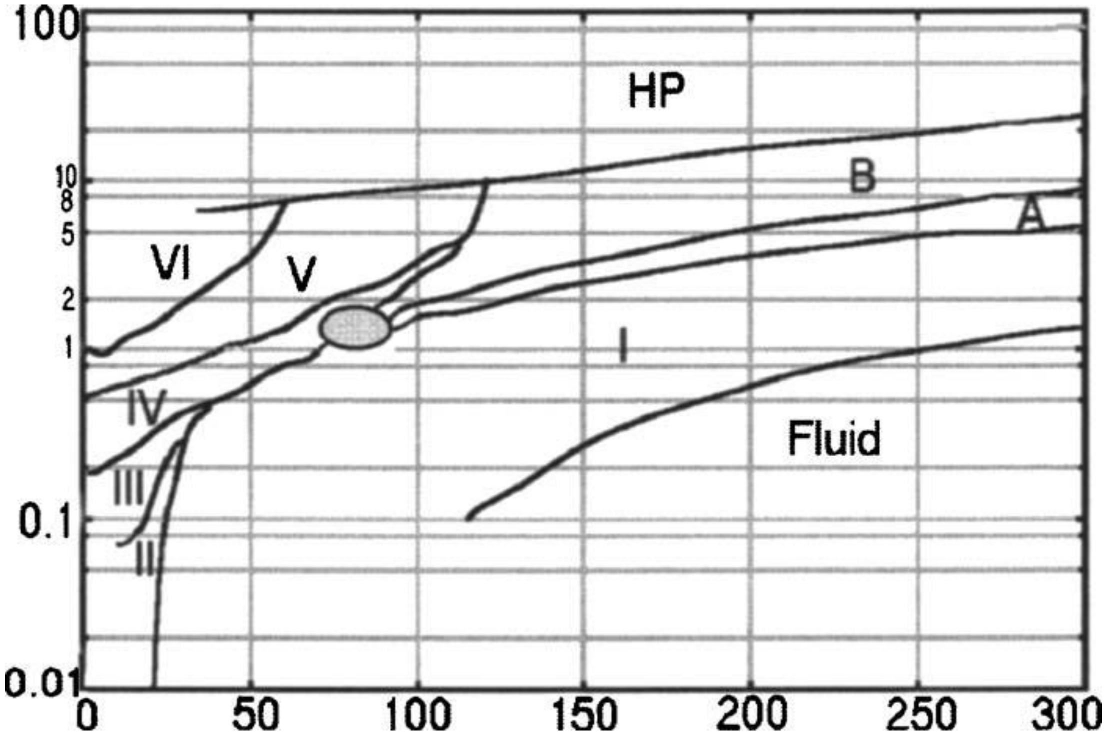

Figure 7: Phase diagram of methane with the Y-axis in the unit of GPa (Giga Pascal) while X-axis in the unit of K (degrees Kelvin)

From the paper Phase transitions of methane using molecular dynamics simulations by S.M. El-Sheikh, K.Barakat and N.M Salem [11], involving 108 and 256 methane molecule system. In their paper, they uses the software MOLDY by Rofson. Phase of methane was distinguish by them by using the forth order cumulant in which a phase transition will be detected when an intersection occurs between the graph of the 2 different size system. The second method being used involves analyzing the caloric curves obtained via simulation in which any changes in the slope of the curves or discontinuity indicates a phase transition. Besides that the translational parameter is used to determine if the phase is in solid or liquid. The rotational order of methane is specified by computing its orientation order parameter. The structure of methane is also determined by calculating the lattice constants of methane. Lastly, the radial distribution function involving the number and distance of nearest and next nearest neighbor is calculated to further justified the type of structure of methane.

There are two parts to the research; the 1st part involves setting the pressure as a constant variable at 100MPa, 300Mpa, 2000MPa, 20Gpa respectively while varying the temperature from 10K to 300K. Simulation on the phase transition of methane under constant pressure as compared with experiment results yields the values tabulated. For the case where pressure is set at 100MPa, it was found that phase transition from phase III to II took place at 29 to 33 K, while at 34 to 38 K transition from phase II to I took place and lastly the melting point is observed at around 121 K as shown in Table 1. An example of caloric curve for the 256 molecule methane at the pressure of 100MPa is as shown in Figure 8.

Table 1: At Pressure=100MPa, the phase transition which took place at temperature K

Transition	**Temperature (K)**	
	Previous Work	**Experiment**
Phase III to II	31 ±2	19
Phase II to I	36 ±2	25
Melting point	121 ±3	115

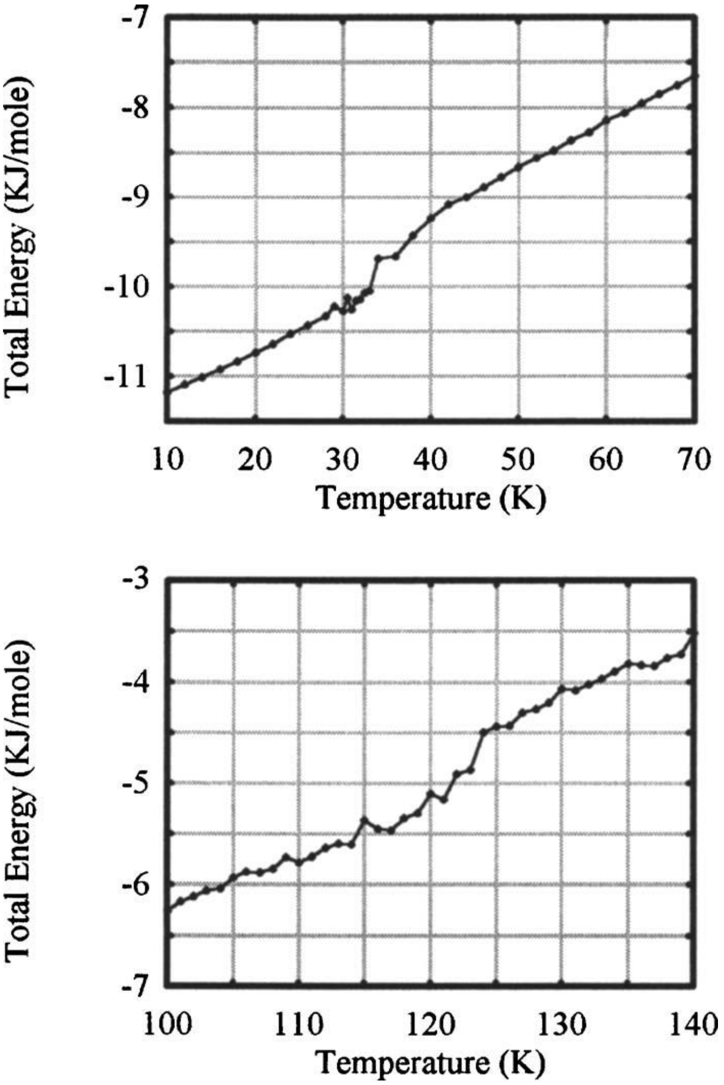

Figure 8: Caloric curves at 100MPa for a 256 molecule methane system

Besides the caloric curves shown above, the forth order cumulant versus temperature at 100MPa which show intersection of the graph as well as an example of translational order parameter and radial distribution function for the pressure setting of 100MPa are as shown in Figure 9, 10, and 11 respectively.

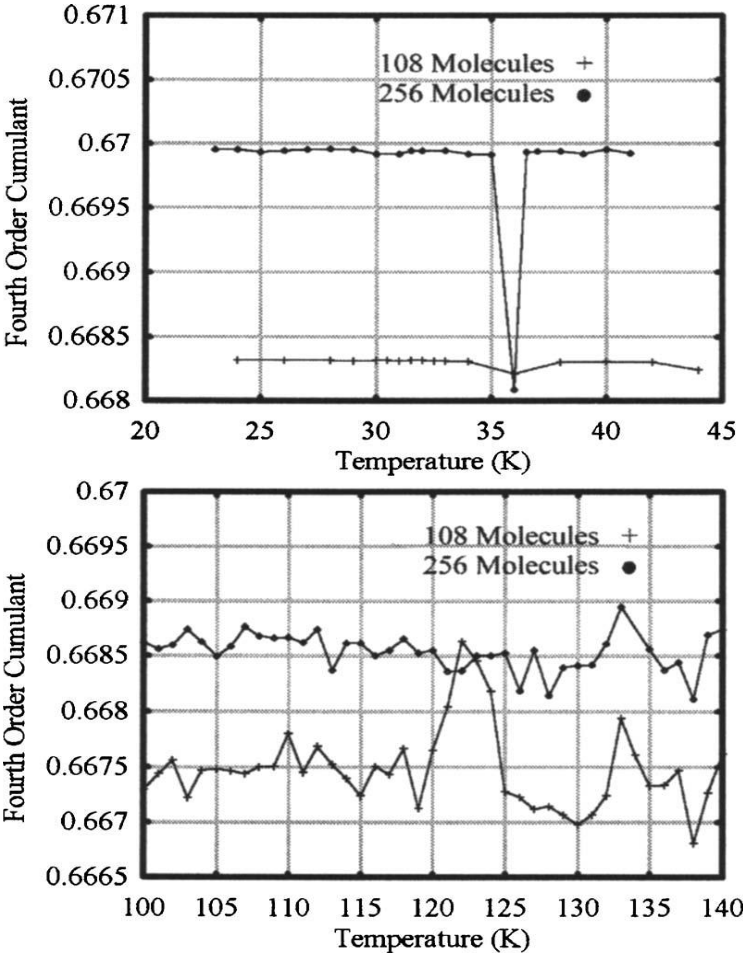

Figure 9: Forth order Cumulant graph at pressure of 100Mpa

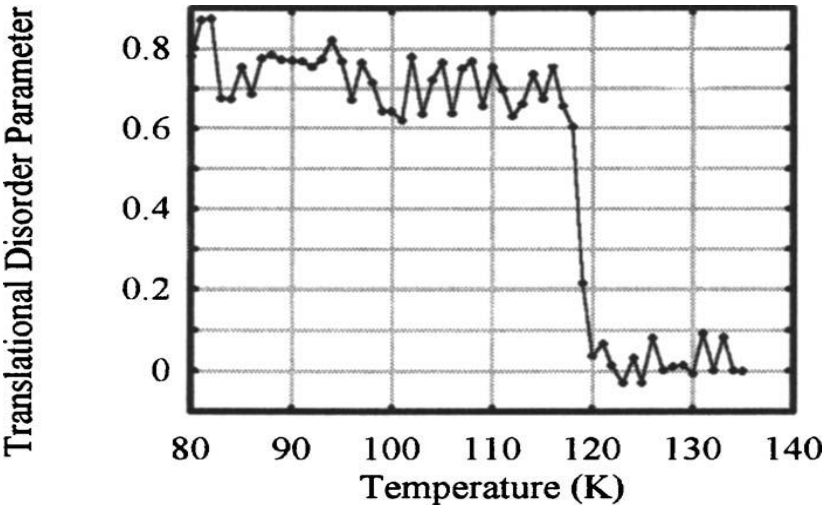

Figure 10: Translational order parameter for pressure setting of 100MPa

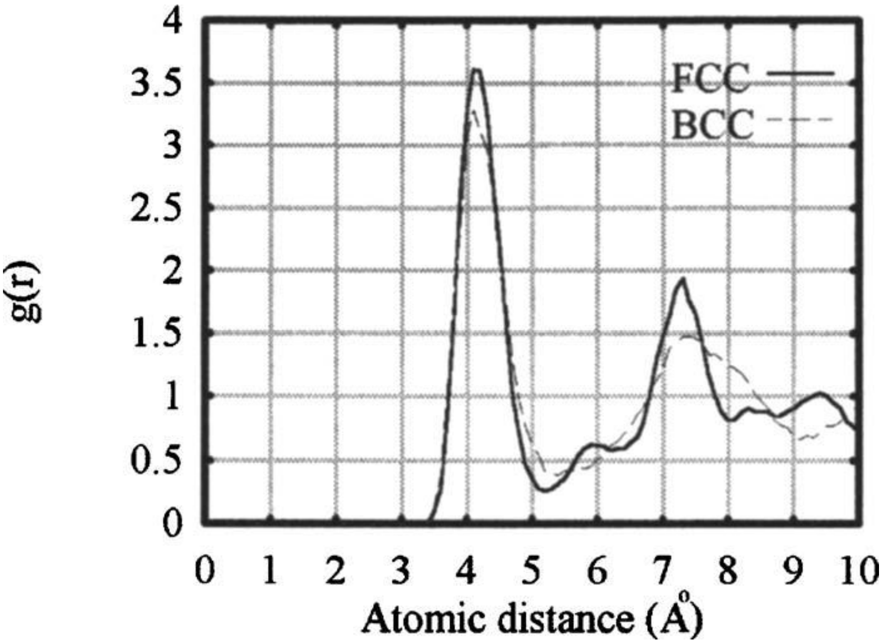

Figure 11: For T=100K and pressure = 100MPa, the radial distribution function of the two system of methane is as shown

For the pressure setting of 300MPa, the temperature in which a phase transition is indicated is as shown in Table 2.

Table 2: At Pressure=300MPa, the phase transition which took place at temperature K

Transition	Temperature (K)	
	Previous Work	Experiment
Phase IV to III	32 ±2	20
Phase III to I	38 ±2	31
Melting Point	161 ±3	155

From the simulation, there is a phase transition from phase IV to III at the temperature around 32 K while phase transition from phase III to I took place at the temperature around 38 K and melting happens between 158 and 164 K.

When pressure is increase to 2000MPa, more phases including those high pressure phases came into play. At the temperature of around 26 K, transition from phase IV to V took place follow by a transition from phase V back to IV at around 82 K. Phase change from IV to B and from B to A took place at around 90K and 110K respectively. Lastly, at temperature around 125 K transition from phase A to I took place as tabulated in Table 3.

Table 3: At Pressure=2000MPa, the phase transition which took place at temperature K

Transition	Temperature (K)	
	Previous Work	Experiment
Phase IV to V	26 ±1	32
Phase V to IV	82 ±2	75
Phase IV to B	90 ±4	92
Phase B to A	110 ±3	107
Phase A to I	125 ±2	128

As for the pressure of P=20GPa, the only detectable phase transition is from HP phase to phase B which happens at around 240 K as shown in Table 4.

Table 4: At Pressure=20GPa, the phase transition which took place at temperature K

Transition	Temperature (K)	
	Previous Work	Experiment
HP Phase to B	240 ±3	260

In the second part of the research, the temperature of the system is set to a constant temperature of 130K, 165K and 295K respectively while varying the pressure of the system from 0 to 30 GPa. Methods of verifying the phase transitions is done similarly as the first part of the research where the fourth order cumulant, caloric curves, translational order parameter, rotational order parameter, lattice constant, radial distribution functions as well as distance between nearest and next nearest neighbors are collected and studied. For the case of constant temperature set at 130K its caloric curves which show a change in its total energy is shown as well by Figure 12(1) and Figure12(2) while the forth order cumulant graph obtained is as shown in Figure 13.

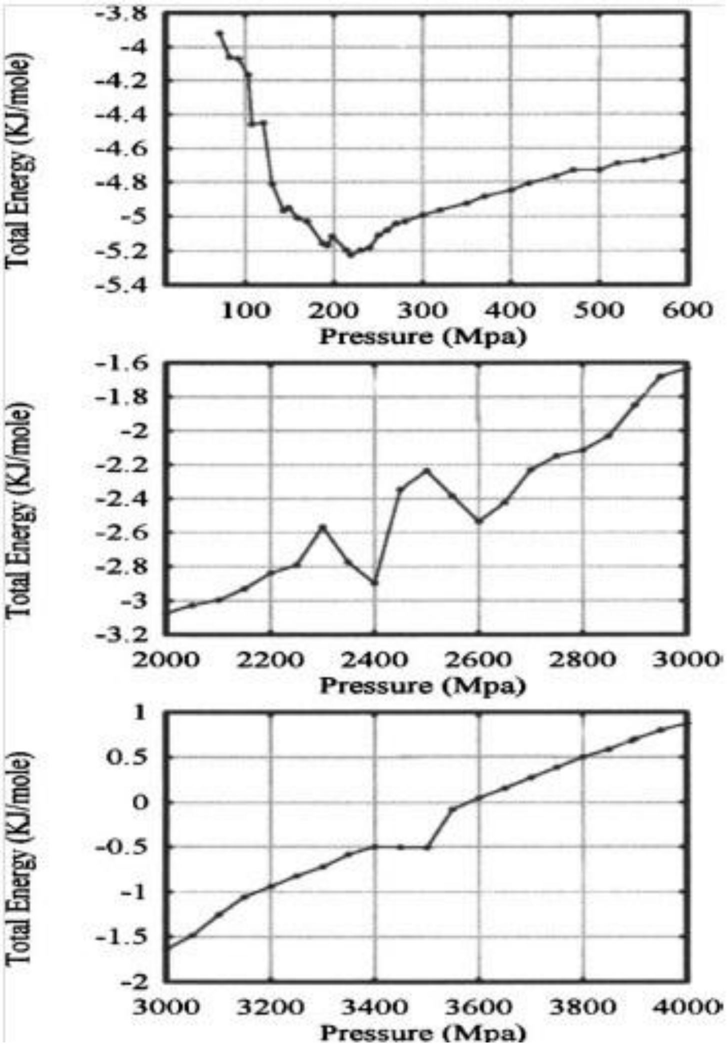

Figure 12(1): Caloric curve for temperature of 130K with varying pressure

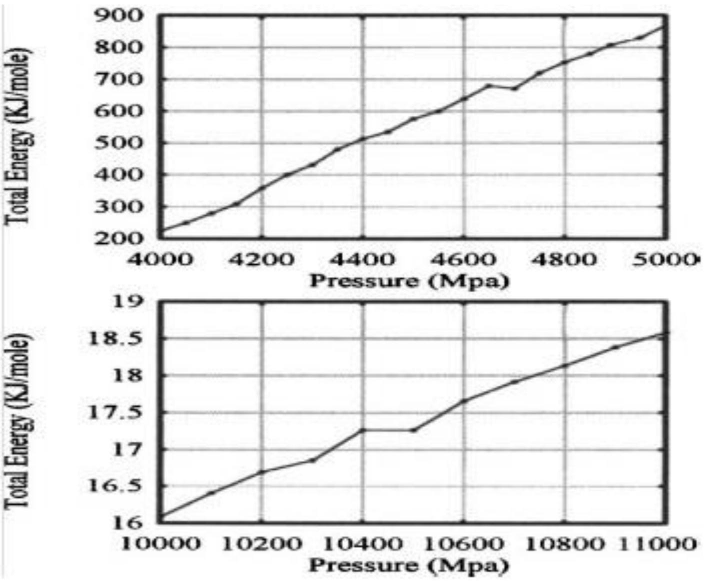

Figure 12(2): Caloric curve for temperature of 130K with varying pressure

The phase transition detected at 130K is as tabulated in Table 5. From the simulation, transition from liquid to phase I took place at around 200MPa while phase I to A happen at around 2400MPa. At 2800±100MPa, phase transition from phase A to B took place. From 3400 to 4800MPa, the methane is in intermediate phases and no obvious transition is detected and the last transition was detected at around 10450MPa.

Table 5: At temperature 130K, the phase transition that took place at pressure (MPa)

Phase Transition	Pressure (MPa)	
	Previous Work	Experiment
Phase liquid to I	200±50	155
Phase I to A	2400±200	2050
Phase A to B	2800±100	2700
Fcc	3600±200	Intermediate Phase
Fct	4600±200	
HP phase	10450±200	10300

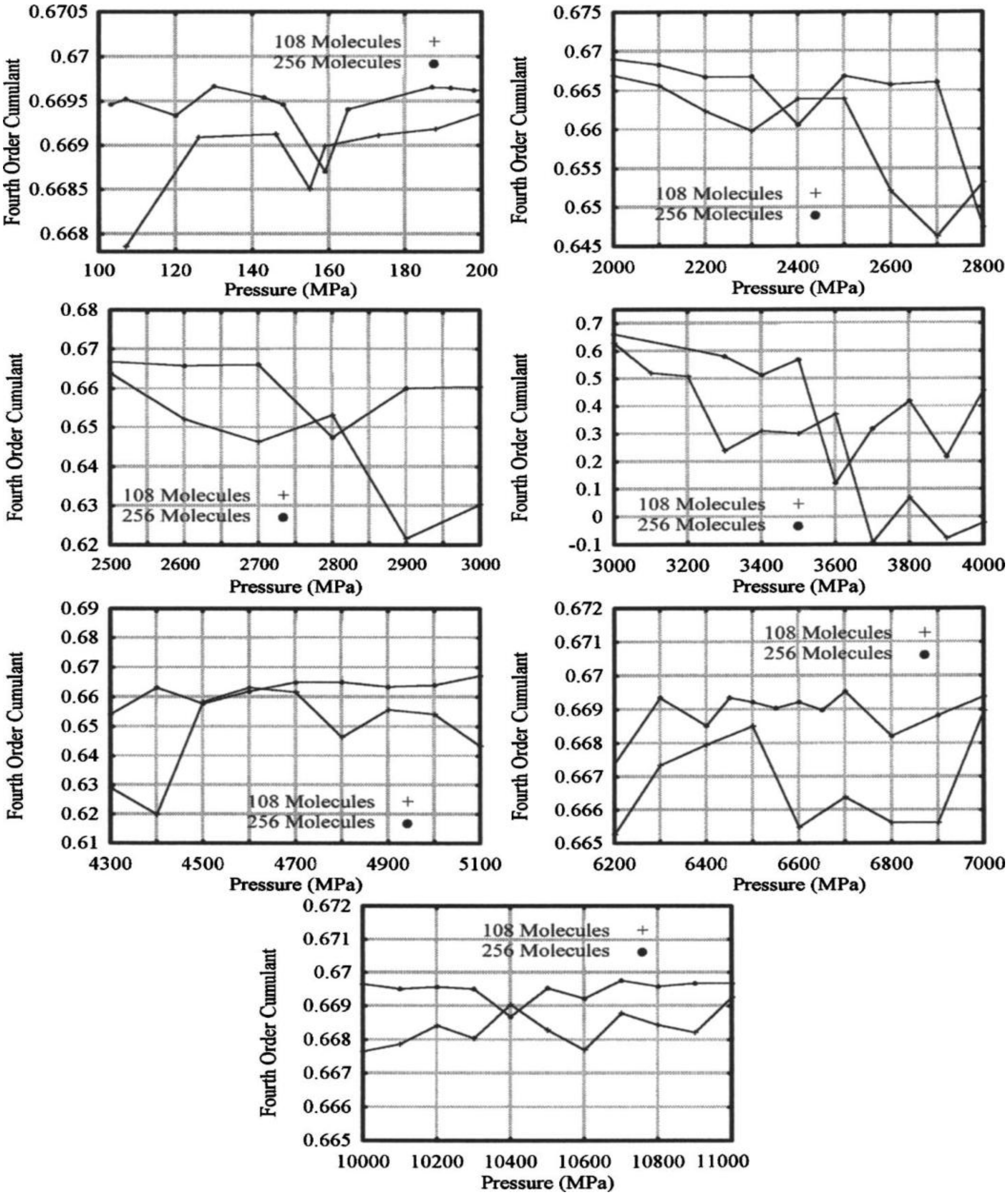

Figure 13: Forth order cumulant graph for simulation with constant temperature of 130k

The transition detected at a constant temperature of 165K is tabulated in Table 6. From the table, it can be observed that for the said temperature, transition from liquid to phase I happens at 242 plus minus 50 MPa. Phase I to A happens when the pressure is at around 3000MPa. Phase transition from A to phase B took place accordingly at 3600±250 MPa. From 4050 to 12250MPa, it is found that the methane is in intermediate phases where it fluctuates between fcc and fct structure. At around 12300MPa the system is in HP phase.

Table 6: At temperature 165K, the phase transition that took place at pressure (MPa)

Phase Transition	Pressure (MPa)	
	Previous Work	Experiment
Liquid to phase I	242 ±50	360
Phase I to Phase A	3000 ±120	2700
Phase A to B	3600 ±250	3700
Fluctuation between fcc and fct	4300 ±250	Intermediate phases
	11700 ±250	
	12000 ±250	
HP phase	12300 ±250	12600

For the case where the temperature is set at 295K, the methane system under test exhibits transitions involving only liquid, phase I, A, B and HP phase as can be observed from its phase diagram (Figure 7, page 17). At the pressure of around 950MPa, the system undergoes transition from liquid to Phase I follow by from phase I to A at the pressure of around 6500MPa. The system enters the intermediate phase at around 7700MPa and changes to Phase B at around 9000MPa. It re-enters another intermediate phase at the pressure range between 9650 to 23000MPa. Finally at the pressure of 23700MPa it changes to the HP Phase. The observations mention above is tabulated in Table 7.

Table 7: At temperature 295K, the phase transition that took place at pressure (MPa)

Transition	**Pressure (MPa)**	
	Previous Work	**Experiment**
Liquid to phase I	950 ±100	1300
Phase I to A	6500 ±400	5300
Fcc	7700 ±300	Intermediate phase
Phase B	9000 ±250	8600
Fluctuates between fcc and fct	9900 ±200	Intermediate phases
	11600 ±250	
	14100 ±250	
	15200 ±350	
	18600 ±400	
	20030 ±400	
	20300 ±300	
	20900 ±300	
	21100 ±300	
	21500 ±300	
	22600 ±400	
HP Phase	23200 ±500	23520

From the values of lattice constant calculated, the lattice parameters of each phase are tabulated as shown in Figure 14 bellow.

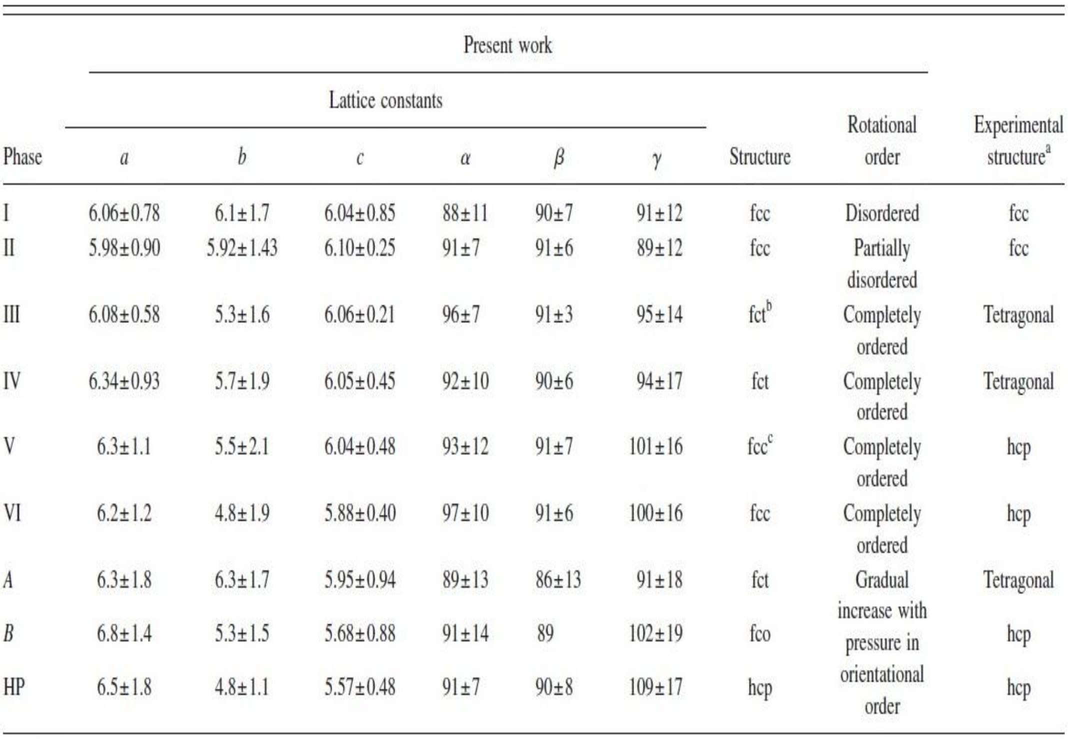

	Present work								
	Lattice constants								
Phase	*a*	*b*	*c*	*α*	*β*	*γ*	Structure	Rotational order	Experimental structure[a]
I	6.06±0.78	6.1±1.7	6.04±0.85	88±11	90±7	91±12	fcc	Disordered	fcc
II	5.98±0.90	5.92±1.43	6.10±0.25	91±7	91±6	89±12	fcc	Partially disordered	fcc
III	6.08±0.58	5.3±1.6	6.06±0.21	96±7	91±3	95±14	fct[b]	Completely ordered	Tetragonal
IV	6.34±0.93	5.7±1.9	6.05±0.45	92±10	90±6	94±17	fct	Completely ordered	Tetragonal
V	6.3±1.1	5.5±2.1	6.04±0.48	93±12	91±7	101±16	fcc[c]	Completely ordered	hcp
VI	6.2±1.2	4.8±1.9	5.88±0.40	97±10	91±6	100±16	fcc	Completely ordered	hcp
A	6.3±1.8	6.3±1.7	5.95±0.94	89±13	86±13	91±18	fct	Gradual increase with pressure in orientational order	Tetragonal
B	6.8±1.4	5.3±1.5	5.68±0.88	91±14	89	102±19	fco		hcp
HP	6.5±1.8	4.8±1.1	5.57±0.48	91±7	90±8	109±17	hcp		hcp

Figure 14: Lattice Constant of different phases of methane

CHAPTER 4: METHODOLOGY

4.1 System Design and Planning

Before implementation of the project, the molecule system of the methane which will be use as part of the input file for the project is design using crystal maker. Crystal maker is a product by Crystal Maker Software Ltd. It focuses on productivity as it allows the user to drag and drop the data files into it and an instant display will be generated by the software in a realistic manor. This software also allows the user to build their required molecular or crystal structure using the information about the material such as its space group to generate bonds among atoms or molecules. Graphical representation available in the software allows extensive view of the generated software. Upon completion of the molecule generation, measurement to the bonding length and bonding angle can be measured as well to verify that the generated output is consistent with the theoretical model [12]. For this project, in order to build a bulk cell of methane molecule, a single methane molecule is first design follow by creating a single cell unit of the bulk methane and finally the bulk methane structure containing 1437 molecules of methane is build up by replicating the single unit cell. The method to build the methane is via coordinate system in which the individual coordinate of the atoms inside a methane molecule is defined and the bond type is added. Once the bond type is defined and the structure is complete, the output file containing the molecule’s coordinate as well as its parameters is generated and it will be used in the next step of this project. Figure 15, 16 and 17 shows a single methane molecule, a single unit cell of methane molecules in face center cubic arrangement as well as the bulk system of the methane molecule respectively.

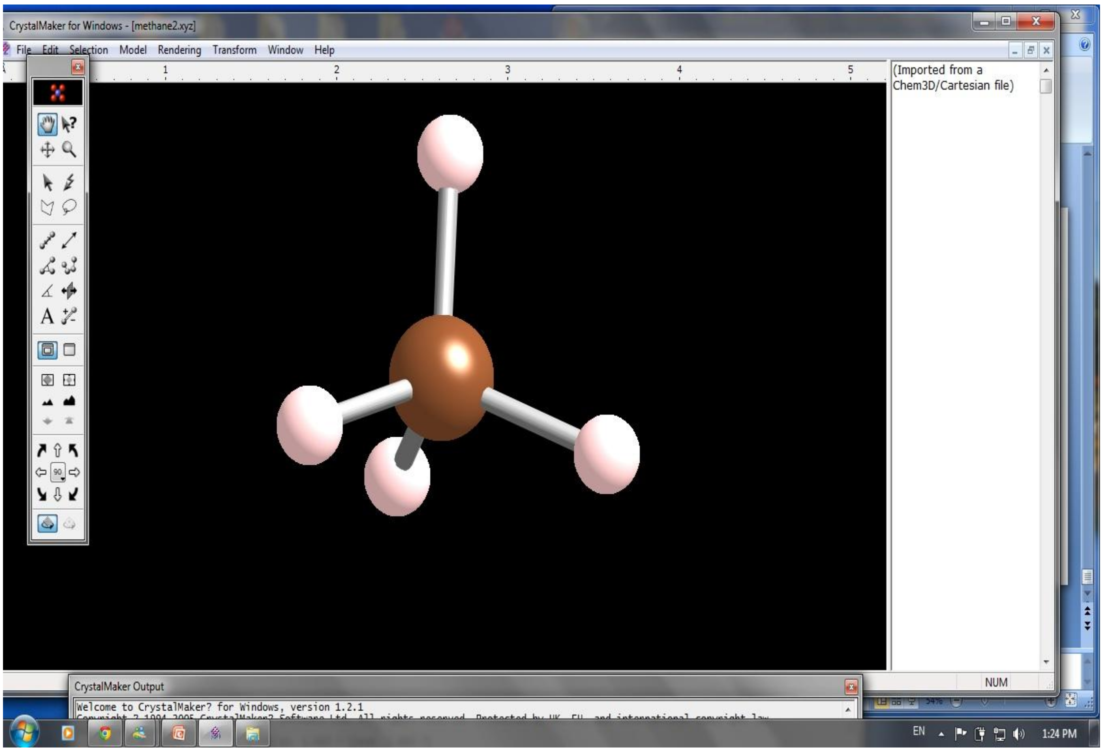

(Imported from a Chem3D/Cartesian file)

```
Welcome to CrystalMaker? for Windows, version 1.2.1
```

Figure 15: Single methane molecule

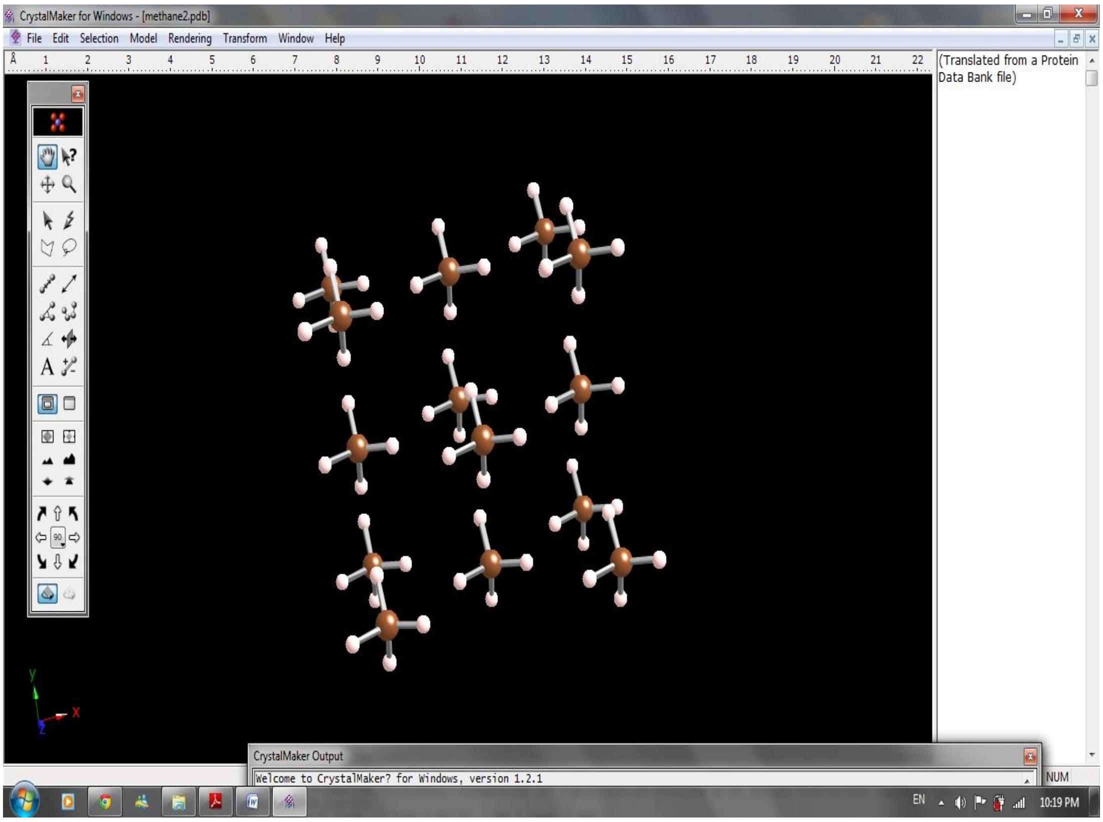

(Translated from a Protein Data Bank file)

```
Welcome to CrystalMaker? for Windows, version 1.2.1
```

Figure 16: single unit cell of methane molecules in FCC arrangement

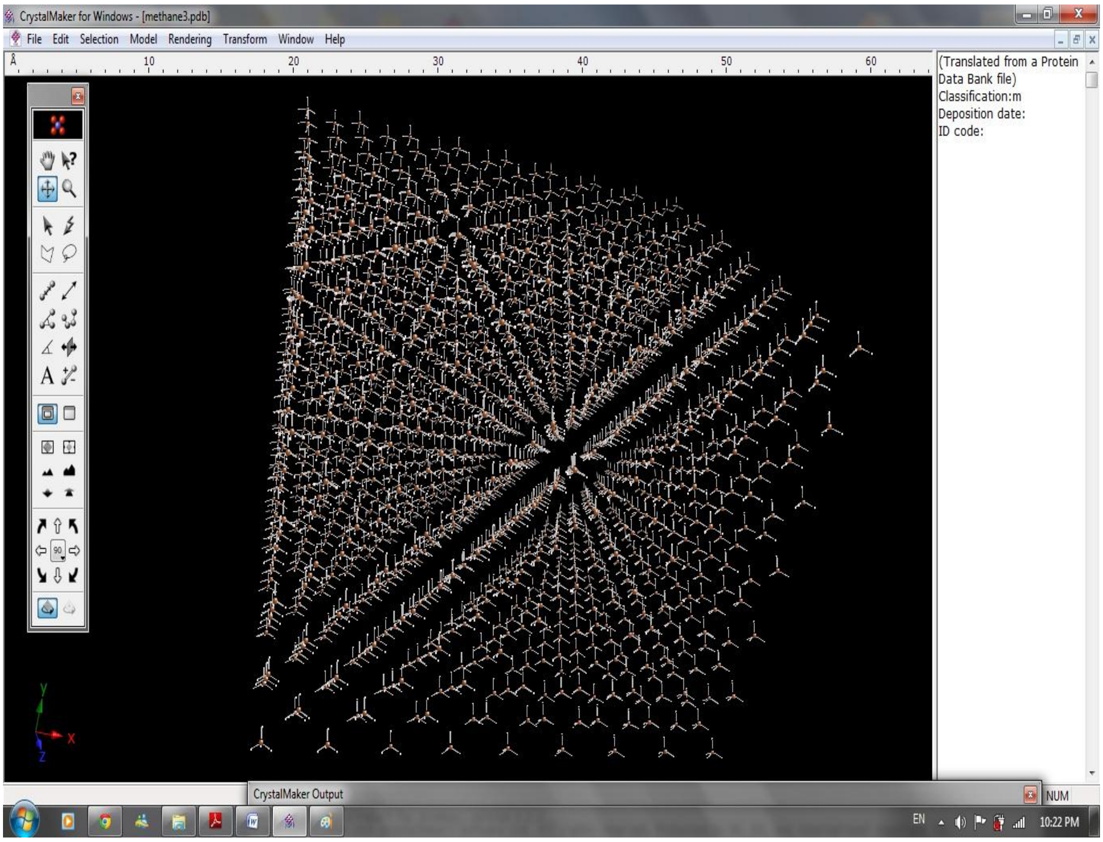

(Translated from a Protein Data Bank file)
Classification:m
Deposition date:
ID code:

Figure 17: Bulk system of the methane molecule

4.2 Implementation and simulation

In this phase of the project, the simulation will be performed. But before that, the software used which is LAMMPS needs to be install in a Linux environment. LAMMPS (Large scale Atomic/Molecular Massively Parallel Simulator) is a open source software distributed by Sandia National Labs under the GNU Public License which models a system of particles in its different state namely liquid gas or solid using classical molecular dynamics code. Modeling of different systems such as atomic, biological, metallic, polymeric etc with different types of force fields and boundary condition imposed is possible with this software. With the help of C++ compilation as well as MPI message passing library support, LAMMPS can perform well in parallel computers [13]. However it can also perform in an acceptable speed on single processor machines. It can be used to model systems ranging u to millions or billions or molecule or atoms by integrating Newton's equation of motion with a variety of initial and boundary conditions and it uses a neighbor list to allow it to avoid lost of particle during the course of simulation. The reason as to the selection of LAMMPS as the software to implement this project can be summarize into the points given below [13]:

- Runs well on both single processor or parallel
- Distributed memory message passing parallelism (MPI)
- For parallelism it uses spatial-decomposition of the simulated domain
- It is a open source distribution
- Portable due to usage of C++
- Capability of using optional library such as MPI and FFT (single processor)
- Many of its code features are also supported by OpenMP, CUDA and OpenCL
- New features and functionality of LAMMPS can be added in easily
- Input script is use to run the software
- Usage of variables, formulas, looping and breaking out of loop have well define syntax

Upon completion of installation, an input script needs to be written to allow the lammps software to execute the commands line by line. LAMMPS execute molecular dynamics simulation to investigate the changes that took place in methane under the influence of changing temperature as well as pressure. Upon completion of the simulation, an output log file will be process to obtain the data and a trajectory file will be use to observe the outcome of the simulation using a software called VMD (Visual Molecular Dynamics).

4.2.1 Initialization

Before the script can be written, the initial configuration of the system need to be obtained or determined by means of literature research or by conducting experiment. In LAMMPS, the dimensionality, boundary condition, atomic positions, time steps, unit cell and simulation box size needs to be tuned.

The initial settings for both parts of the experiment are as describe bellow. The units are set to real [14], which means that the quantities specified in the input script as well as the output values of the simulation is set to real where energy is in terms of $Kcal/mole$, temperature in terms of degrees K and pressure is measured in atmospheres [13]. The boundary conditions are set in periodic mode in all Cartesian direction. The atom style of the system is set to full in which the bonds and angles involved both molecular and charge which is suitable to describe organic molecules.

4.2.2 Implementation of Force Field

The interactive potential of a system needs to be defined as well. Therefore it is important to choose a suitable empirical potential as a function of time. Among the available choices, the force field which is implemented for this project is the Lennard-Jones potential with coulombic cutoff [14]. An example of other types of force fields available to describe molecular structure is as shown in Figure 18. The potential parameters of the system are set as such, both the bond style and angle style is set as harmonic. For the bond coefficient, the bond strength is set at 340.0 and the bond length is set at 1.09 Armstrong between carbon and hydrogen atoms while for the angle coefficient it is set at 33.0 with an angle of 107.8 [14].

The pair coefficient between two carbon atoms is set at 0.66 Armstrong for the Lennard-Jones cutoff and 3.5 Armstrong for the coulombic cutoff. Similarly, the pair coefficient between two hydrogen atoms is set to 0.03 and 2.5 respectively.

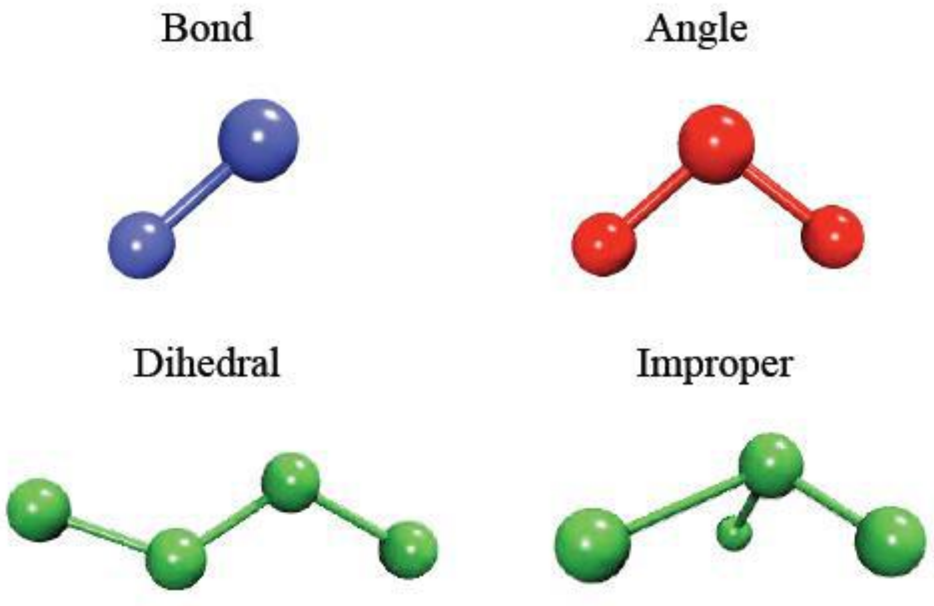

Figure 18: Force Fields used in molecular structure

4.2.3 Assigning Ensemble and performing simulation

Before the simulation can be done, the process of thermalization needs to be done to ensure that the system is in thermal equilibrium or in other terms, being at a state where the energy of the system is at its minimum. To achieve this, ensemble needs to be implemented. Usually for this purpose, micro canonical ensemble (NVT) is used where the system runs at constant volume, temperature and molarities. Time integration is done on the Nose-Hoover style non-Hamiltonian equation to generate position and velocities. After that the simulation is done using canonical ensemble (NVE) where the system runs at a constant molarity, energy and volume.

For this project, there is two parts to it. The first part involves the constant pressure simulation while the second part involves the constant temperature simulation. For both the simulation, the NVT ensemble is used to minimize the energy of the system by invoking and executing the command “nve” in LAMMPS. Next, the energy of the system is further minimize by calling the function “minimize” follow by using a langevin thermostat to dissipate the remaining “hot spot” in the system for 10000 time steps. After executing the preliminary energy minimization of the system, the simulation can be started.

4.3 Constant pressure simulation

For the simulation in which constant pressure is involve, the NPT isobaric ensemble is first used to increase the pressure from 0.00001 atm to the desired pressure namely 100MPa, 300MPa, 2000MPa, and 20GPa which in atmosphere units are 986.92326 atm, 2960.76980 atm, 19738.46534 atm, and 197384.6534 atm respectively using 10000 timesteps. Once the required pressure is achieved, the simulation continues by maintaining the desired pressure using the NPT isobaric ensemble while increasing the temperature from 1 degrees Kelvin to 300 degrees Kelvin using 50000 timesteps. In the meanwhile, the program is also set to output a trajectory file in which it allows the changes in the molecule to be observed via VMD.

Upon completion of simulation, the output file will be used for analysis. In order to obtain the caloric curves of the system, the total energy of the system at the output of each timestep is plotted against temperature. From the caloric curve plotted, any obvious disturbance on the continuity of the curve can be determined as a change in the phase of methane. Besides that, the volume versus temperature graph is also plotted to observe if any changes to the volume of the system which will indicates a change in phase. Lastly the radial pair distribution function will also be obtained to determine the phase of the methane under simulation. Radial pair distribution [15] [16] can be calculated by the equation:

$$g(r) = 4\pi\rho r^2 \delta r$$

Where r is the radial distance, $\rho = \frac{N}{V}$ where N is the total number of atoms and V is the volume of the model and g(r) represents the possibility of finding an atom in a δr shell at a distance of r from another atom.

The Binder fourth order cumulant and the translational order parameter is not being use during the analysis of the results in this simulation because it requires extensive understanding of chemistry involving order parameters, director vectors, lattice states and many others.

4.4 Constant temperature simulation

As for the simulation where constant temperature is needed while the pressure is being varied, after the preliminary energy minimization is done, the system's temperature is bring to the desired temperature by using the NVT command and running it for 10000 timesteps. The temperature being use is at 130 degrees Kelvin, 165 degrees Kelvin, and 295 degrees Kelvin respectively. Once the desired temperature is achieved, the system's pressure is being varied from 1atm to 296076.9801atm (30GPa) using the NPT isobaric ensemble while maintaining the temperature at the desired value using 50000 timesteps. Similarly with the previous simulation setting, a trajectory file is output as well.

Once simulation is completed, the caloric curve is obtained by plotting the total energy versus the pressure of the system. The volume versus pressure graph is also plotted to determine any changes in the phase of the system. Lastly, the radial pair distribution is calculated as well.

CHAPTER 5: RESULTS AND ANALYSIS

5.1 Constant pressure simulation

5.1.1 Pressure set at 100MPa

The caloric curves of this simulation are as plotted in Figure 19, 20 and 21. From it, it can be observed that at around 18 $°K$ a change in phase from III to II took place and at around 27 $°K$ another transition from phase II to I occur which is in comparison, quite similar to the values obtained via literature. The solid methane system melts at around 118 $°K$. This is supported by the slight steep change in the volume of the system as well which is shown in Figure 22.

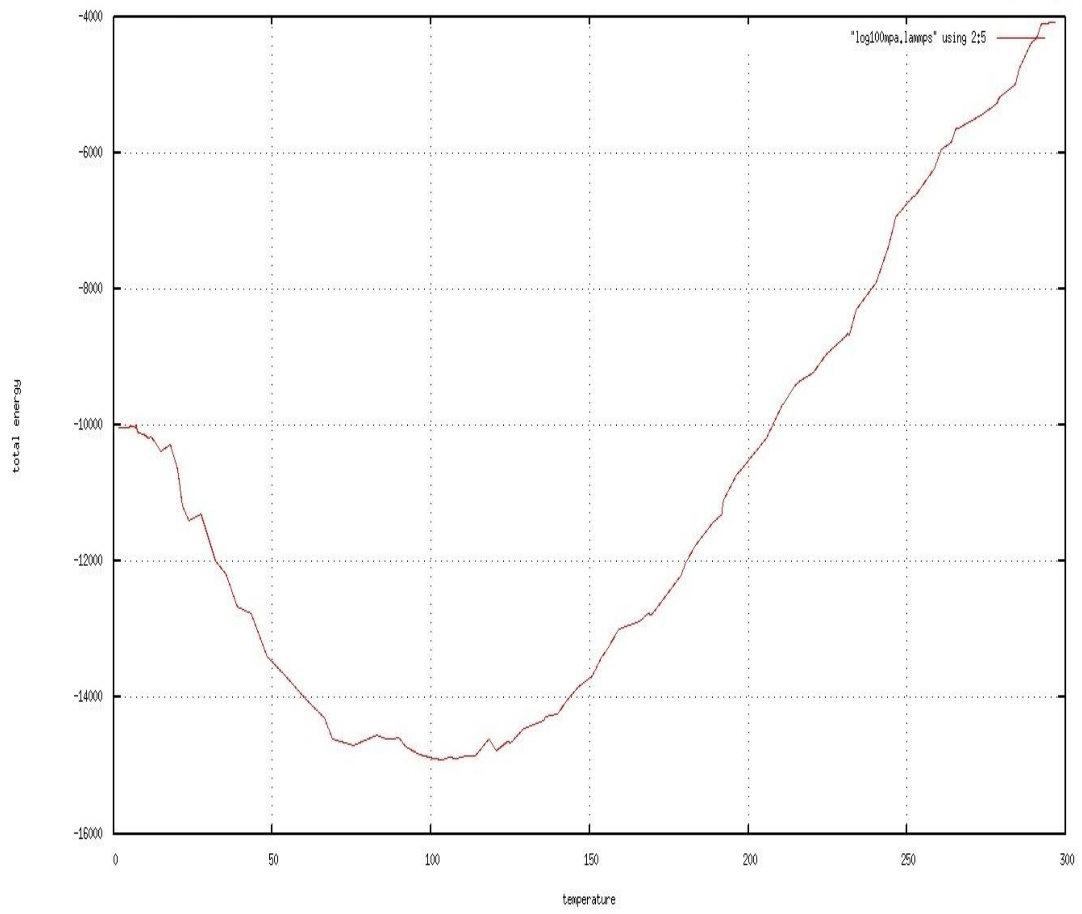

Figure 19: Full view of the caloric curve for the system with constant pressure of 100MPa

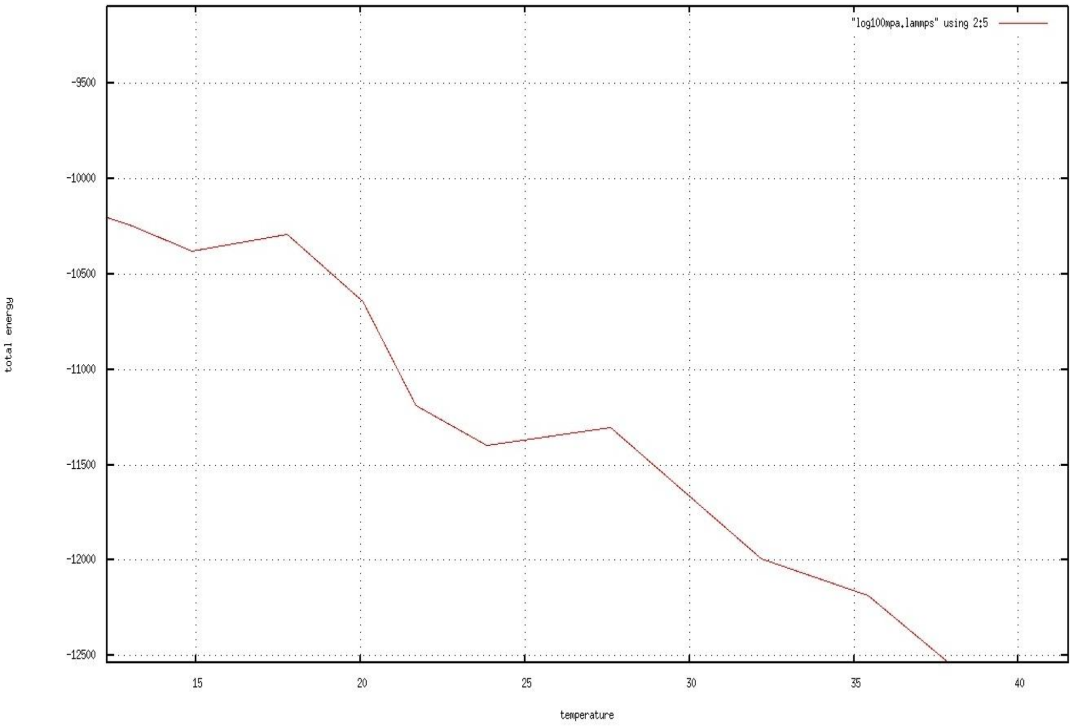

Figure 20: close up view of the discontinuity of the system with constant pressure of 100MPa

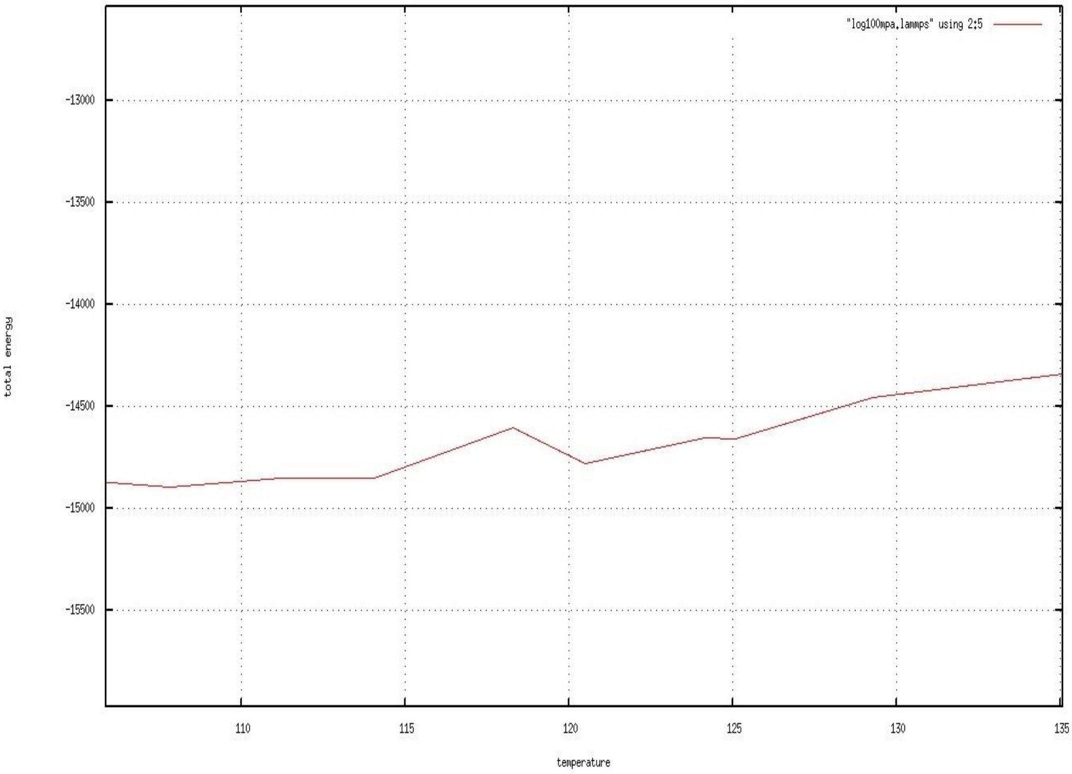

Figure 21: close up view of the 2nd discontinuity of the system with constant pressure of 100MPa

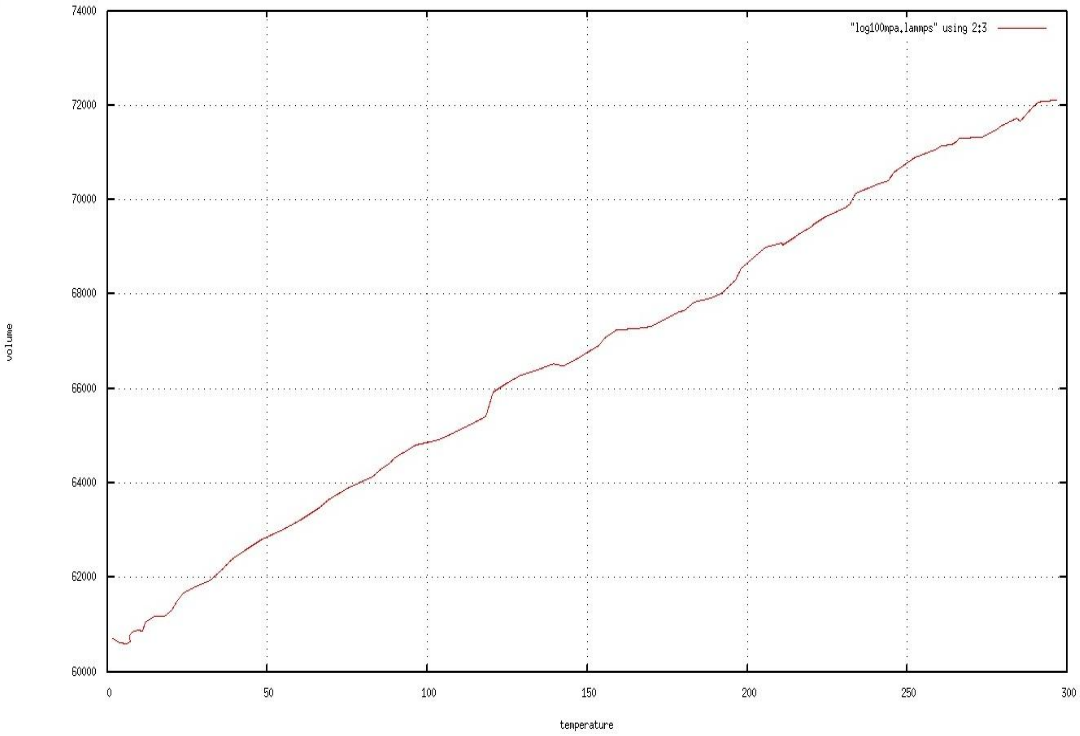

Figure 22: Volume versus temperature graph of the system with constant pressure of 100MPa

Besides that, from the radial distribution function, it can also be observed that initially, the system is in solid state as it has a high probability of finding another atom at a distance of around 4 Armstrong and the high amount of sharp peaks detected as shown Figure 23 supports it. After the melting point, the amount of peaks reduces. The probability of finding another atom at the distance around 4 Armstrong decreases to around 2.5 times as shown in Figure 24. As the heating continues, the amount of peaks continues to reduce and the probability of finding a molecule being as close as 4 Armstrong reduces to around 2 times as shown in Figure 25. This phenomenon is expected as with the increase of temperature, the molecules obtain more kinetic energy to move around freely and thus tends to be further apart from each other. However, it is still in the liquid state as a gaseous state will yield a radial distribution function graph with fewer peaks and a smooth damping curve.

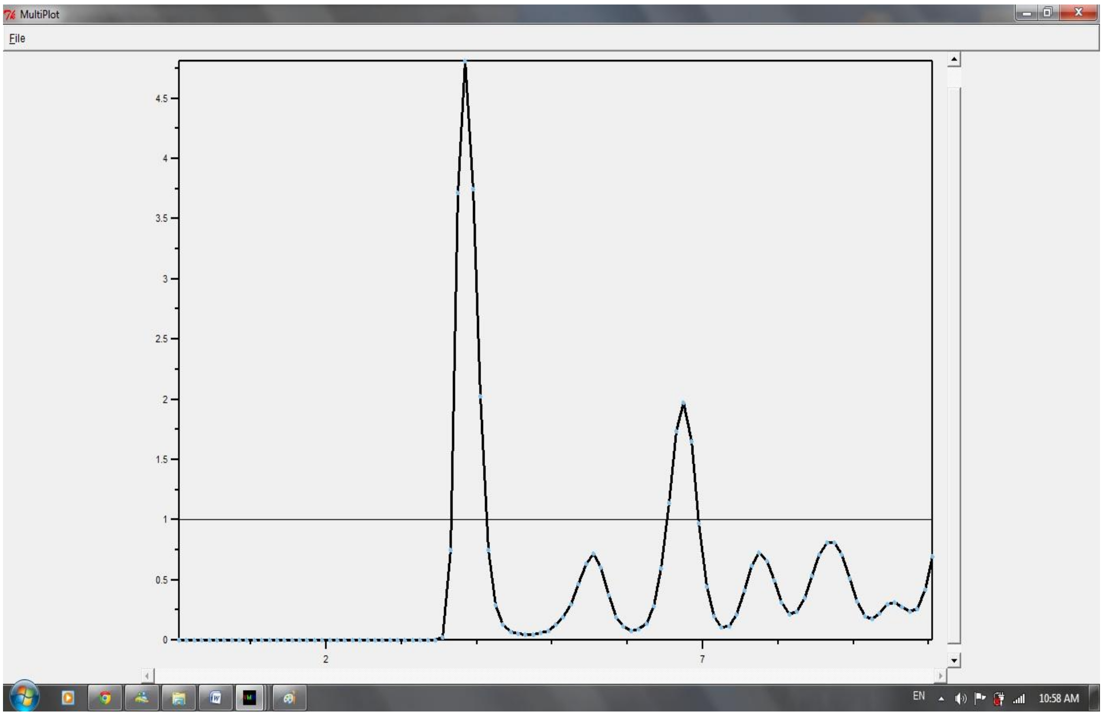

Figure 23: radial distribution function plot of the 100MPa system's initial condition

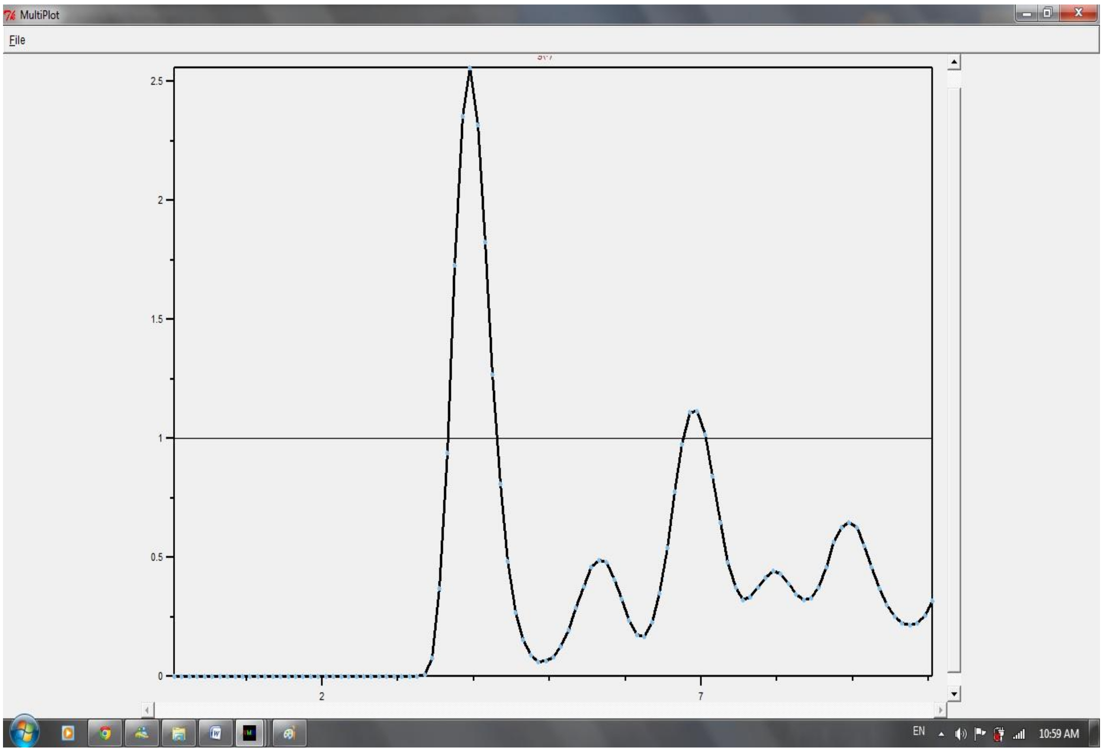

Figure 24: radial distribution function plot of the 100MPa system's after melting (118°K)

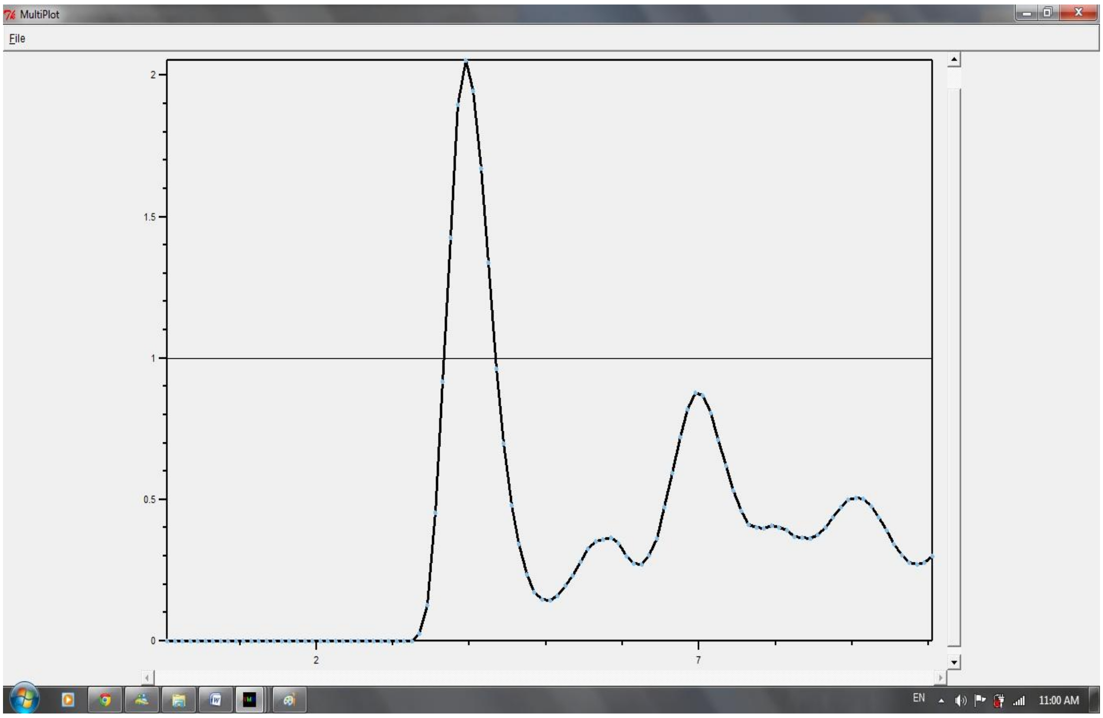

Figure 25: radial distribution function plot of the 100MPa system's at around 250°K

The values obtained via simulation are tabulated in table 8 bellow in comparison with the values obtained via literature.

Table 8: Phase transitions that took place at 100MPa (2)

Transition	Temperature (K)		
	Present Work	**Previous Work**	**Experiment**
Phase III to II	17.784	31 ±2	19
Phase II to I	27.604	36 ±2	25
Melting point	118.299	121 ±3	115

5.1.2 Pressure set at 300MPa

For this setting of the simulation, it is observed that changes from phase IV to III took place at around 29 °*K* follow closely by another transition from phase III to I at around 39°K . The melting of the system took place at the temperature of around 157°K. The full via of the caloric curve is as shown in Figure 26 while a close up view of the region of interest is shown in Figure 27 and 28.

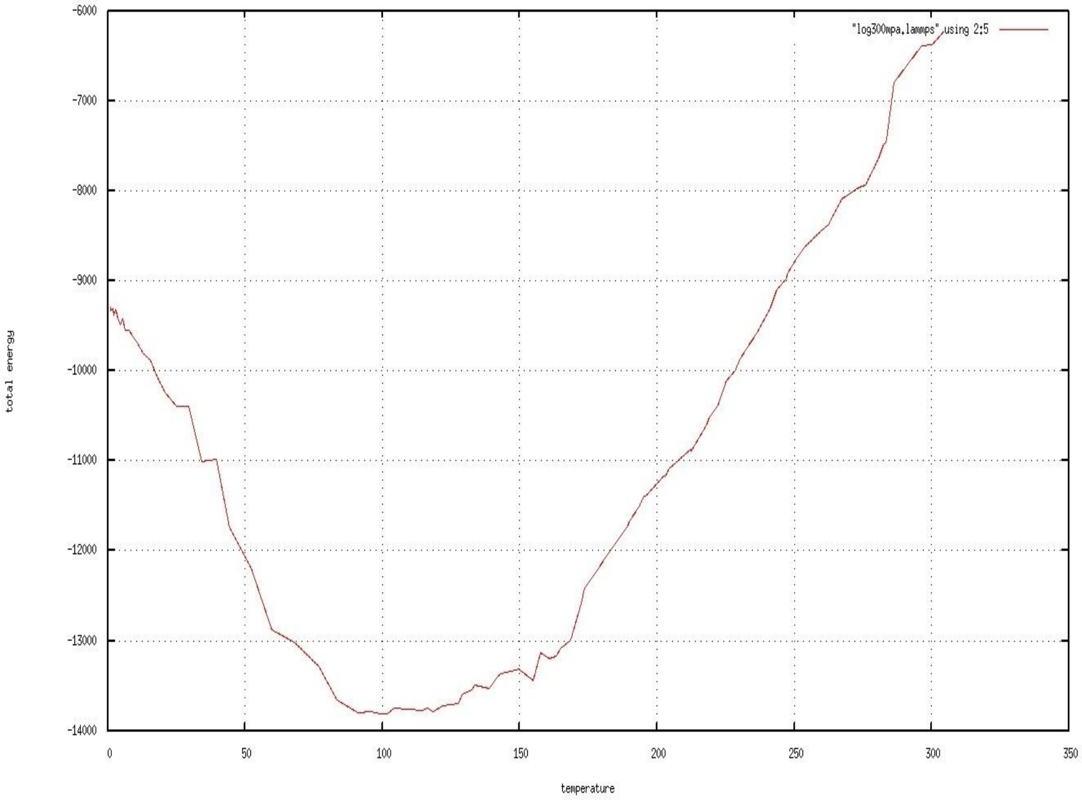

Figure 26: Full view of the caloric curve for the system with constant pressure of 300MPa

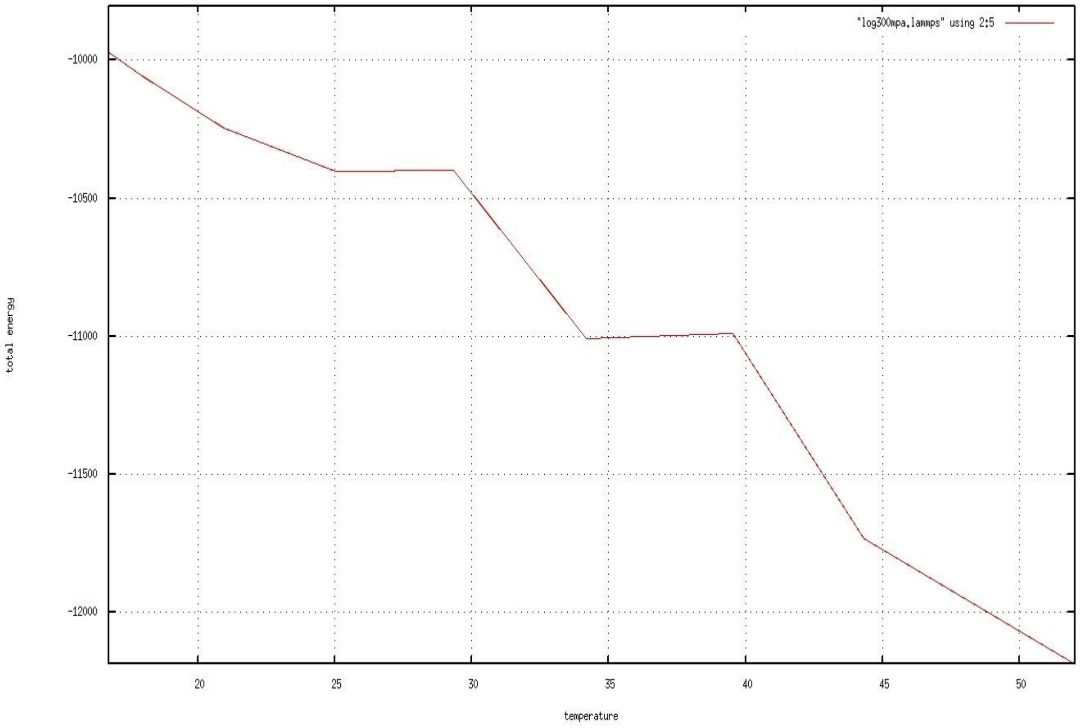

Figure 27: Close view of the 1st region of interest in the caloric curve for the system with constant pressure of 300MPa

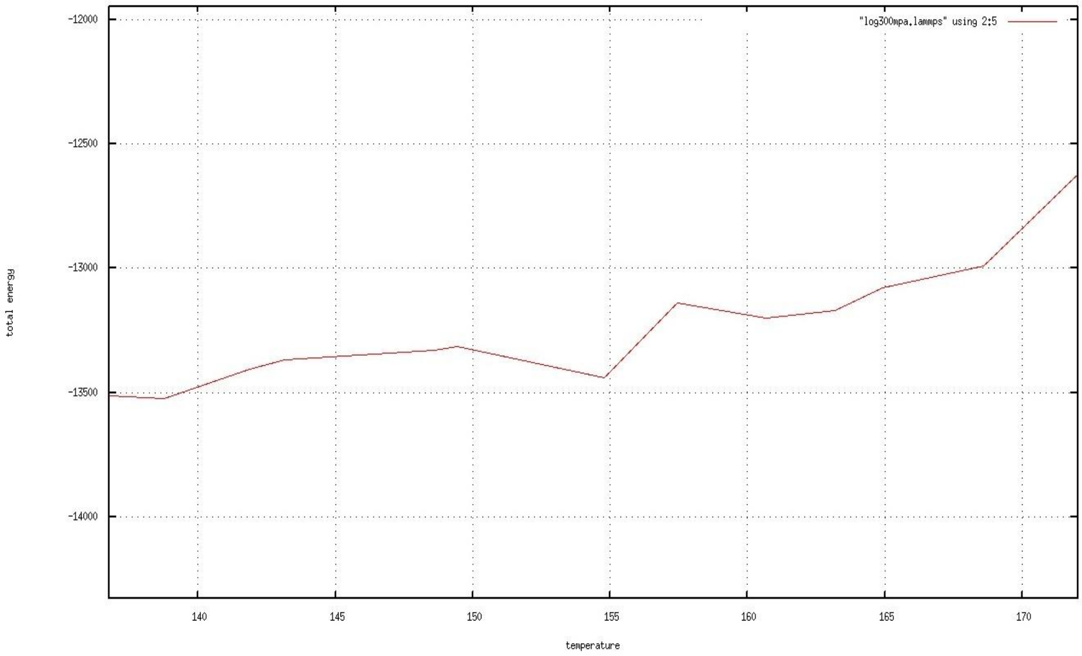

Figure 28: Close view of the 2nd region of interest in the caloric curve for the system with constant pressure of 300MPa

The plot of volume versus temperature shown in Figure 29 for this simulation which has a slight steep increase in volume at the region near the melting point which is around 157°K.

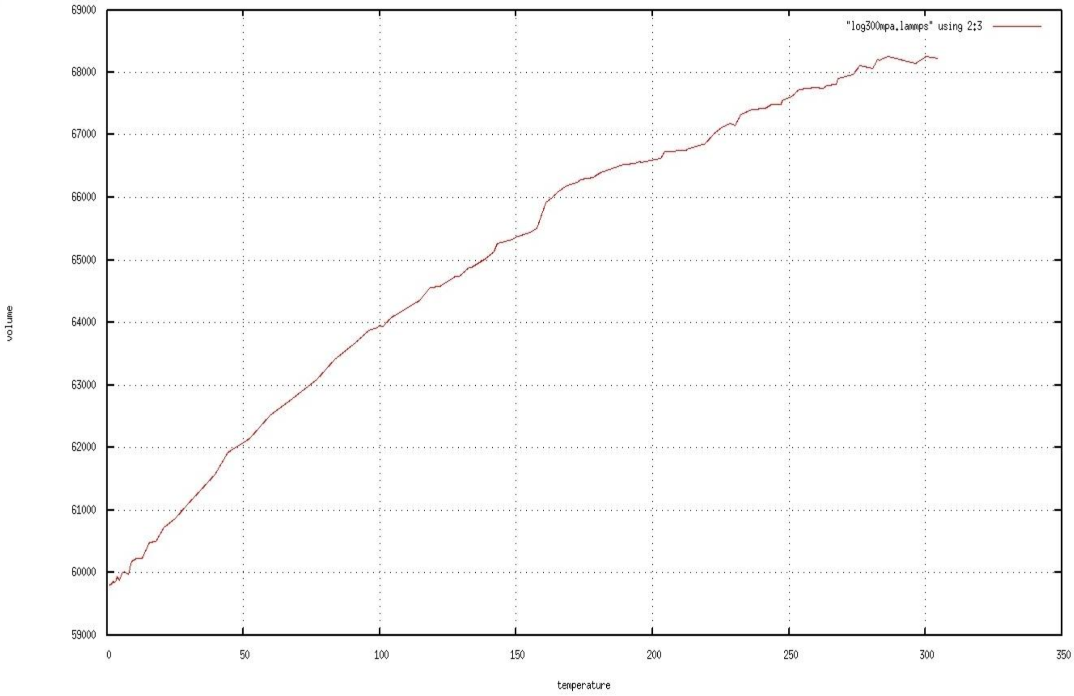

Figure 29: Volume versus temperature plot of the simulation with 300MPa constant pressure

The initial graph of the radial pair distribution is the same as that obtained in the previous simulation as shown in Figure 30. However after the melting point, the probability of finding a methane molecule at around 4 Armstrong decrease to 3times which is slightly higher than that of the 100MPa constant pressure simulation which is due to the fact that the pressure is higher thus forcing the molecules to be closer to each other (Figure 31). As the temperature continue to rise, the probability reduce to around 2.1 times at the end of the simulation and the observation stated earlier still holds true were the 1st peak detected in the 300MPa constant pressure is still slightly higher than that of the 100MPa simulation (Figure 32).

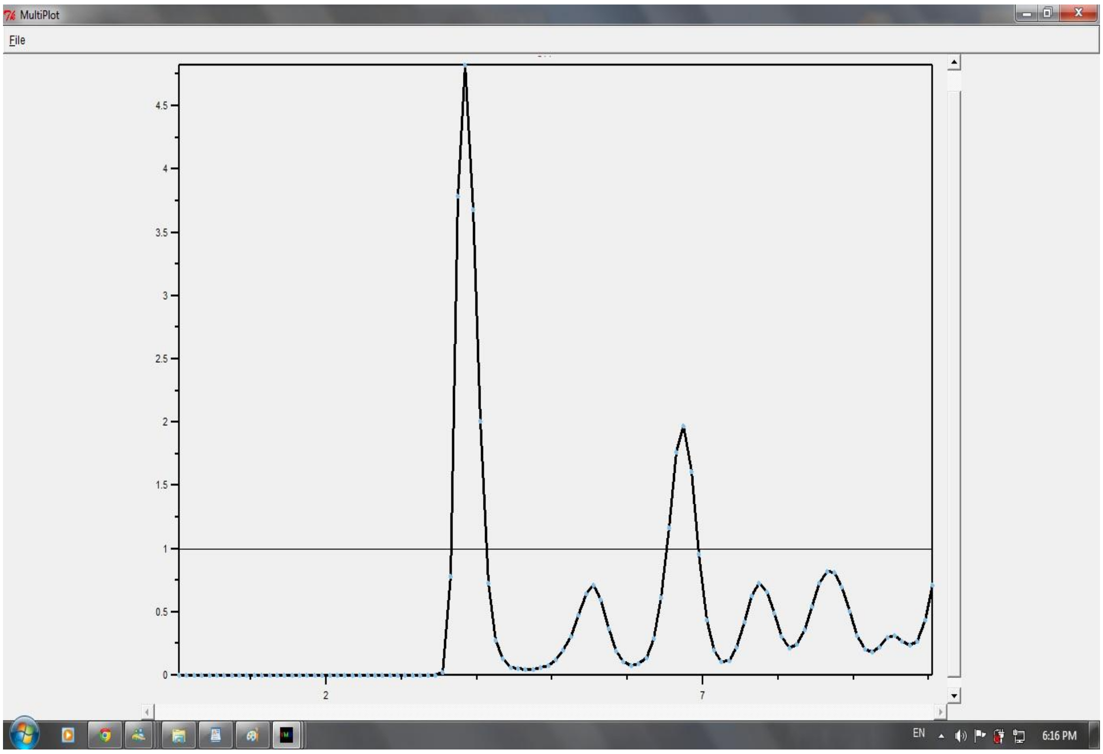

Figure 30: radial distribution function plot of the 300MPa system's initial condition

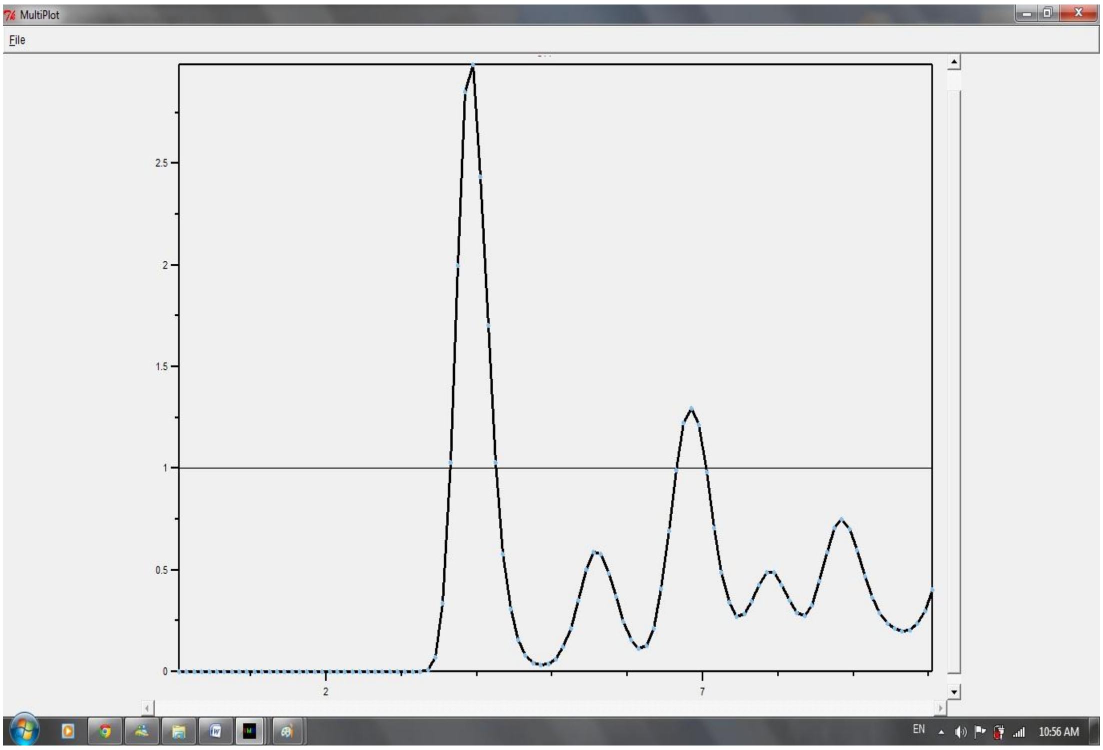

Figure 31: radial distribution function plot of the 300MPa system after melting point

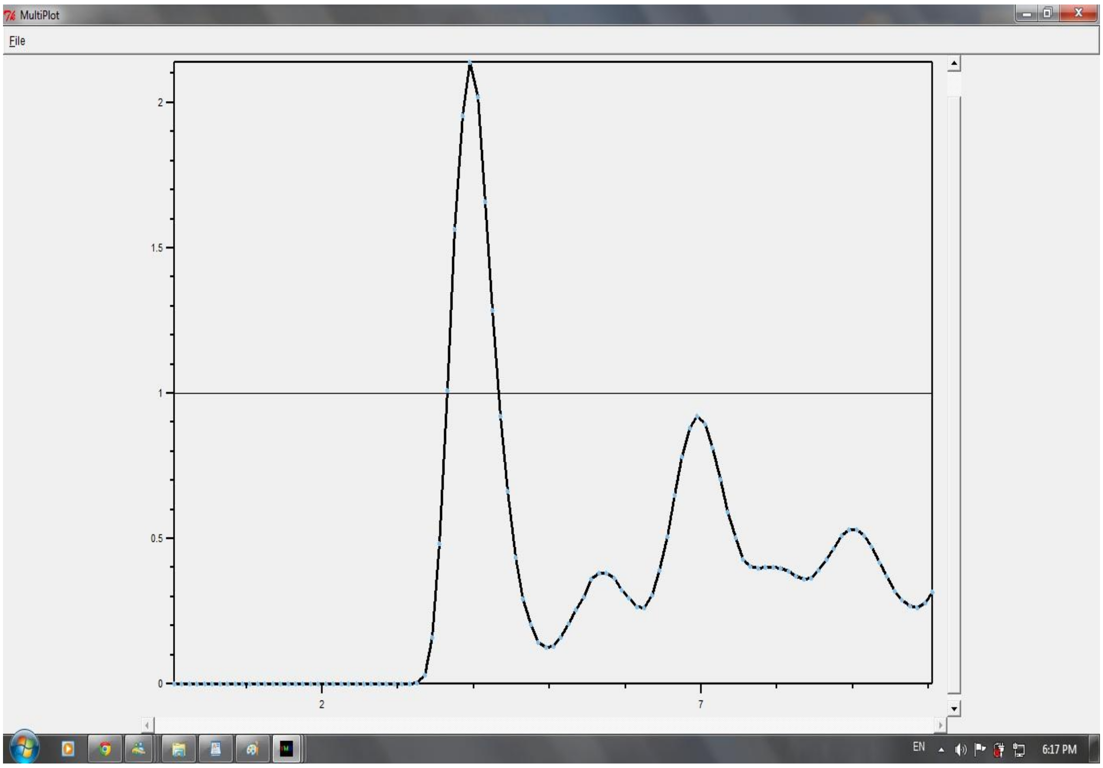

Figure 32: radial distribution function plot of the 300MPa system at the end of simulation

Table 9: Phase transitions that took place at 300MPa (2)

Transition	Temperature (K)		
	Present Work	Previous Work	Experiment
Phase IV to III	29.342	32±2	20
Phase III to I	39.541	38±2	31
Melting Point	157.458	161±3	155

5.1.3 Pressure set at 2000MPa

In this simulation setting, a few spikes in the caloric curve are detected as shown in Figure 33, 34 and 35. The first one detected is around 28 to 29 $°K$ which indicate a transition from phase IV to V. The transition from phase V to IV took place at around 79 $°K$ follow by transition from phase IV to B at around 94$°K$. Other than that, a transition at around 114$°K$ shows a transition from phase B to A and from phase A to I at around 128 $°K$. The volume versus temperature graph shows an increase in volume with temperature without any high fluctuation as shown in Figure 36. In Figure 37, the initial condition of the radial pair distribution function graph shows that the molecules in the system is more closely pack as the subsequent peaks after the first peak shows a higher probability of a molecule is in that distance when compare with the graph obtain in the previous two simulation setting which is due to the higher pressure applied. It is also observed that in Figure 38, despite increase in pressure, not many changes in terms of the probability in the peaks are detected. At the end of the simulation, there is a slight decrease of the probability in the 1st peak of the graph as shown in Figure 39.

Table 10: At Pressure=2000MPa, the phase transition which took place at temperature K (2)

Transition	Temperature (K)		
	Present Work	Previous Work	Experiment
Phase IV to V	29.565	26±1	32
Phase V to IV	79.420	82±2	75
Phase IV to B	94.399	90±4	92
Phase B to A	113.487	110±3	107
Phase A to I	128.721	125±2	128

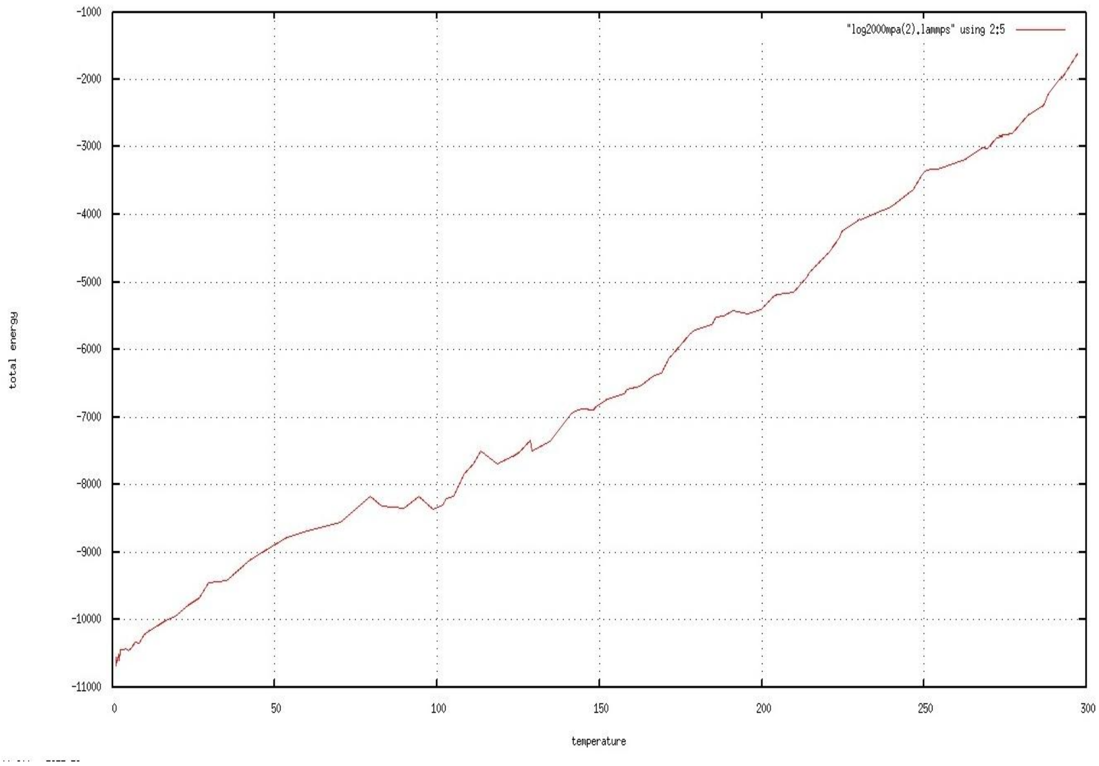

Figure 33: Full view of the caloric curve for the system with constant pressure of 2000MPa

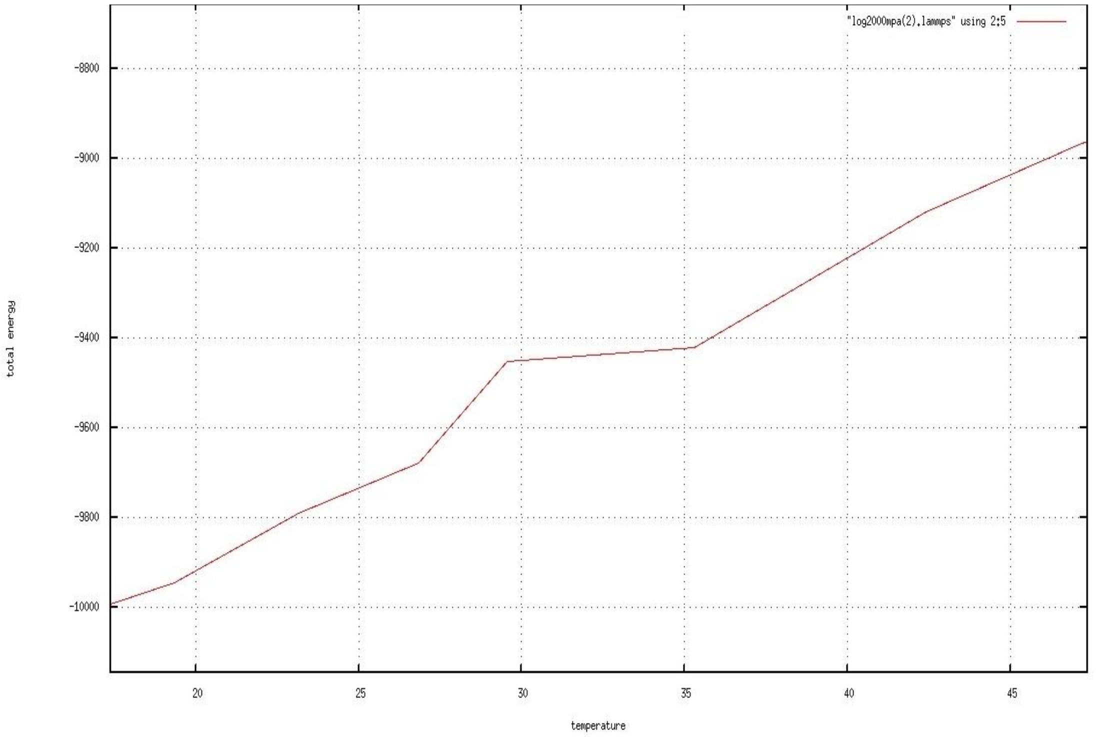

Figure 34: Close view of the 1st region of interest in the caloric curve for the system with constant pressure of 2000MPa

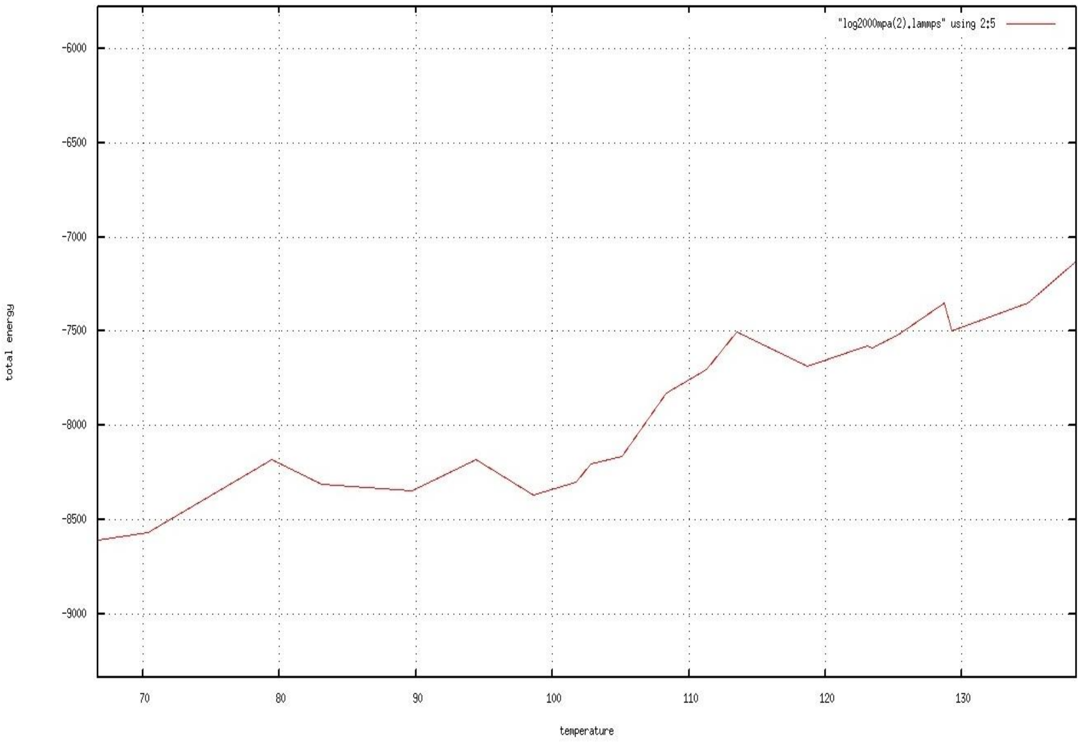

Figure 35: Close view of the 2nd region of interest in the caloric curve for the system with constant pressure of 2000MPa

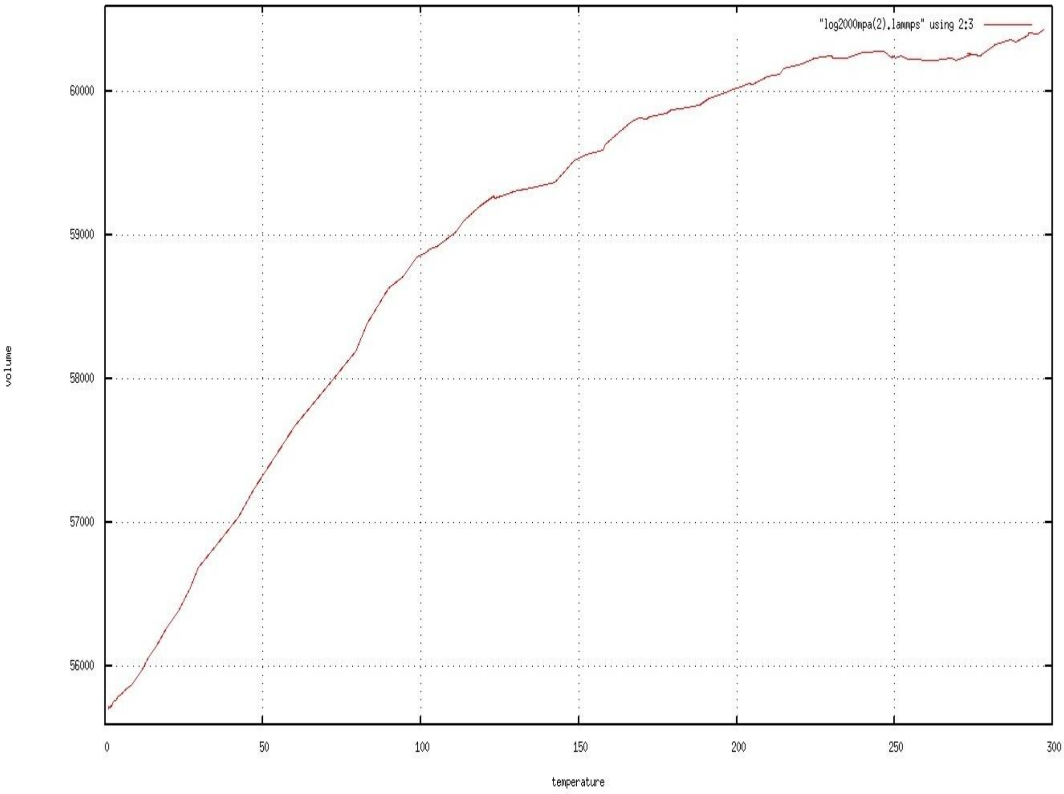

Figure 36: Volume versus temperature plot of the simulation with 2000MPa constant pressure

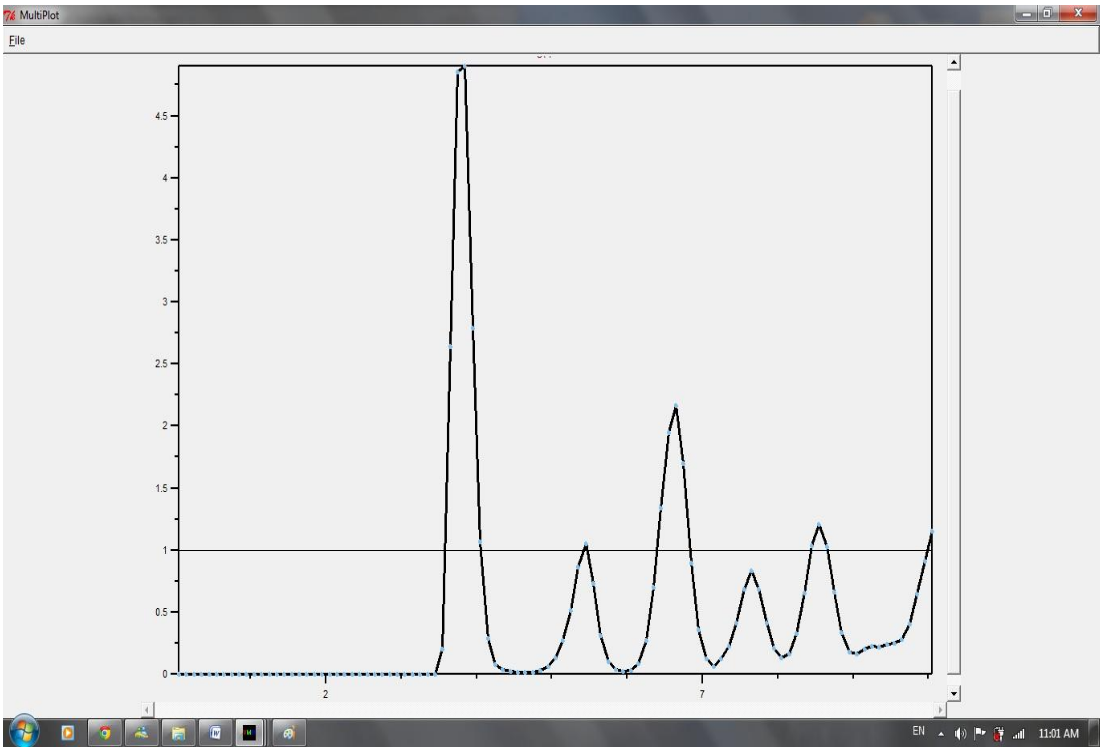

Figure 37: radial distribution function plot of the 2000MPa system's initial condition

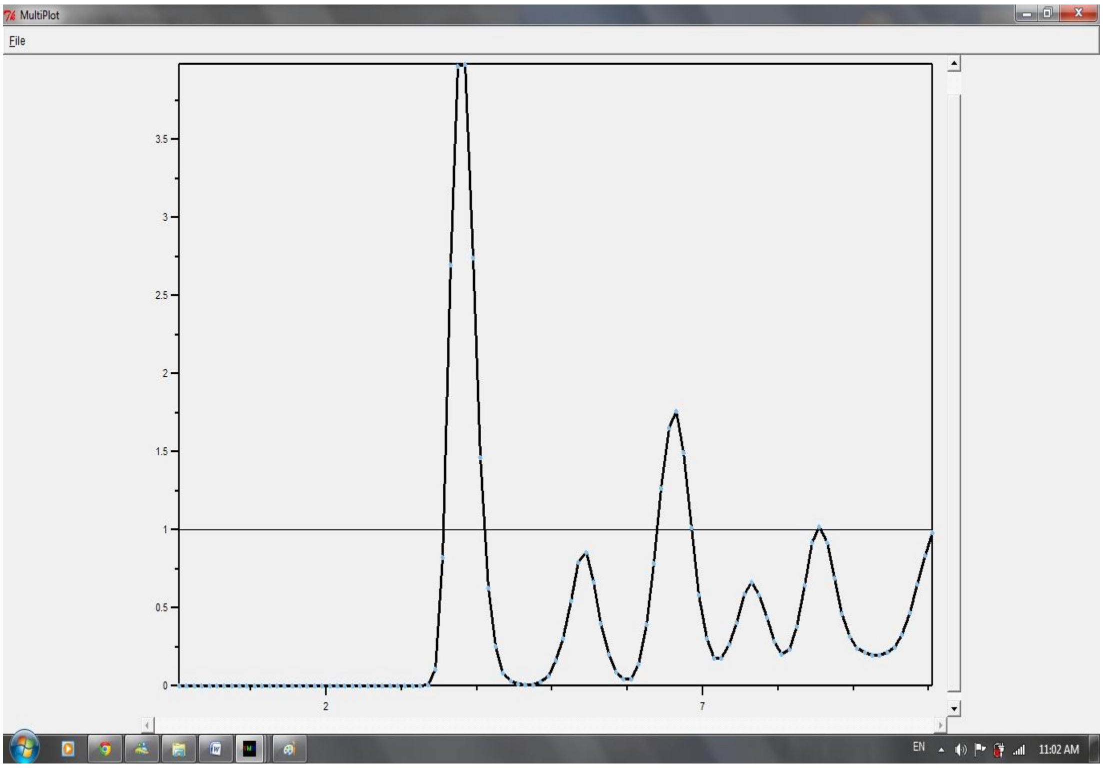

Figure 38: radial distribution function plot of the 2000MPa system at the middle of simulation

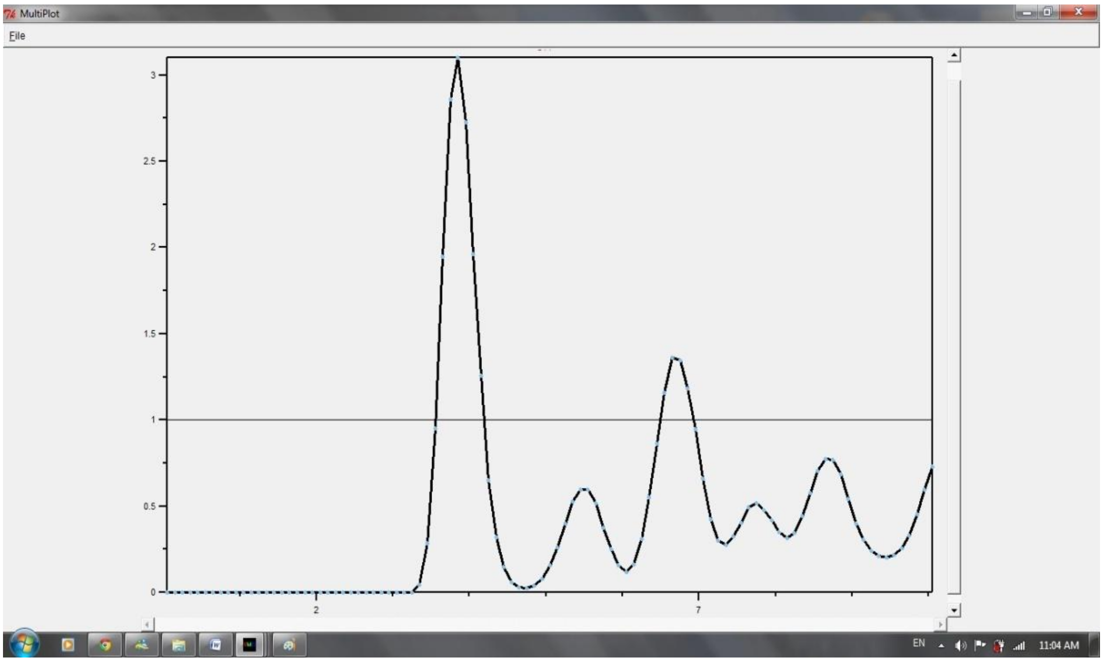

Figure 39: radial distribution function plot of the 2000MPa system at the end of simulation

5.1.4 Pressure set at 20GPa

For this part of the simulation, due to the extreme high pressure, the only detectable phase transition took place at around 242°K from phase HP to B as shown in Figure 40 and 41. Figure 42 of the graph volume versus temperature also shows a stable increase of volume with temperature. As for the pair radial distribution function graph also shows that the system is in solid state throughout the whole simulation as the probability of finding a molecule at around 3.5 Armstrong is around 4.5 to 5 times as likely in all taken sample timesteps as shown in Figure 43, 44 and 45.

Table 11: At Pressure=20GPa, the phase transition which took place at temperature K (2)

Transition	**Temperature (K)**		
	Present Work	**Previous Work**	**Experiment**
HP Phase to B	241.087	240±3	260

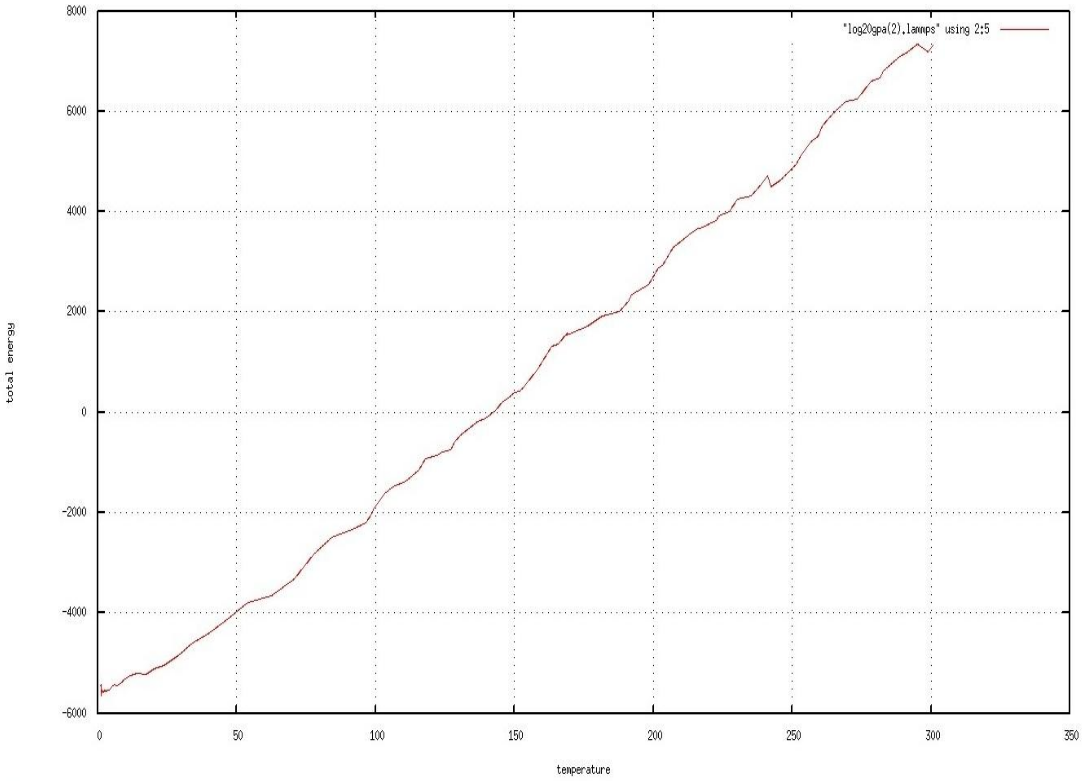

Figure 40: Full view of the caloric curve for the system with constant pressure of 20GPa

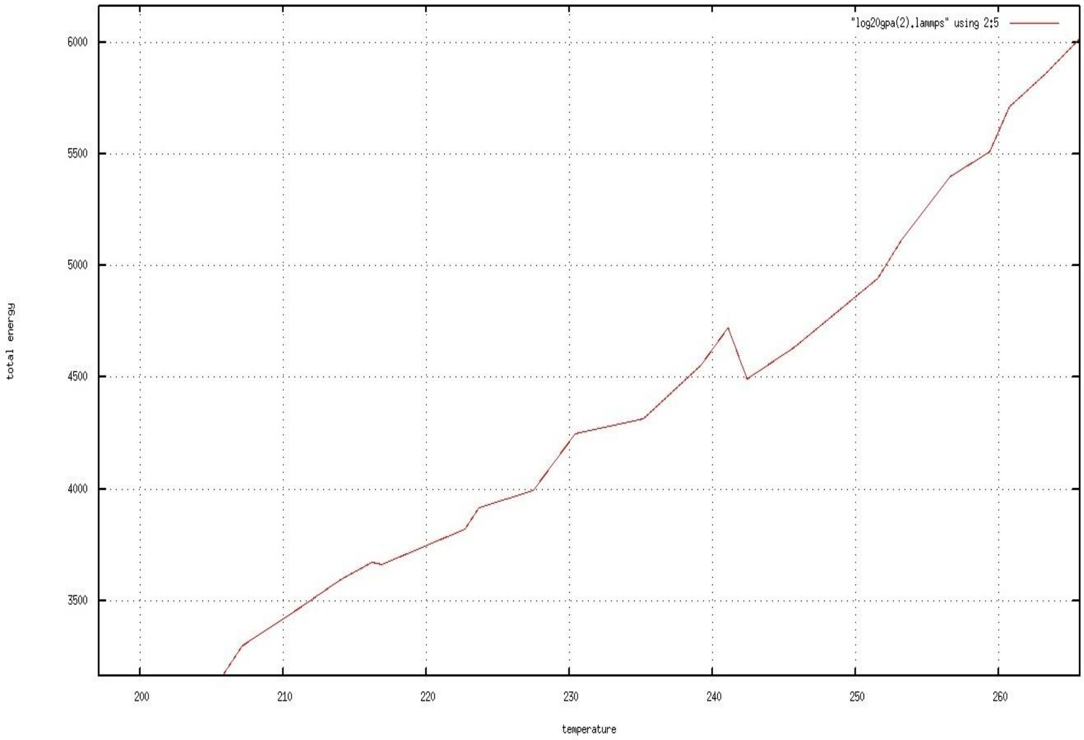

Figure 41: Close view of the region of interest in the caloric curve for the system with constant pressure of 20GPa

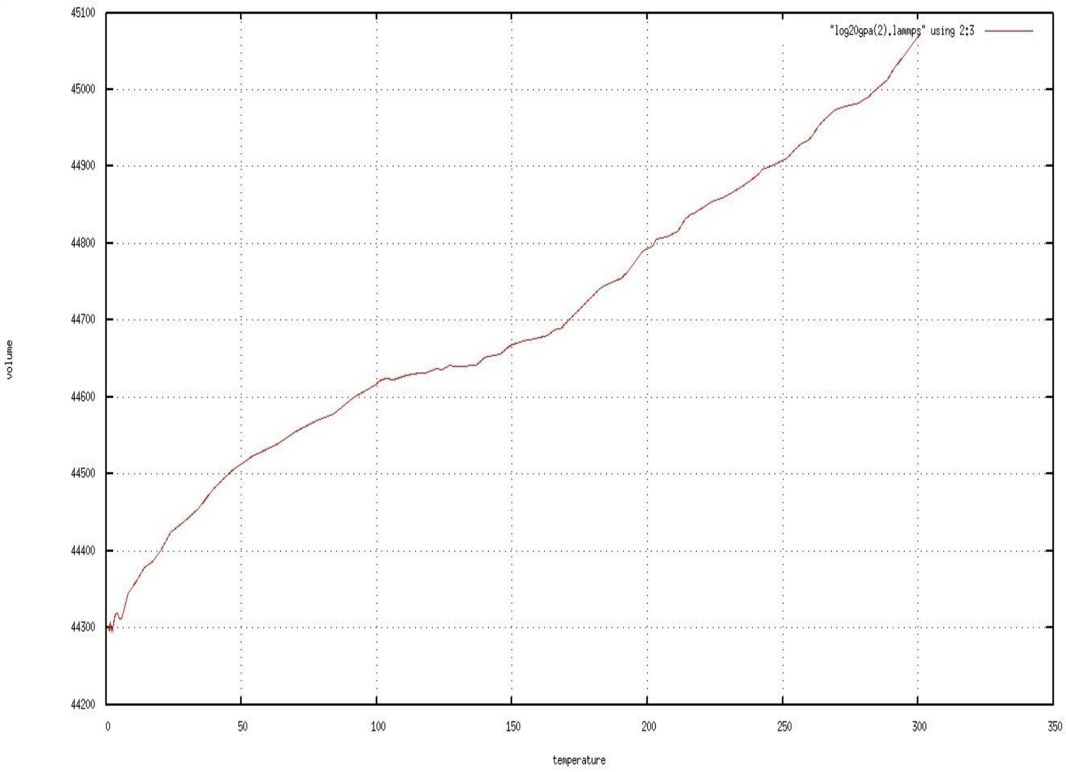

Figure 42: Volume versus temperature plot of the simulation with 20GPa constant pressure

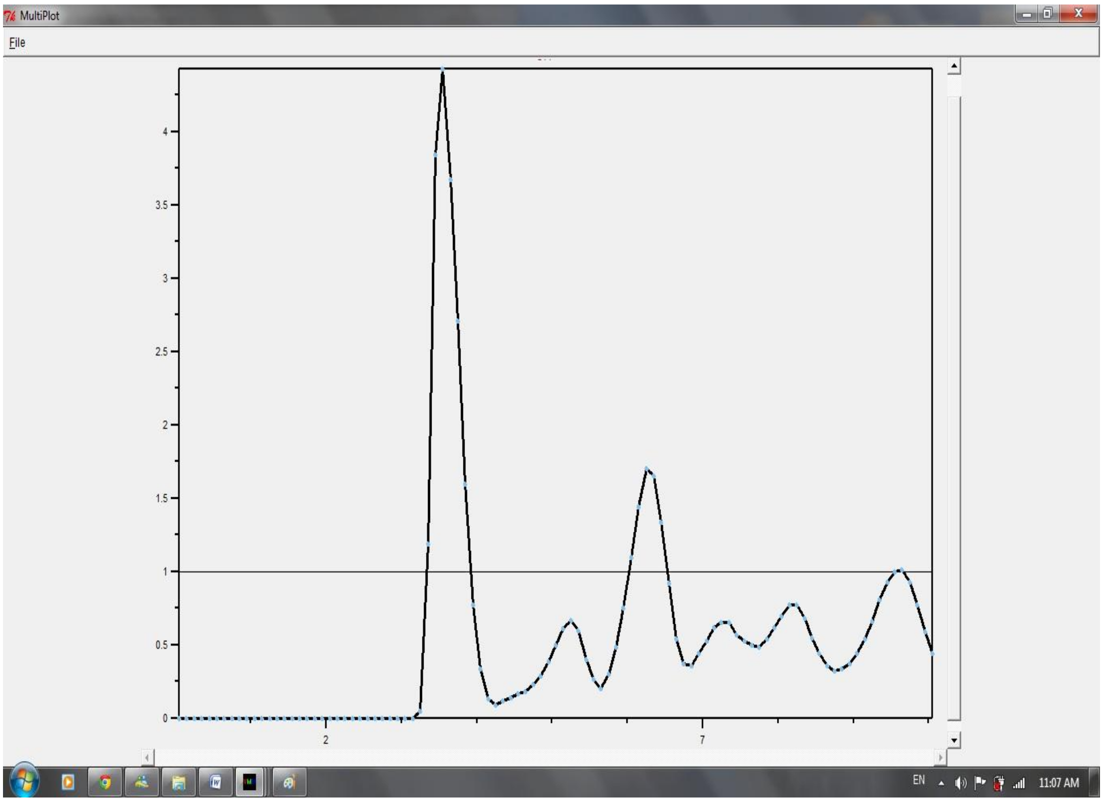

Figure 43: radial distribution function plot of the 20GPa system’s initial condition

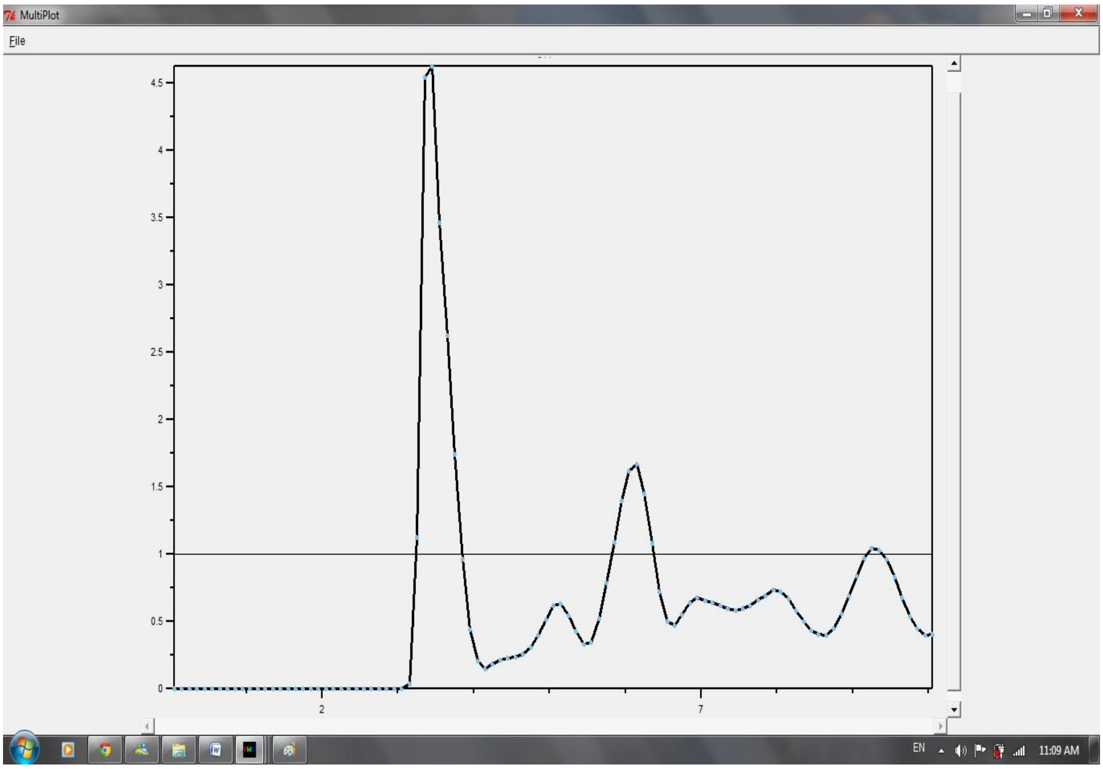

Figure 44: radial distribution function plot of the 20GPa system at the middle of simulation

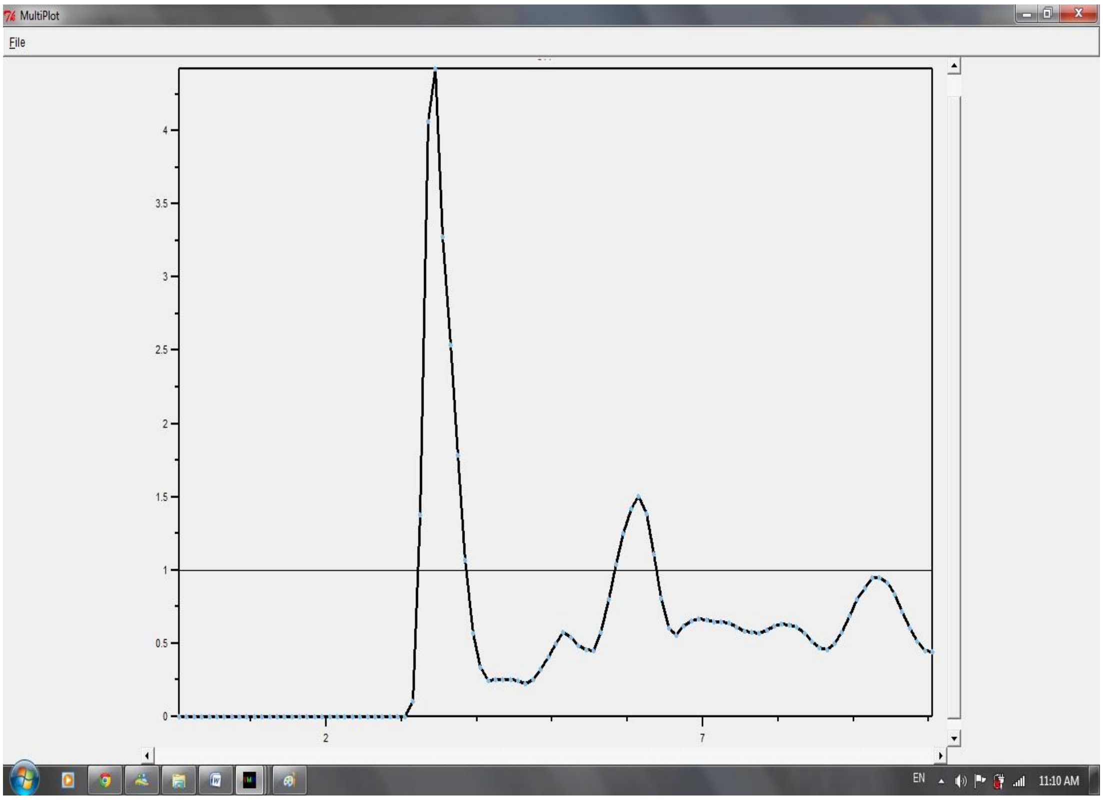

Figure 45: radial distribution function plot of the 20GPa system at the end of simulation

5.2 Constant temperature simulation

5.2.1 Temperature set at 130°K

After rising the temperature to 130°K, and increase the pressure is done. From the graph, the detected transition is around 175.556 MPa from liquid to I phase and from I to A phase at around 1994.001 MPa. Phase A to B transition took place at around 2904.739 MPa. Transition to the HP phase is at around 10167.051 MPa. These are shown in the caloric curves depicted by Figure 46, 47 and 48. The volume versus pressure graph shows a slight discontinuity when it changes from liquid to phase I and continue to decrease with increasing pressure as shown in Figure 49. Figure 50, 51 and 52 shows the radial pair distribution function graph and it can be observe that initially, the 1st peak have a probability of 2.3 times which indicates that the system is mostly in liquid form, however with increasing pressure, the value of the 1st peak shot up to 5 times as likely to find a molecule at the distance of 3.5 Armstrong.

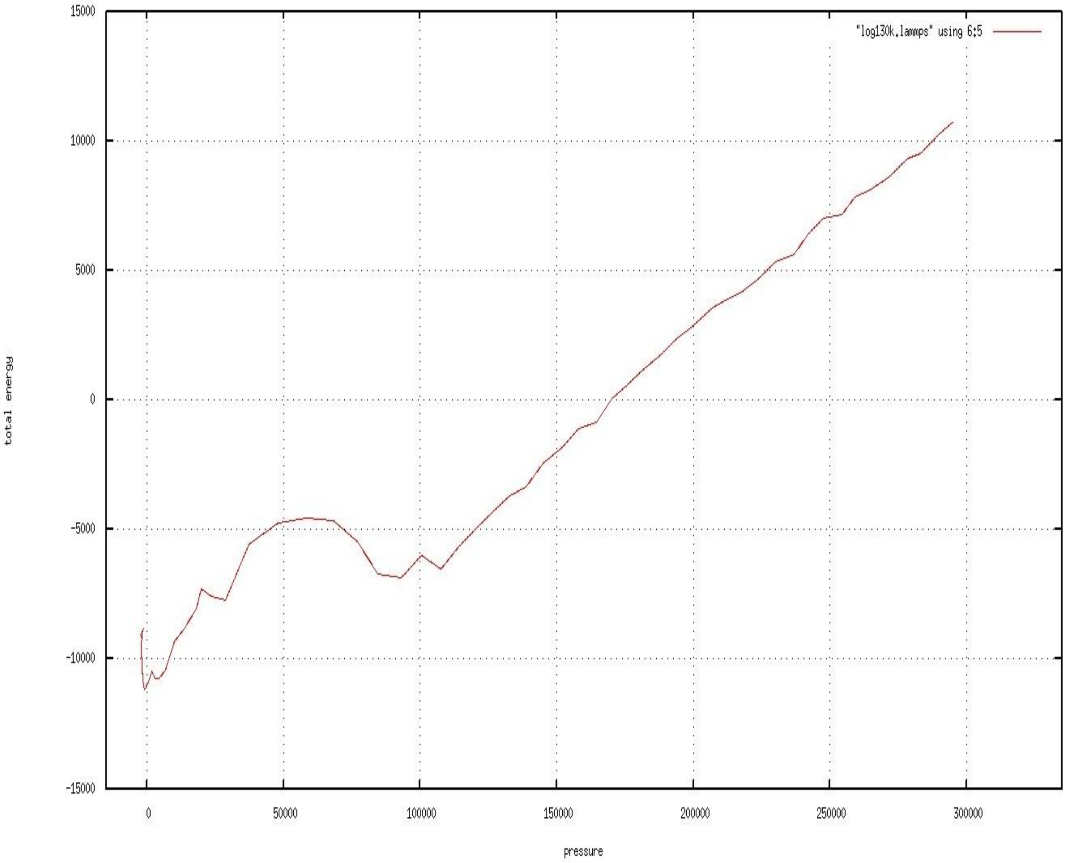

Figure 46: Full view of the caloric curve for the system with constant temperature of 130°K

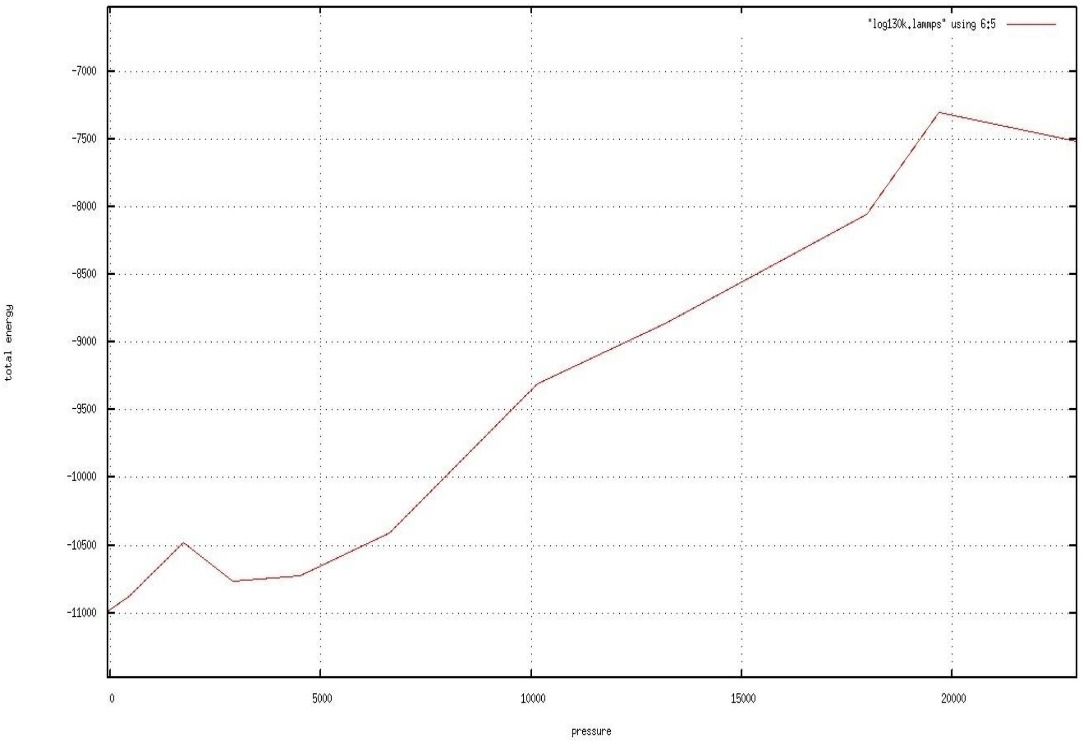

Figure 47: Close view of the 1st region of interest in the caloric curve for the system with constant temperature of 130°K

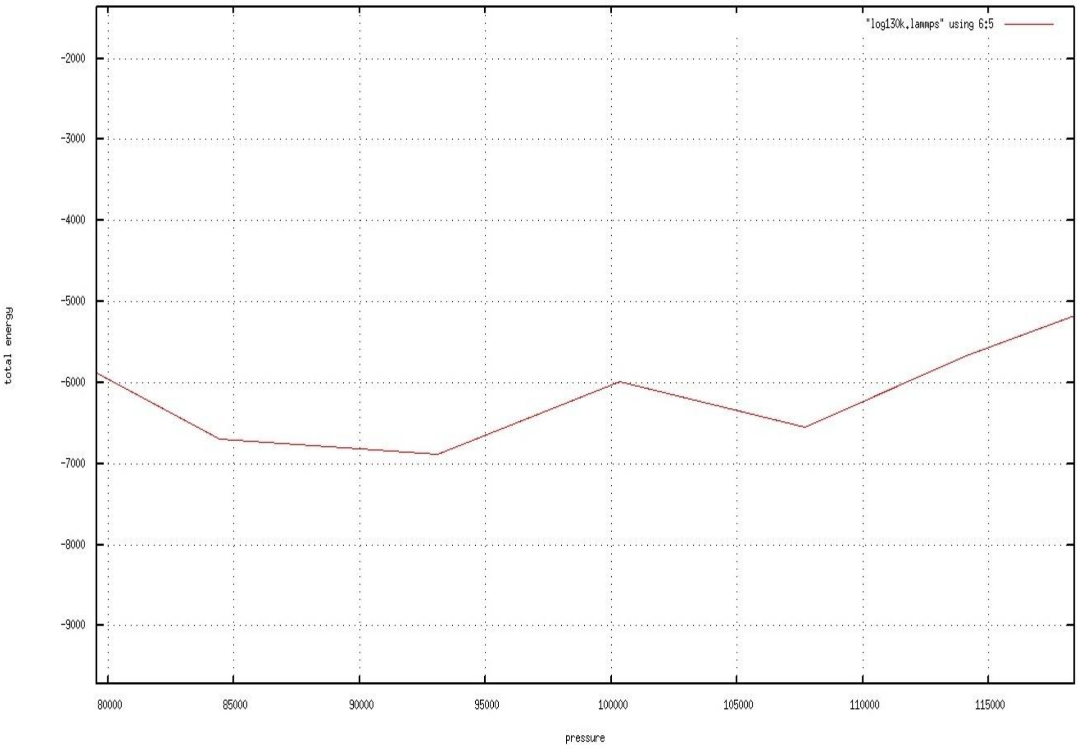

Figure 48: Close view of the 2nd region of interest in the caloric curve for the system with constant temperature of 130°K

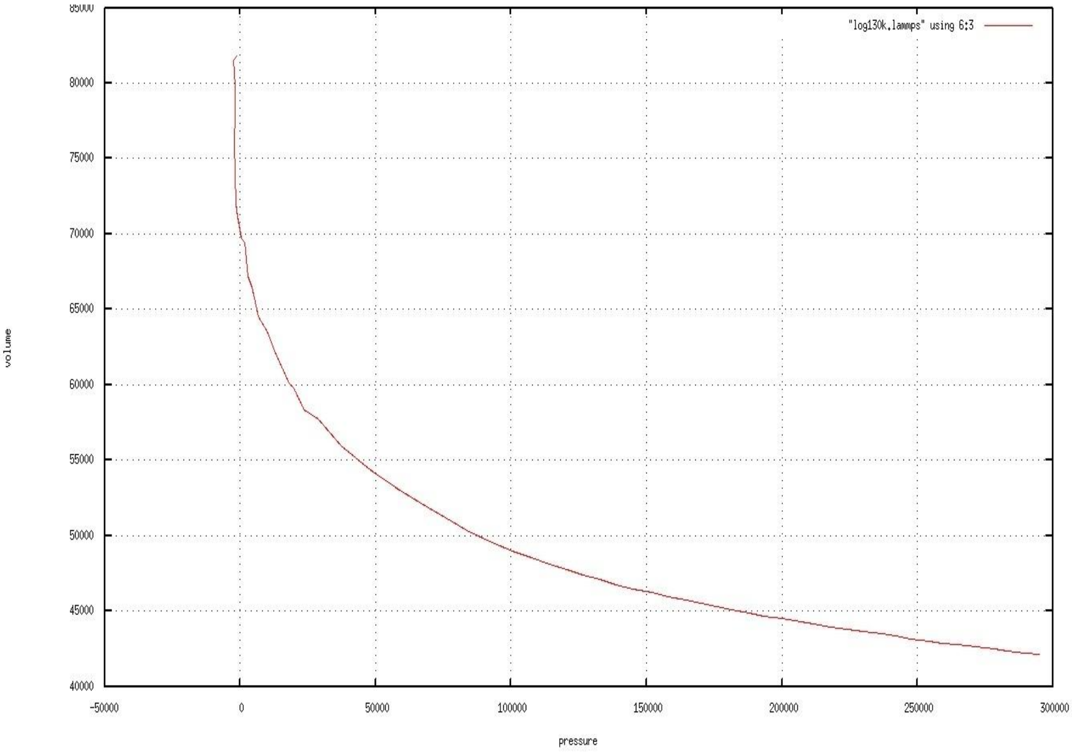

Figure 49: Volume versus pressure plot of the simulation with constant temperature of 130°K

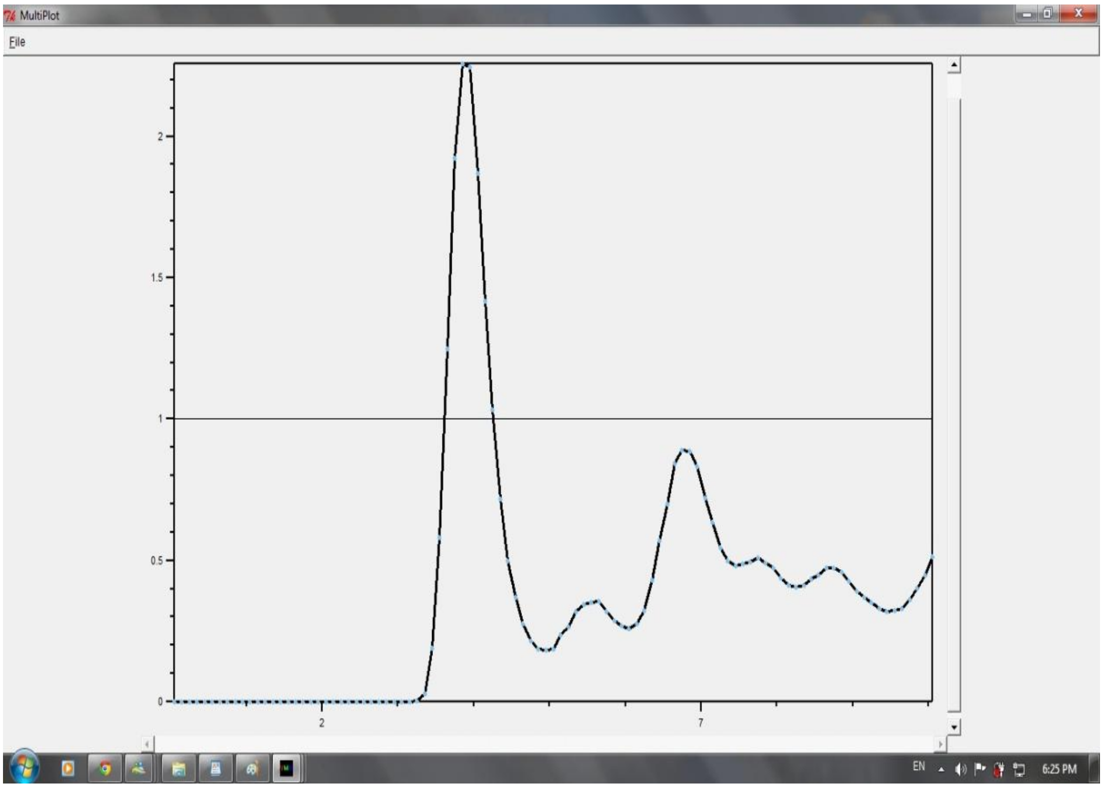

Figure 50: radial distribution function plot of the system's initial condition with constant temperature of 130°K

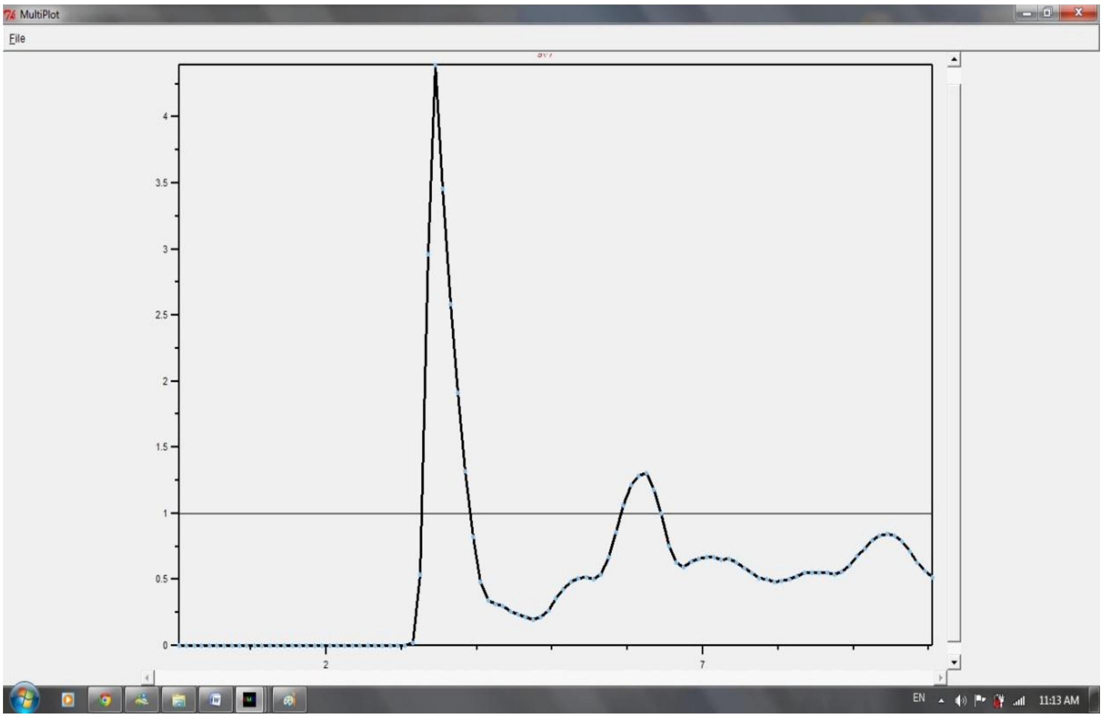

Figure 51: radial distribution function plot of the system at the middle of simulation with constant temperature of 130°K

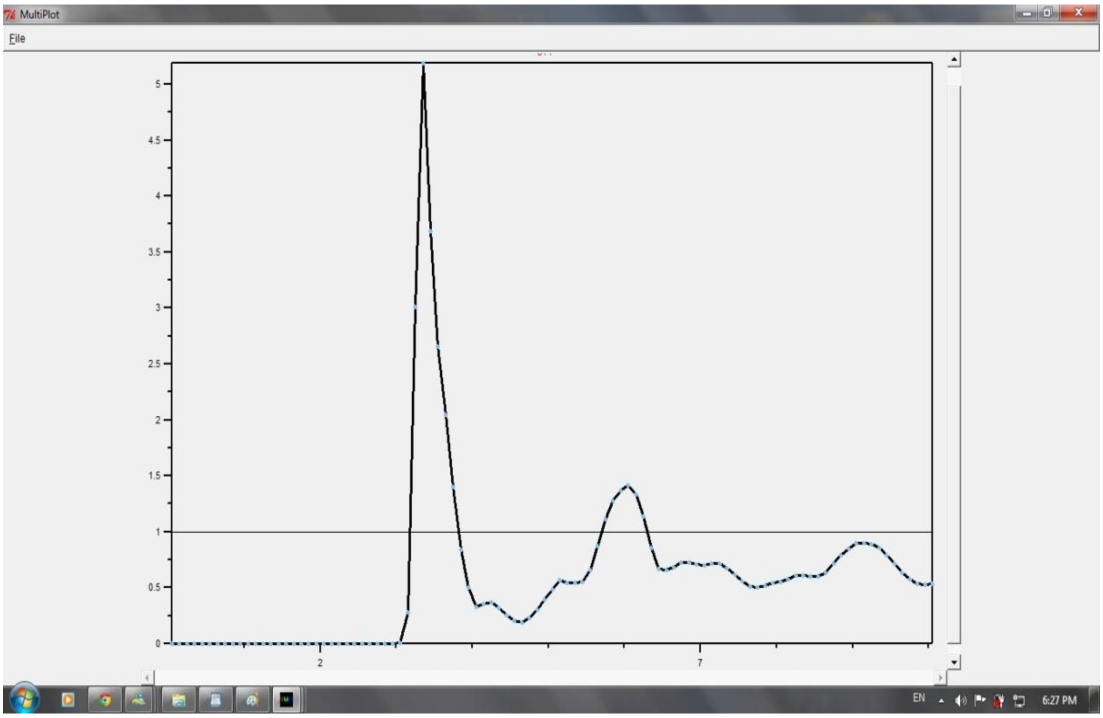

Figure 52: radial distribution function plot of the system at the end of simulation with constant temperature of 130°K

Table 12: At temperature 130K, the phase transition that took place at pressure (MPa) (2)

Phase Transition	**Pressure (MPa)**		
	Present Work	**Previous Work**	**Experiment**
Phase liquid to I	175.556	200±50	155
Phase I to A	1994.001	2400±200	2050
Phase A to B	2904.739	2800±100	2700
Fcc	-	3600±200	Intermediate Phase
Fct	-	4600±200	
HP phase	10167.051	10450±200	10300

5.2.2 Temperature set at 165°K

At the temperature of 165°K, the transition from liquid to phase I took place at around 252.105MPa follow by from phase I to A at 2550.737MPa and from phase A to B at 3842.694MPa. Phase HP took place at around 12780.834MPa as plotted in the graph on Figure 53, 54 and 55. Similar changes is observed in this simulation setting as that with the simulation at 130°K for the volume versus pressure plot as well as the radial pair distribution function plot. However for the radial pair distribution function plot, the value of the 1st peak is lower due to the fact that the molecules have more energy and tends to be further apart.

Table 13: At temperature 165K, the phase transition that took place at pressure (MPa) (2)

Phase Transition	**Pressure (MPa)**		
	Present Work	**Previous Work**	**Experiment**
Liquid to phase I	252.105	242±50	360
Phase I to Phase A	2550.737	3000±120	2700
Phase A to B	3842.694	3600±250	3700
Fluctuation between fcc and fct	-	4300±250	Intermediate phases
	-	11700±250	
	-	12000±250	
HP phase	12780.834	12300±250	12600

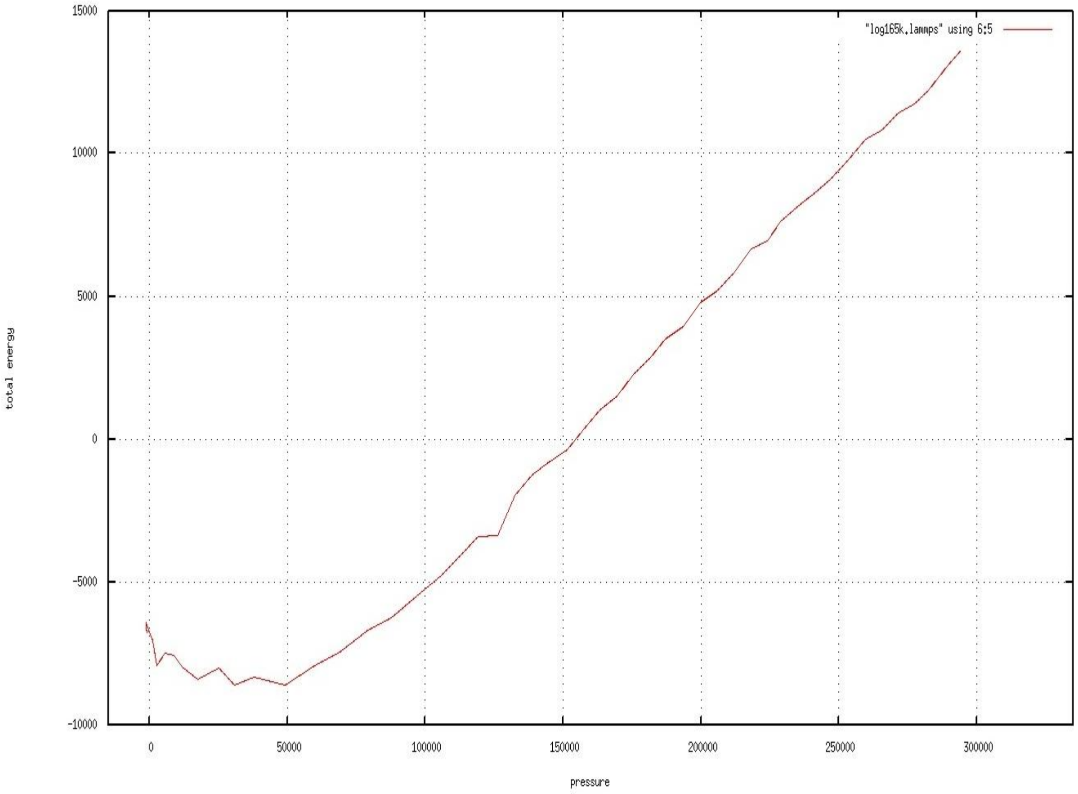

Figure 53: Full view of the caloric curve for the system with constant temperature of 165°K

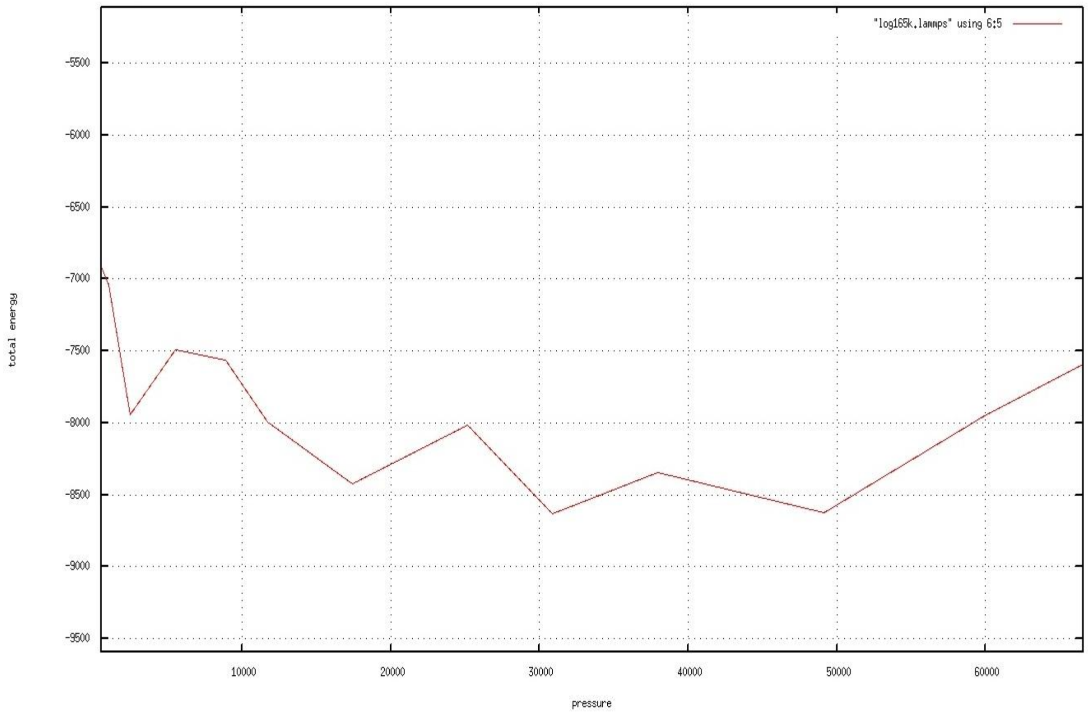

Figure 54: Close view of the 1st region of interest in the caloric curve for the system with constant temperature of 165°K

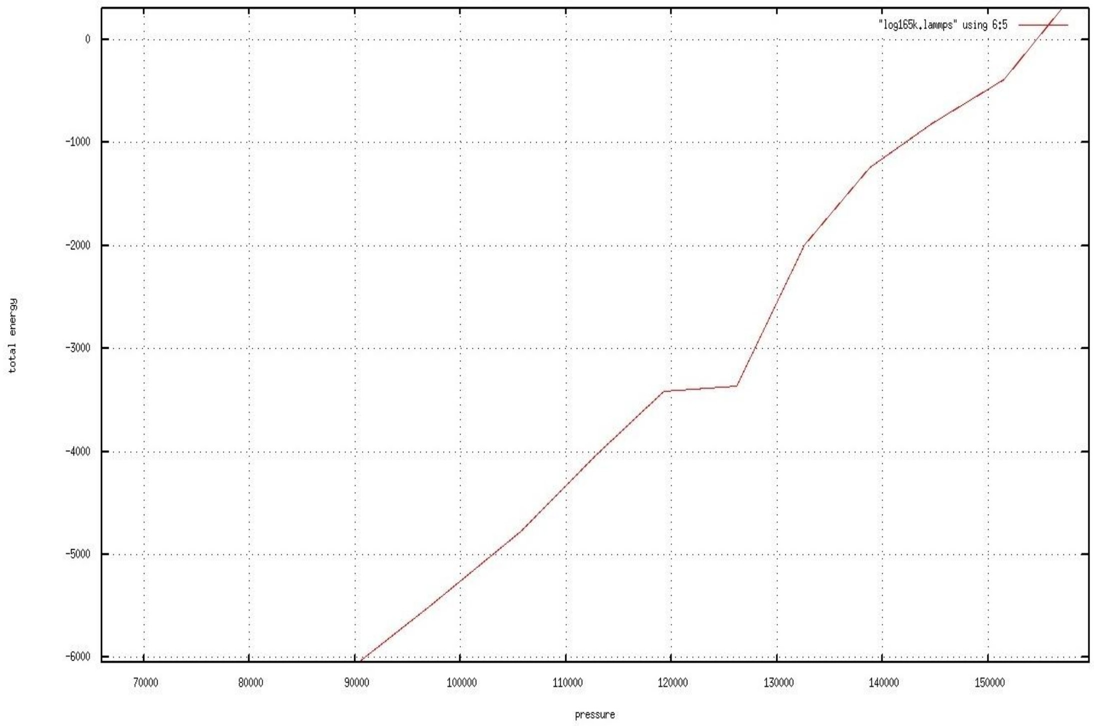

Figure 55: Close view of the 2nd region of interest in the caloric curve for the system with constant temperature of 165°K

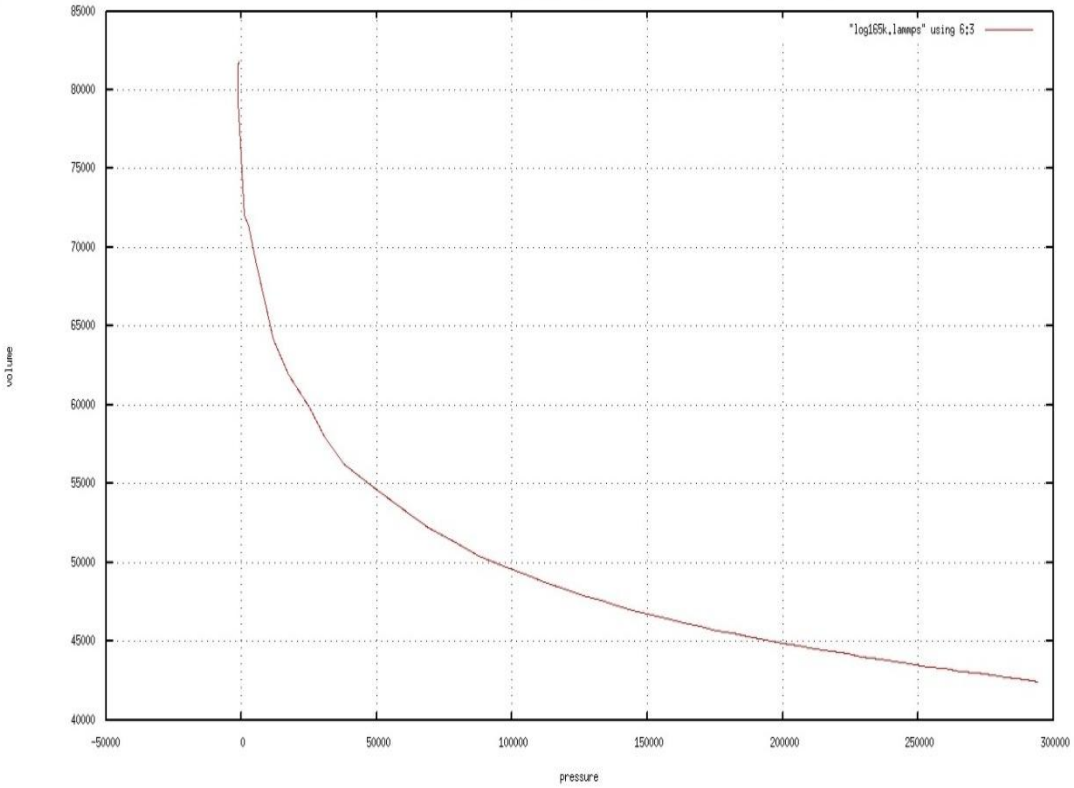

Figure 56: Volume versus pressure plot of the simulation with constant temperature of 165°K

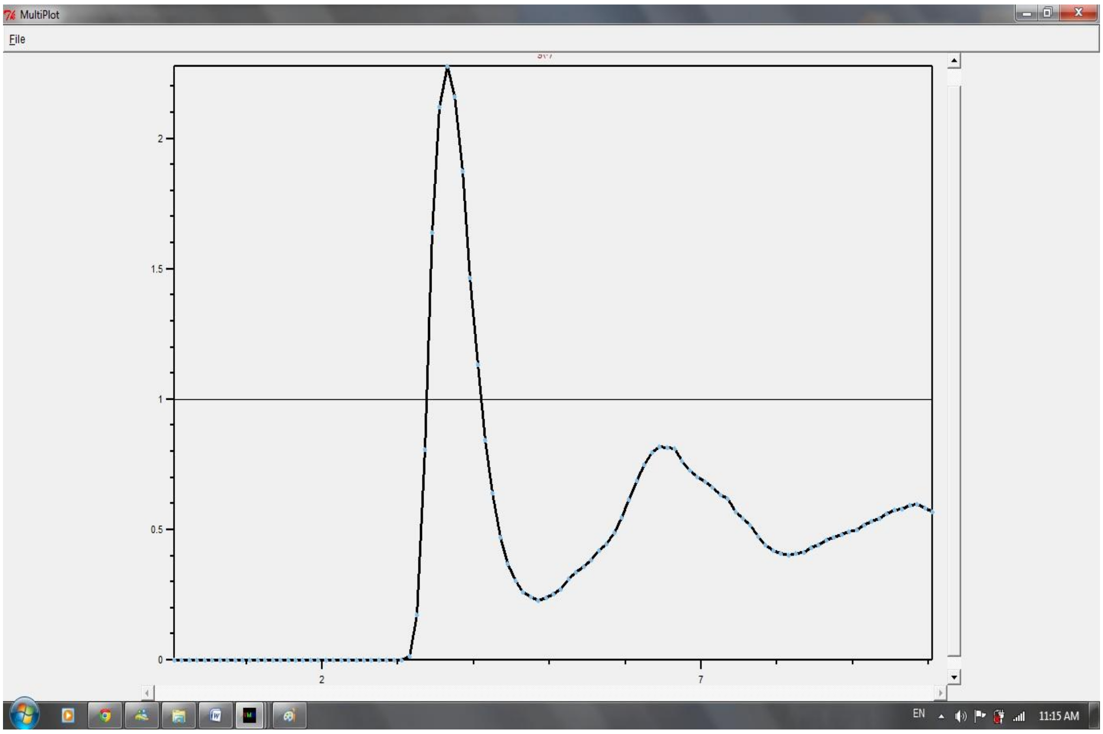

Figure 57: radial distribution function plot of the system's initial condition with constant temperature of 165°K

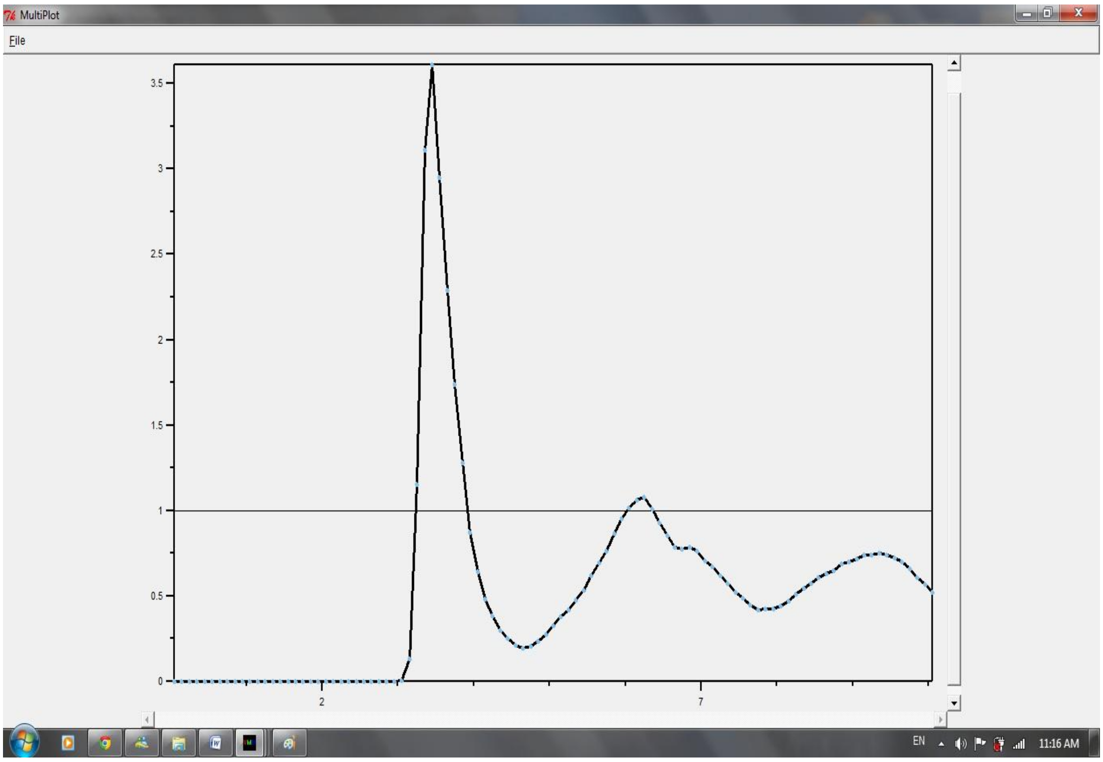

Figure 58: radial distribution function plot of the system at the middle of simulation with constant temperature of 165°K

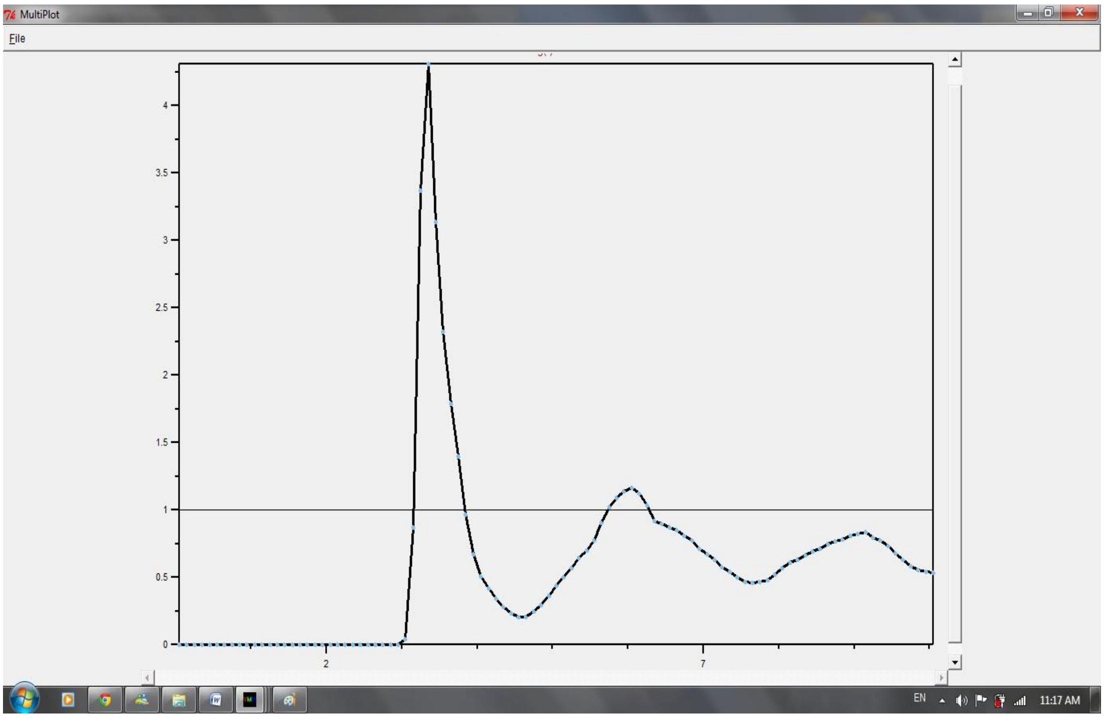

Figure 59: radial distribution function plot of the system at the end of simulation with constant temperature of 165°K

5.2.3 Temperature set at 295°K

For the simulation with temperature set at 295°K the caloric curves shown in Figure 60, 61 and 62 are obtained, the transition from liquid to phase I took place at around 1392.376MPa. A successive transition from phase I to A happens at 5042.514MPa and enters phase B at 8432.785MPa. At around 22737.326MPa the methane system enters the HP phase. From the volume versus pressure plot (Figure 63) as well as the radial pair distribution function plot, it can be observed that similar changes took place with increasing pressure. For the radial pair distribution function plot, the value of the 1st peak is even lower when compare with the simulation having a temperature of 165lower due to the fact that the molecules have more energy at 295 °K and tends to be further apart. The amount of peaks detected also reduces due to the same reason.

Table 14: At temperature 295K, the phase transition that took place at pressure (MPa) (2)

Transition	Pressure (MPa)		
	Present work	**Previous Work**	**Experiment**
Liquid to phase I	1392.376	950 ±100	1300
Phase I to A	5042.514	6500 ±400	5300
Fcc	-	7700 ±300	Intermediate phase
Phase B	8432.785	9000 ±250	8600
Fluctuates between fcc and fct	-	9900 ±200	Intermediate phases
	-	11600 ±250	
	-	14100 ±250	
	-	15200 ±350	
	-	18600 ±400	
	-	20030 ±400	
	-	20300 ±300	
	-	20900 ±300	
	-	21100 ±300	
	-	21500 ±300	
	-	22600 ±400	
HP Phase	22737.326	23200 ±500	23520

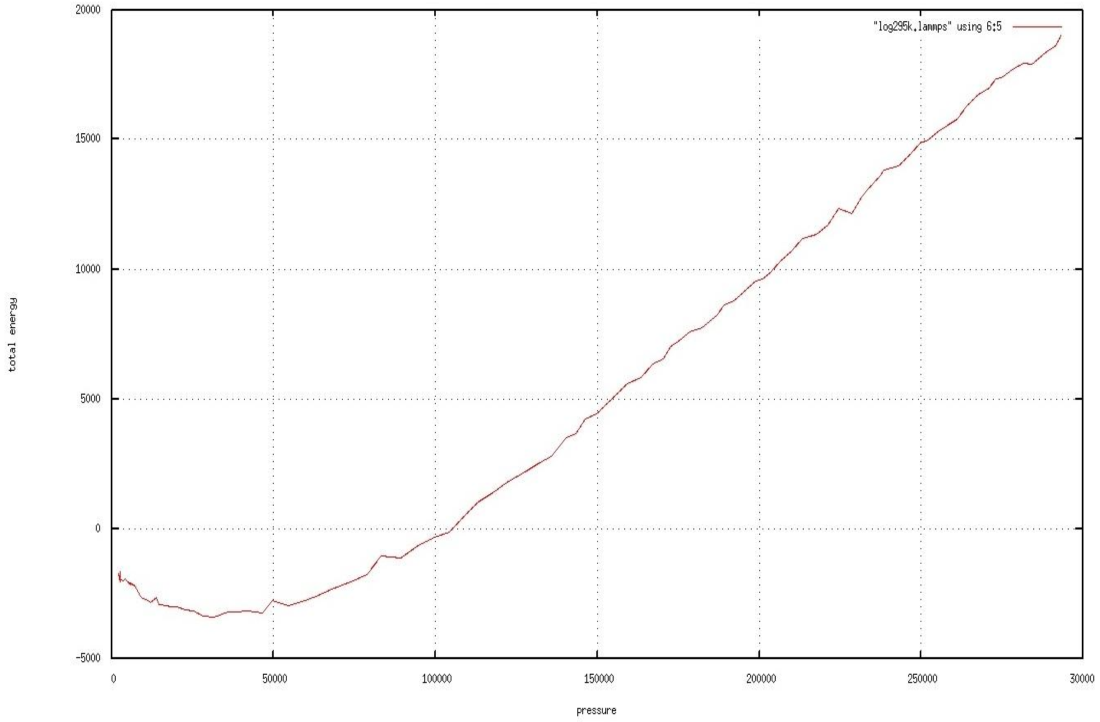

Figure 60: Full view of the caloric curve for the system with constant temperature of 295°K

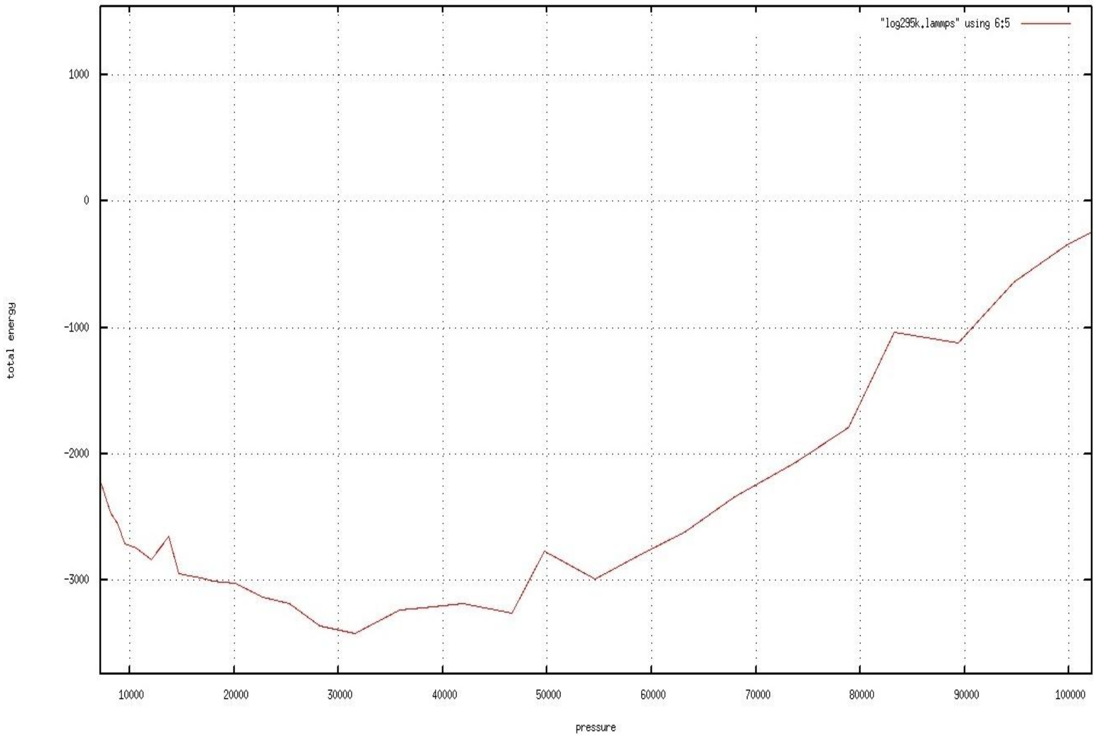

Figure 61: Close view of the 1st region of interest in the caloric curve for the system with constant temperature of 295°K

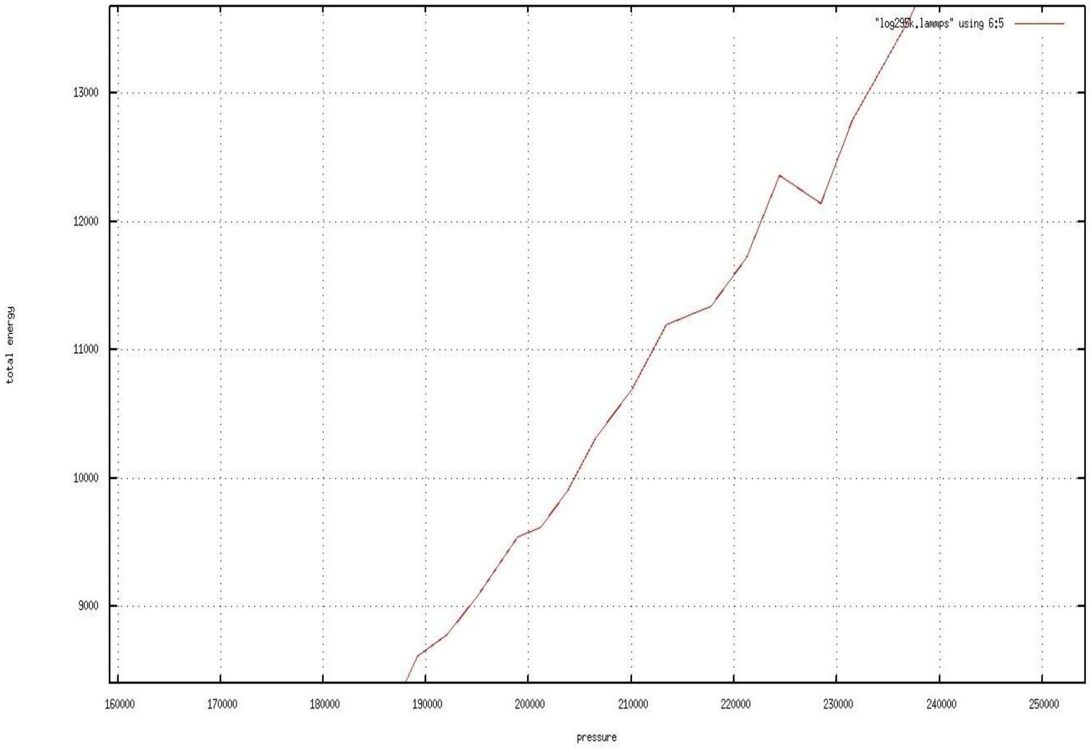

Figure 62: Close view of the 2nd region of interest in the caloric curve for the system with constant temperature of 295°K

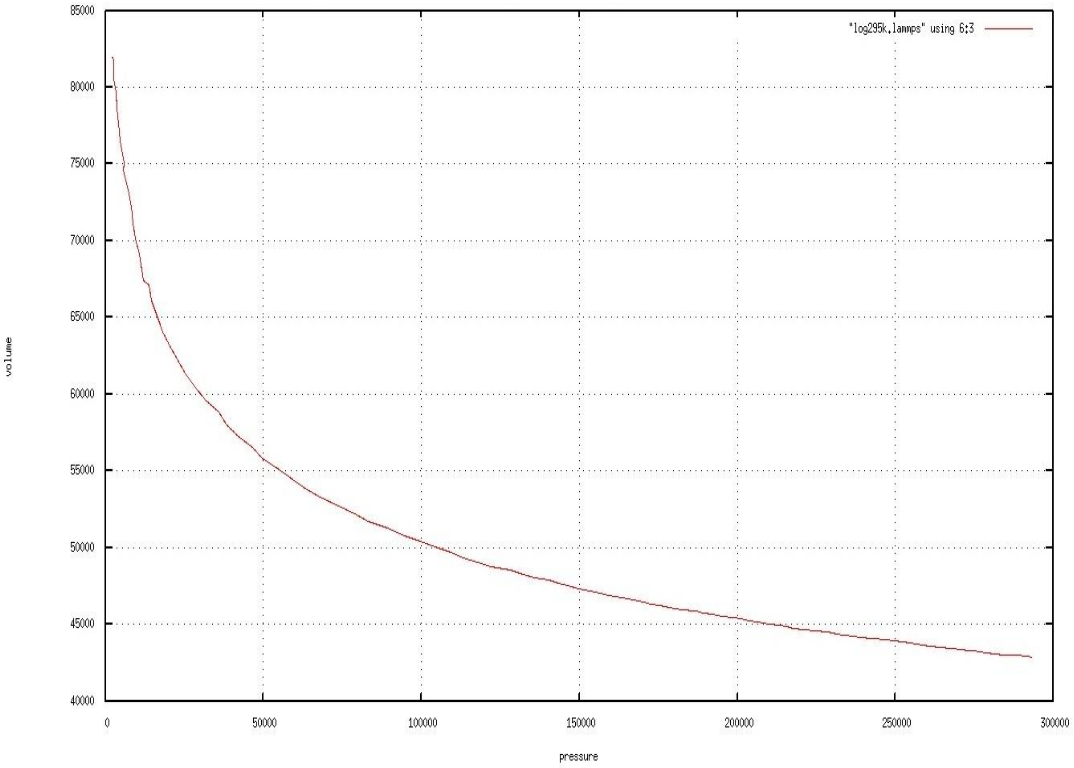

Figure 63: Volume versus pressure plot of the simulation with constant temperature of 295°K

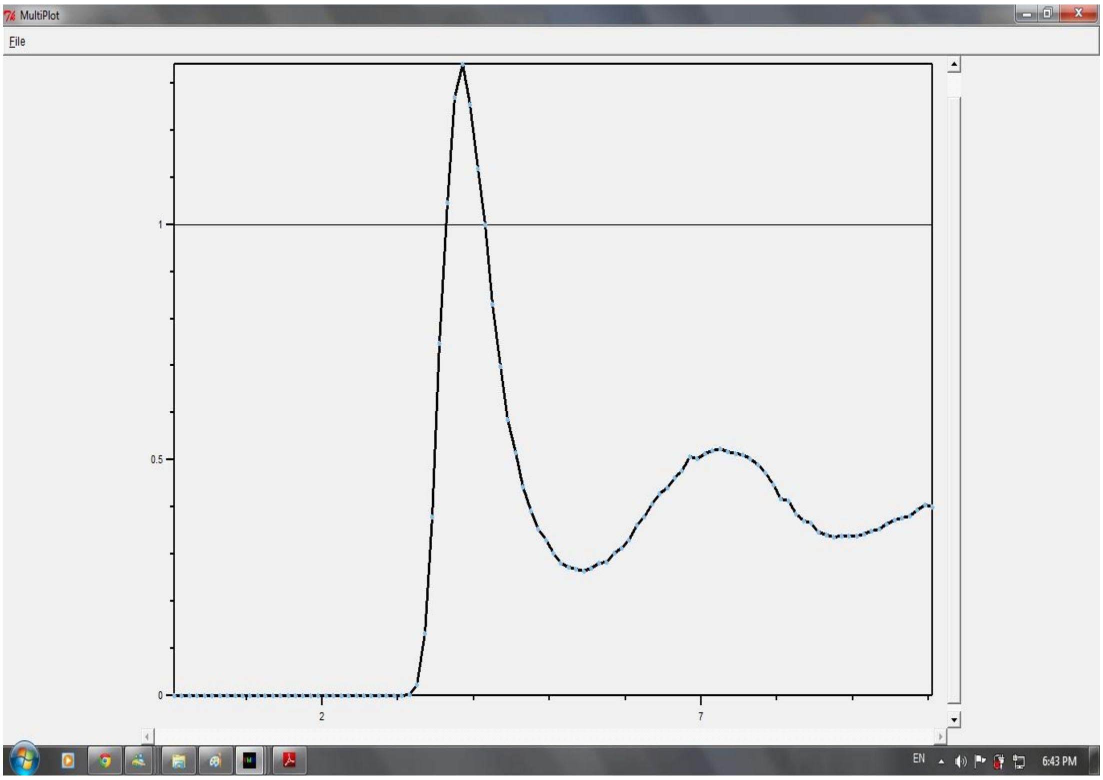

Figure 64: radial distribution function plot of the system's initial condition with constant temperature of 295°K

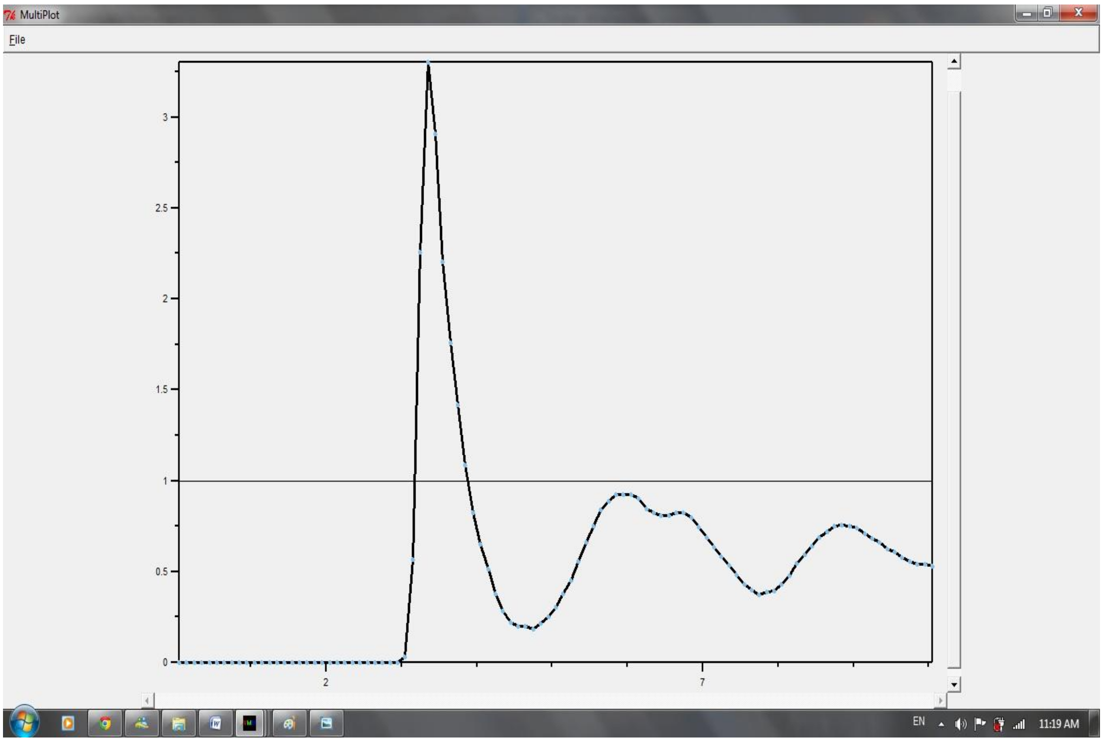

Figure 65: radial distribution function plot of the system at the middle of simulation with constant temperature of 295°K

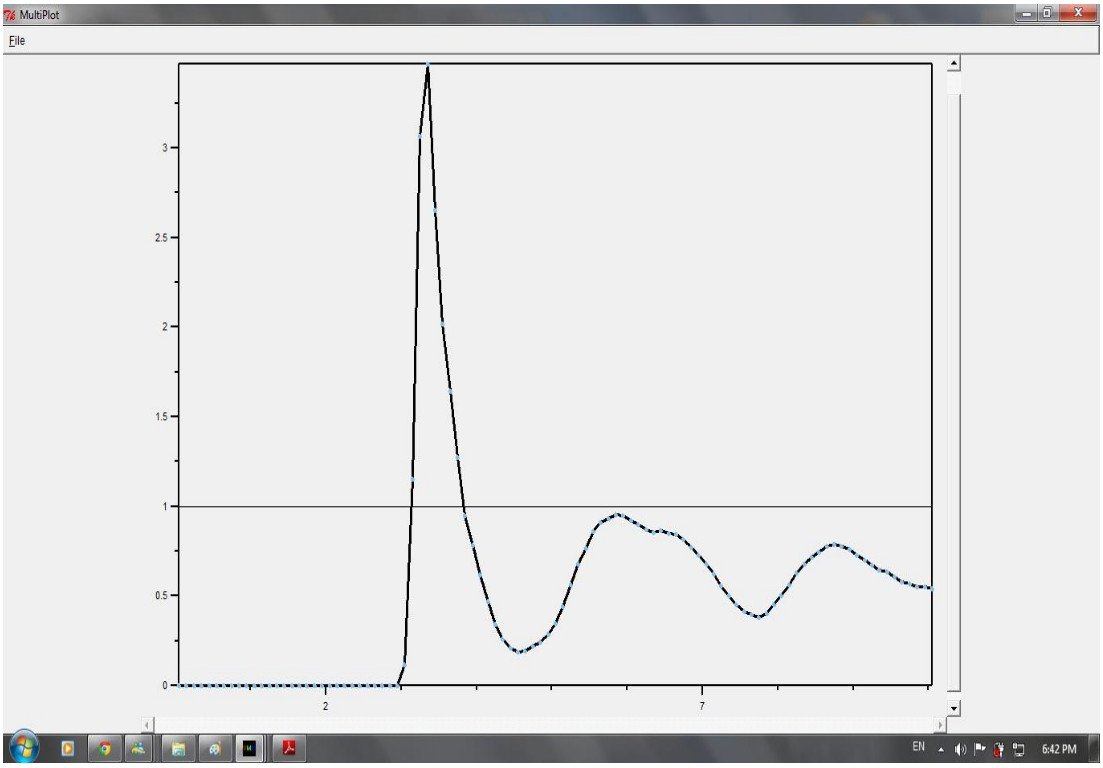

Figure 66: radial distribution function plot of the system at the end of simulation with constant temperature of 295°K

CHAPTER 6: CONCLUSION AND RECOMMENDATIONS

6.1 Conclusion

From the molecular dynamics simulations it can be seen that the results obtain do not differ much from the previous research done. That implies that the force field value being use is quite accurate as well as an incorrect force field will create a large different in the results obtain as well as possible simulation failure. Besides that it also shows that the Lennard-Jones pair potential can adequately describe the interactions between methane molecules. The used of a large size simulation system also increase the accuracy of the results obtain as LAMMPS runs simulation via sampling the data at each interval based on statistical approach. It can also be concluded that under high pressure, methane maintains at a solid state which will allow easier transportation or storage.

6.2 Recommendations

In order to further increase the accuracy of the simulation results obtained, a better force field can be obtain via using better methods to find it’s values. The damping factor when executing the barostating and thermo stating can be further fine tune to allow the molecules under simulation is well relaxed before allowing the temperature and pressure to rise. Besides that, a better energy minimization technique can be implemented or by increasing the time taken to perform energy minimization can further reduce the initial energy of the system. By increasing the sampling rate, it can also increase the accuracy of the data obtain to get a better result at the cost of higher computing or simulation time.

Integrating the advance knowledge of chemistry into the research by using forth order cumulant as well as rotational order parameter as done by S.M El-Sheikh in his paper [11] will further help to verify the accuracy of the data.

References

[1] M.J. McPherson “Subsurface Ventilation and Environmental Engineering” Chapman and Hall, ISBN 13: 9780412353000 ISBN 10:0412353008, 01April, 1993

[2] Michael P.Allen “Introduction to Molecular Dynamics Simulation” Computational Soft Matter: From Synthetic Polymers to Proteins, Lecture Notes, Norbert Attig, Kurt Binder, Helmut Grubm ̈uller, Kurt Kremer (Eds.), John von Neumann Institute for Computing, Julich, NIC Series, Vol. **23**, ISBN 3-00-012641-4, pp. 1-28, 2004.

[3] Ju Li “Basic Molecular Dynamics” In S. Yip, editor, Handbook of Materials Modeling, chapter 2.8. Kluwer Academic Publishers, 2005

[4] Rapaport, D.C. “The Art of Molecular Dynamics Simulation”, Cambridge University, 1996. ISBN# 0521445612

[5] Joy Woller “The Basics of Monte Carlo Simulations”, Unniversity of Nebraska-Lincoln Physical Chemistry Lab (Chem 484), Spring 1996
http://www.chem.unl.edu/zeng/joy/mclab/mcintro.html

[6] W. Press, “Structure and Phase Transitions of Solid Heavy Methane”, J.Chem. Phys. 56, 2597 (1972)

[7] E. Gregoryanz, M. J. Clouter, N. H. Rich, and R. Goulding, Phys Rev B 58, 2497 (1998)

[8] A. J. Nijman, M. Sprik and N. J. Trappeniers, “A high pressure NMR study of solid methane II. Coupled and uncoupled relaxation of the Zeeman and tunnel system in ordered four spin system” Physica B+C Volume 98, Issue 4, March 1980

[9] M. M. Thiéry, D. Fabre, and K. Kobashi, “Raman spectra of solid CH_4 under high pressure. III. New high pressure phases in solid CH_4 and CD_4” J. Chem. Phys. 83, 6165 (1985)

[10] M. Prager, W. Press, A. Heidemann, and C. Vettier, “Rotational tunneling in CH_4 under pressure (CH_4 III)” J. Chem. Phys. 77, 2577 (1982)

[11] S.M. El-Sheikh, K.Barakat, N.M. Salem “Phase transitions of methane using molecular dynamics simulations” The journal of chemical physics 124, 124517 (2006)

[12] Crystal maker software http://www.crystalmaker.com/, Last visited: 20 March 2012

[13] LAMMPS Molecular Dynamics Simulator http://lammps.sandia.gov/, Last visited: 20 March 2012

[14]Learning lamps and forcefield parameter
https://sites.google.com/site/akohlmey/software/topotools/topotools-tutorial---part-2
Last visited: 10 March 2012

[15] Radial Distribution Function
http://www.iams.sinica.edu.tw/lab/jlli/thesis_andy/node14.html, Last visited: 21 March 2012

[16] Radial Distribution Function http://www.ks.uiuc.edu/Research/vmd/plugins/gofrgui/,
Last visited: 21 March 2012

[17] S.M. El-Sheikh "A phase transition for solid methane" Chemical Physics Letters
247(1995) 159-162

[20] M.S.A. El Kader "On high pressure phase transitions in solid methane" Chemical Physics 277 (2002) 77-81

[21] Roland H. Stote, Institut de Chimie LC3-UMR 7177,Université Louis Pasteur, Strasbourg France "Introduction to Molecular Dynamics Simulation"

Appendix A

Command script for constant pressure simulation of 100MPa:

```
units real
boundary P P P
atom_style full
read_data datafcc.step2a
pair_style lj/cut/coul/cut 12.0
bond_style harmonic
angle_style harmonic
pair_modify mix geometric tail yes
special_bonds lj/coul 0.0 0.0 0.5
pair_coeff 1 1 0.66 3.5
pair_coeff 2 2 0.03 2.5
bond_coeff 1 340.0 1.09
angle_coeff 1 33.0 107.8
velocity all create 1.0 53244 dist gaussian mom no rot no
fix 1 all nve
run 100
minimize 1.0e-4 1.0e-6 100 1000
timestep 0.25
reset_timestep 0
neighbor 1.5 bin
neigh_modify every 10 delay 20 check yes
thermo 500
thermo_style custom step temp vol pe etotal press
velocity all scale 1.0
fix        2 all langevin 1.0 1.0 50.0 6243
dump   2 all atom 1000 methaneout.lammpstrj
dump_modify 2 image yes scale no
run 10000
```

```
unfix 1
unfix 2
fix       6 all npt temp 1.0 1.0 50 iso 0.00001 986.92326 500
run 10000
unfix 6
fix       5 all npt temp 1.0 300.0 150 iso 986.92326 986.92326 500
run 50000
```

Appendix B

Command script for constant temperature simulation of 130°K:

```
units real
boundary P P P
atom_style full
read_data datafcc.step2a
pair_style lj/cut/coul/cut 12.0
bond_style harmonic
angle_style harmonic
pair_modify mix geometric tail yes
special_bonds lj/coul 0.0 0.0 0.5
pair_coeff 1 1 0.66 3.5
pair_coeff 2 2 0.03 2.5
bond_coeff 1 340.0 1.09
angle_coeff 1 33.0 107.8
velocity all create 1.0 53244 dist gaussian mom no rot no
fix 1 all nve
run 100
minimize 1.0e-4 1.0e-6 100 1000
timestep 0.25
reset_timestep 0
neighbor 1.5 bin
neigh_modify every 10 delay 20 check yes
thermo 500
thermo_style custom step temp vol pe etotal press
velocity all scale 1.0
fix         2 all langevin 1.0 1.0 50.0 6243
dump   2 all atom 1000 methaneout.lammpstrj
dump_modify 2 image yes scale no
run 10000
```

```
unfix 1
unfix 2
fix       1 all nvt temp 1.0 130.0 50
run 10000
unfix 1
fix      5 all npt temp 130.0 130.0 150 iso 0.00001 296076.9801 5000
run 50000
```